A SOL-GELLO APPROACH

TO THE SYNTHESIS

OF NANOCRYSTALLINE MATERIALS

By

AMANDA J. NICHOLS

Bachelor of Science in Chemistry
Oklahoma Christian University
Oklahoma City, OK
2003

Submitted to the Faculty of the
Graduate College of the
Oklahoma State University
in partial fulfillment of
the requirements for
the Degree of
DOCTOR OF PHILOSOPHY
July, 2008

A SOL-GELLO APPROACH

TO THE SYNTHESIS

OF NANOCRYSTALLINE MATERIALS

Dissertation Approved:

Dr. Allen Apblett

Dissertation Adviser

Dr. Warren Ford

Dr. Nicholas Materer

Dr.LeGrande Slaughter

Dr. Jim Smay

Dr. A. Gordon Emslie

Dean of the Graduate College

ACKNOWLEDGEMENTS

I would like to sincerely thank my research advisor, Dr. Allen W. Apblett, for his outstanding guidance, patience, and encouragement. I appreciate the flexibility I was given to work and the many things I learned from him during my graduate career. My gratitude extends to the other members of my advisory committee: Dr. Ford, Dr. Materer, Dr. Slaughter, and Dr. Smay for their advice, suggestions, and time.

I would also like to acknowledge my fellow graduates and friends for their assistance and encouragement. I appreciate the help of the Chemistry Department office staff during my time here at OSU.

I want to acknowledge my family. I am thankful to my added family for their support and help especially this summer. I wish to thank my parents for their love, encouragement, and support throughout my entire education. My deepest thanks go to my husband, Josh, for his continual encouragement and support. Thank you for the hours of encouraging talks and caring for our son Joshua Casen when I needed to work extra at the end.

Finally, I am thankful to God for this opportunity to further my education and the peace I felt during the stressful times.

"We are hard pressed on every side, but not crushed…" 2 Corinthians 4:8

"He brought me out into a spacious place; he rescued me because he delighted in me." Psalm 18:19

TABLE OF CONTENTS

Chapter Page

LIST OF TABLES

Table Page

LIST OF FIGURES

Figure Page

Figure Page

Figure Page

CHAPTER I

GENERAL INTRODUCTION

BACKGROUND AND AIM OF RESEARCH:

Within the realm of materials science, chemistry is used to synthesize materials. Chemistry allows for better methods to arise in making a material. Traditionally, solid state reactions were used, but extremely high temperatures (~1000ºC or more) and extended heating times are needed. There are factors that can affect sintering: particle size, particle packing, and particle shape [1]. The smaller the particle size, the lower the sintering temperature needed. Therefore, small particles have less distance to travel to fuse together. In addition, smaller particles have higher surface energies than larger particles so the sintering process rate will increase as well. The better the particles are packed together (uniform packing), the faster the sintering rate. Since particles are closer together, there are more contact areas where the particles can begin to fuse together. Aggregation occurs when particle packing is non-uniform. Finally, regular-shaped particles will sinter slower than irregular-shaped particles. Irregular-shaped particles sinter faster due to their higher surface area to volume ratio.

Purity problems can plague a solid state reaction due to other phases forming. Some steps can be taken to lessen or eliminate the problems of high sintering temperatures and impurities, such as achieving smaller particle sizes (e.g. grinding) to

increase diffusion rates or using processes that promote a thorough mixture (e.g. precursor method or sol-gel processing) [1]. These steps can lead to low-temperature synthesis reactions.

An active method in research is developing such low-temperature synthesis processes. The distance required for diffusion of cations, and hence the time and temperature required for a reaction, are decreased when the cations are closer together. In the precursor method, the different cations are ideally dispersed on the atomic level in the correct stoichiometric ratio in the same solid precursor. There are two types of precursor methods: one is where the products are a result of redox reactions and the other type does not involve any change in the oxidation states of the cations. In sol-gel chemistry, molecular precursors are homogeneously distributed in a sol then after gelation, the solvent is removed. Metal alkoxides can be used to form a metal oxide in this manner [1].

One of the most popular areas of research involves nanomaterials. Nanomaterials are materials that can have unique properties when the particle size is between 1-100 nm. Nanocrystalline materials, being the most investigated type of nanomaterial, have grains that are in the nanometer dimension range [1]. As mentioned above, nanosized-precursors increase the rate of solid state reactions.

The purpose of this research was to develop a low-temperature process that can prepare nanocrystalline materials. The basis of this method is having nanosized particles distributed equally in the precursor state that will increase the reaction rate and decrease the temperature needed to synthesize the material. Figure 1-1 illustrates this model using the yttrium aluminum garnet (YAG) synthesis route (with Y^{3+} and Al^{3+} ions) as an

example. Box 1 represents normal hydrolysis. A gradient is formed between the two hydrolyzed metals because aluminum hydrolyzes faster. The cations must cross a large area in order to react with one another and form YAG. Boxes 2 and 3 are representations of gelatin networks with the metal ions distributed in each pore or "tiny beaker". With an increase of gelatin content, the matrix has thicker walls and more walls leading to smaller "beakers". There is a continuous phase due to the gelatin network. The confinement of the cations in a smaller area restricts the degree of segregation of metal ions during hydrolysis. In turn, this will facilitate the synthesis of the final material at low temperature.

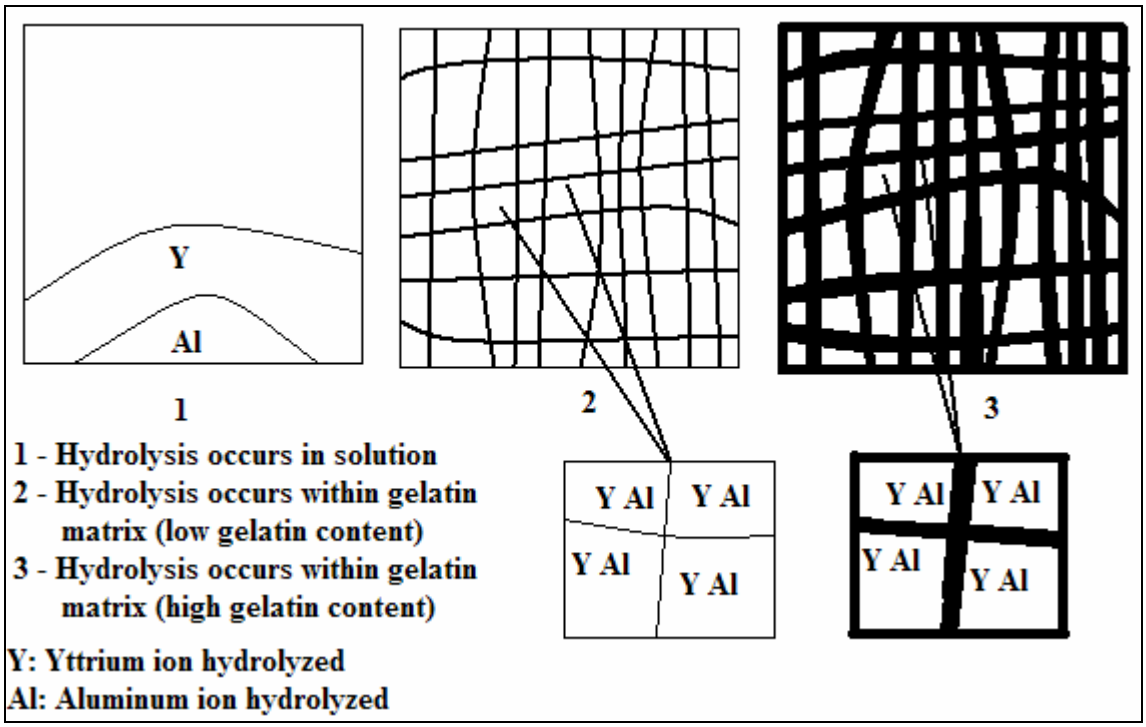

Figure 1-1: Model of the sol-gello method.

This process was applied to the synthesis of different materials; specifically, a garnet, a ceramic, and a biomaterial. Record low crystallization temperatures will be

achieved. The gelling agent will serve to control factors such as crystallization temperature and crystallite size.

GARNETS: BACKGROUND AND STRUCTURE

Garnets are a group of complex oxides with the general formula $A_3B_2X_3O_{12}$. A is an element that is large (~1 Å) and has a coordination number of eight. The A ions are arranged in a distorted cubic environment. The B ions lie in the octahedral sites while X ions lie in the tetrahedral sites [2]. Figure 1-2 shows a representation of the garnet structure. The structure is a network of tetrahedral, octahedral, and the distorted cubic arrangements (or eightfold triangular dodecahedron) [3].

There are different groups within the garnet family. One group of garnets have yttrium or another rare earth metal as the A ions while the B and X ions are as Fe^{3+} [2]. Although garnets occur naturally, most of the garnet research is concerned with the synthetic garnets. Probably the most researched garnet initially was yttrium iron garnet (YIG) ($Y_3Fe_5O_{12}$) [3]. YIG was first discovered to be a useful microwave device material [4] then YIG along with other rare earth iron garnets (ReIG) were found to be ferrimagnetic [5]. Another research area for garnets is the development of magnetic bubble devices for computer memory technology [6].

YTTRIUM ALUMINUM GARNET (YAG)

YAG: APPLICATIONS

Once solid state lasers arrived on the research front, an effective laser host was found in yttrium aluminum garnet (YAG) ($Y_3Al_5O_{12}$). YAG serves as the host for the neodymium ion which is laser active. Nd^{3+}:YAG lasers are considered high power [2].

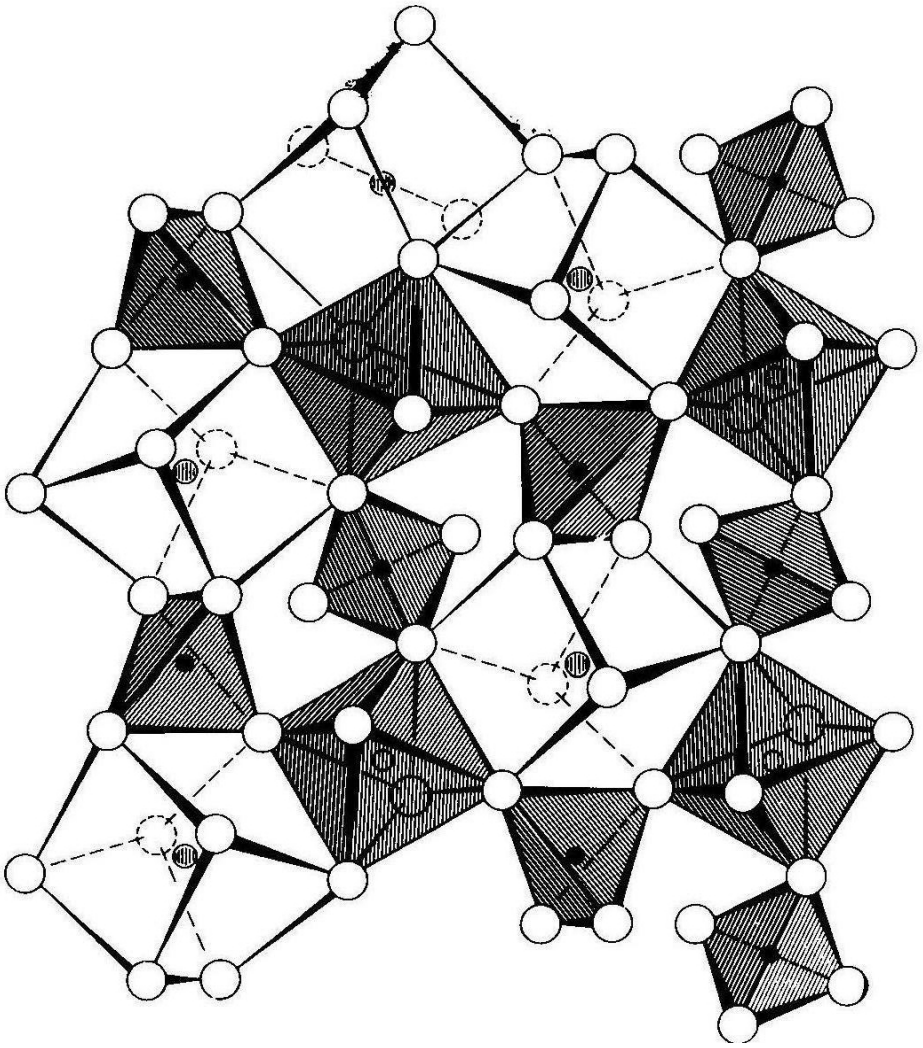

Figure 1-2: Garnet structure [3].

Another important optical property that is being explored for YAG is its infrared transparency in the range of 3-5 μm. This makes it useful for such applications as missile domes [7]. An additional application for YAG is as a pressure and temperature sensor. YAG is doped with samarium, and Sm:YAG films can be prepared via a glycine-nitrate process where the solutions are spin-cast into thin films [8]. YAG can be doped with terbium or europium in order to prepare nanoparticle, bright phosphors. These phosphors

are needed for applications in better cathode-ray tubes that are used in high-resolution display devices such as high density televisions (HDTVs) and projection televisions (PTVs). YAG:Tb can be obtained by a flux method with a single firing [9] or along with YAG:Eu, by a simple sol-gel method [10].

Besides the optical applications, YAG holds a firm place in ceramics used for refractories and industry. Due to its corrosion resistance, YAG has been used in refractory coatings [11]. YAG has also been used in melt growth composites which have outstanding strength, oxidation resistance, and thermal stability at high temperatures. A possible application for such a material includes use in a gas turbine system [12].

YAG: SYNTHESIS METHODS

Most synthesis techniques focus on preparing polycrystalline YAG because of the difficulty in obtaining a single YAG crystal. If needed, powders can then be pressed into pellets and sintered so that translucent disks can be acquired for optical applications as discussed above [13]. YAG has been prepared in a variety of ways. Conventionally, the solid-state reaction method has been used to prepare YAG (see Eq. 1-1).

$$3\ Y_2O_3\ (s) + 5\ Al_2O_3\ (s) \rightarrow 2\ Y_3Al_5O_{12}\ (s) \qquad \textbf{Eq. 1-1}$$

Sintering temperatures are as high at 1600-1850ºC, and 1800ºC is needed to acquire optical properties that are similar to a single crystal of YAG [14]. High calcination temperatures lead to coarsening of the microstructures. Homogeneously mixing the cations can lead to lower sintering temperatures. In order to achieve a homogeneous mixture of yttrium and aluminum ions, yttrium and aluminum nitrates can be mixed and then thermally decomposed above 1000ºC to yield YAG [15]. Combustion synthesis can be used to prepare a YAG precursor via a reaction between an oxidizer (nitrate) and a

fuel (glycine). Micron-sized YAG particles are obtained without other phases present at 1050ºC [16].

Other wet-chemical processes can be used to synthesize YAG precursors that crystallize to YAG at lower temperatures. The citrate gel process entails making a gel of aluminum and yttrium nitrates and citric acid. After drying the gels, a heat treatment will produce YAG particles. Using the citrate gel process, YAG can be crystallized above 800ºC without impurities such as $YAlO_3$ and $Y_4Al_2O_9$ present. The particle size ranged from 20-70 nm [17]. Implementing microwave heating, the citrate gel process can achieve pure YAG crystallization at 600ºC with a particle size of approximately 40 nm [18].

The hydrothermal method has been used to make YAG as well. Temperatures of 500-600ºC and pressures of 70-170 MPa were needed to form phase-pure YAG [19]. Other hydrothermal methods use an organic media instead of water. The organic media can be a glycol, hence, the method is referred to as a glycothermal method. A suspension was made of aluminum isopropoxide, yttrium acetate, and 1-4-butanediol and autoclaved at 300ºC and under 4-5 MPa. YAG particle size was approximately 30 nm [20].

A precipitation method can be used to make YAG. Again yttrium and aluminum nitrates are used, but in this method ammonium hydroxide carbonate is used as a precipitant to produce yttria and alumina powders. Once the powders are heated to 1100ºC, only the YAG phase is present. The particles are just smaller than 100 nm [21]. YAG can also be crystallized at 800ºC using a liquid metal carboxylate (2-[2-(2-methoxy) ethoxy] ethoxyacetic acid) (MEEA) as a precursor. Aluminum nitrate and

$Y(MEEA)_3$ were put in solution and then dried yielding an amorphous product, $Y_3Al_5(MEEA)_9(NO_3)_{15}\cdot 49H_2O$, which is the YAG precursor product [22].

Another method focuses on the precipitation of hydroxides using three different precursors: nitrates, isopropoxides, and isopropoxides chelated with ethyl acetoacetate. First, yttrium and aluminum nitrates are put into solution, and the hydroxide is precipitated when ammonium hydroxide is added. 1000ºC had to be reached before only the YAG phase is present. The second method involves aluminum and yttrium isoproxides that are diluted with 2-propanol then hydrolyzed with the alcohol-water mixture. Then the hydroxide is dried under pressure at 80ºC. Pure-phase YAG was not reached even at 1100ºC. Finally, the modified alkoxide process dictates that yttrium isoproxide and ethyl acetoacetate are mixed and refluxed in an alcohol. Then aluminum isoproxide is added to the reflux followed by an alcohol-water hydrolysis. The hydroxide obtained here is also dried under pressure at 80ºC. Like the nitrate method, the hydroxide had to be heated to 1000ºC to obtain pure-phase YAG powder [23].

Sol-gel chemistry has been used to synthesize YAG powders as well. One method complexed the metal ions with ethylene glycol creating a gel. The gel was dried at 120ºC then the precursor gel was heated to 1000ºC to obtain only the YAG phase. Another method used an alkoxide route to produce pure YAG at 700ºC. The alkoxide route employed a suspension of aluminum tert-butoxide dissolved in isopropyl alcohol and $[Y_3(O^tBu)_9(^tBuOH)_2]$ [24]. A similar sol-gel method used non-alkoxides (yttrium and aluminum nitrates complexed with ethylene glycol) to prepare YAG nanocrystallites at 800ºC [25].

SPINEL

SPINEL: STRUCTURE AND APPLICATIONS

Spinel ($MgAl_2O_4$) consists of a cubic close packed arrangement of oxide ions with magnesium ions in an eighth of the tetrahedral holes and aluminum ions in the octahedral holes (Figure 1-3). Each oxygen ion is surrounded tetrahedrally by three aluminum ions and one magnesium ion. There are many compounds that have the spinel structure and most are oxides [2].

Spinel traditionally has been used for refractory applications [26,27]. Perhaps the most common known use of spinel is as a catalyst support [28]. Research has explored implementing spinel into different applications. Spinel can be used as a radiation-resistant insulating material [29]. Other possible uses of spinel include applications as a missile dome material [30] and a humidity sensor [31].

SPINEL: SYNTHESIS METHODS

Spinel is conventionally made by a solid-state reaction between alumina and magnesia. Extremely high temperatures of 1450-1800ºC are needed to make spinel. Mineralizers can lower the firing temperature, but impurities and low reactivity then becomes problems [32]. For this reason, other preparation routes have been investigated to synthesize pure spinel at lower temperatures.

Chemical preparation methods can have more control over homogeneity, purity, particle shape, size, and distribution. A spinel precursor can be made by homogeneously mixing two metal ions together. The pyrolysis of the precursor allows for lower preparative temperatures and quicker reaction rates [22].

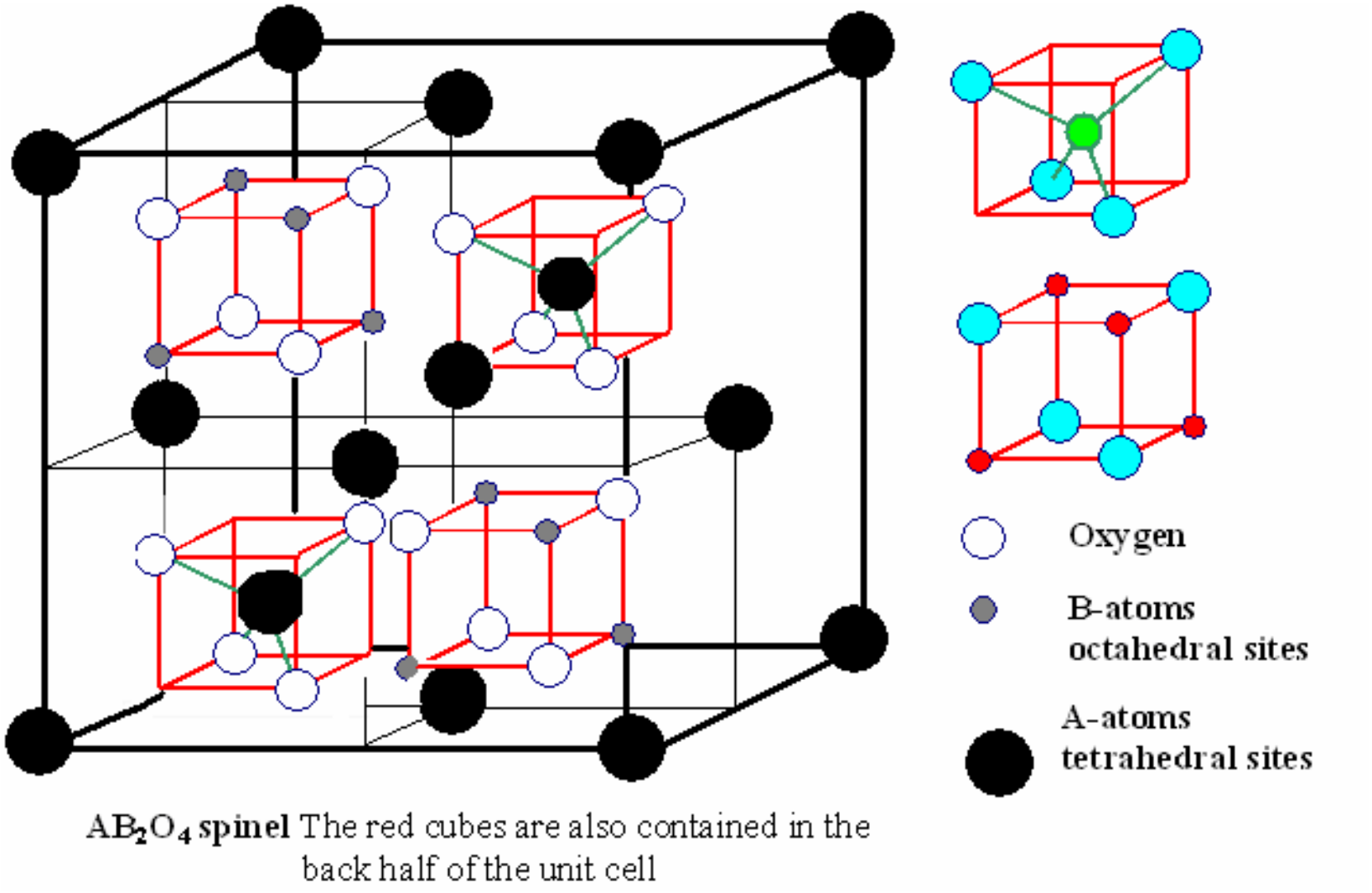

Figure 1-3: Spinel structure [33].

Normal micelle microemulsion methods have been employed to make spinel nanoparticles [34]. In this technique, a metal ion is surrounded by a surfactant with a layer of water around the surfactant. The water layer controls the particle size, allowing the synthesis of nanoparticles to be made [35]. Using aqueous solutions of magnesium nitrate, aluminum nitrate, and sodium dodecyl sulfate, the normal micelle is created. Ammonium hydroxide is added to increase the pH, but the pH has to be tightly controlled or impurities in the spinel will form. The micelles are initially heated to 650ºC where spinel begins to crystallize. After heating for 20 hours at 800ºC, 20 nm spinel nanoparticles are obtained with a surface area of 79 m^2/g.

One chemical preparation method involved using liquid salt precursors, specifically 2-[2-(2-methoxy)ethoxy]ethoxyacetate (MEEA) salts. These MEEA salts can not only chelate metal ions but also solvate them as well [22]. Magnesium and aluminum salts are made and then reacted together to prepare a spinel precursor. For example,

$$Al(O_2CCH_3)_2\cdot(OH) + 2\ MEEAH + H_2O \rightarrow Al(MEEA)_2OH\cdot H_2O + 2\ CH_3CO_2H \quad \textbf{Eq. 1-2}$$

$$Mg(NO_3)_2 + 2\ Al(MEEA)_2OH\cdot H_2O \rightarrow MgAl_2(MEEA)_4(OH)_2(NO_3)_2\cdot 2H_2O \quad \textbf{Eq. 1-3}$$

This spinel precursor can be heated and begins to crystallize spinel at 700ºC. Pure spinel is formed above 900ºC.

Another spinel preparation method focused on using a polymer-like spinel precursor. This precursor is an oligomeric alkoxide: $N(CH_2CH_2O)_3HMg[N(CH_2CH_2O)_3Al]_2$ easily prepared by reacting aluminum hydroxide

and magnesium oxide triethanolamine ($N(CH_2CH_2OH)_3$) in ethylene glycol. Due to the facile, one-step method, Waldner coined the synthesis procedure as the OOPS (Oxide One-Pot Synthesis) Method [36]. Spinel with $MgCO_3$ present is formed at 600ºC but once heated to 1200ºC, only spinel is there. At 900ºC, the spinel has a surface area of 90 m^2/g.

Not only do liquid precursors ensure a quicker, more facile synthesis of spinel, but implementing sol-gel methods also can aid in spinel formation, and, particularly, nanocrystalline spinel. Parmentier explored two possible routes of making a sol-gel spinel precursor [37]. One method used magnesium nitrate and aluminum sec-butoxide as the metal ion sources that are dissolved in isopropanol where a sol-gel is formed. The other method reacted solid magnesium and aluminum under reflux with methoxyethanol. Hydrolysis with a water/methoxyethanol solution resulted in a sol-gel spinel precursor. The second method produced pure nanocrystalline spinel (6-34 nm) at 800ºC.

BIOMATERIALS

Bone is the second most implanted material [38]. The best orthopedic implant materials are biocompatible, mechanically strong, wear-resistant, and made at a reasonable cost [39]. The biochemical response caused by the implant material in the host tissue dictates whether that material is termed bioactive, or bioinert, or worse [40]. Metal implants can have loosening or rejection by the surrounding tissue while some ceramics can cause inflammation and bone marrow depletion [41]. Bioinert materials cause no reaction while bioactive materials act like natural tissue, in this case, specifically like bone. Some common bioinert ceramics used for implants include

alumina and zirconates. While these implants are nonreactive, they tend to be brittle and difficult to mold [40]. Bioactivity is in a sense a gluing effect and sometimes is referred to as bonding osteogenesis. For the bioactive material, there is a deposition of collagen and hydroxyapatite from the host tissue onto the surface of the implant material [42]. The natural tissue grows into the bioactive implant material. Hydroxyapatite and calcium phosphates have been shown to encourage the release of cytokines and proteases that help bone resorption [41]. To increase the flexibility of a ceramic implant, a polymer can be mixed or cross-linked with the ceramic. This hybrid implant material not only has the bioactivity from the inorganic portion, but it also possess the flexibility with the organic part. An example of a polymer-ceramic implant material is ORMOSIL (organically modified silicate) that is a network of polydimethylsiloxane (PDMS)-poly(tetramethylene oxide) (PTMO)-CaO-SiO_2-TiO_2 [43]. Another similar hybrid makes the hydroxyapatite portion when soaked in simulated body fluid (SBF) [44].

HYDROXYAPATITE

Bone mineral can be represented by the formula $Ca_{8.3}(PO_4)_{4.3}(CO_3)_x(HPO_4)_y(OH)_{0.3}$ where x increases and y decreases as age increases [1]. The ideal bone substitute would imitate natural tissue in its size, consistency, and function. As it degrades, the bone substitute needs to become like the surrounding tissue; if it does not degrade, the bone substitute has to be tolerated by the body and not cause infection. Hydroxyapatite is a good candidate for a bone substitute due to its bioactivity. It can be used as a permanent bone substitute for small and large implants. Hydroxyapatite implants have proven successful: after 11 years of a knee implant, there was no change and after 12 years, there was only minor loss of motion [40]. About 3

weeks are needed for hydroxyapatite-coated implants to attach to bone and 7 weeks are needed to ensure that the bonding between the coating and the natural tissue is strong enough [45].

Not only is hydroxyapatite used as a bulk implant or a coating for implants, but it is also added to injectable bone cements to promote osteoconductivity. Bone cements can be used as a filler for spinal fusions or for fractures [46].

The basic apatite structure is hexagonal [47]. The structure of hydroxyapatite has a skeleton of phosphate tetrahedra (Figure 1-4 top). Within one unit cell, the phosphate tetrahedra can be divided into two layers or channels. The first channel has two calcium ions in each unit cell while the second channel has walls made up of oxygen atoms and calcium ions (Figure 1-4 bottom) [48].

Many synthesis routes exist for preparing hydroxyapatite. Hydroxyapatite can be formed via solid state reactions. Sodium phosphate reacting with calcium nitrate have been shown to produce hydroxyapatite using microwave heating [49], and calcium phosphate and calcium carbonate can be calcined to higher temperatures (1000-1300ºC) to make hydroxyapatite [50]. Hydrothermal processes have had success in synthesizing hydroxyapatite though control over pH and temperature. Hydroxyapatite can be prepared by treating corals and algae with a hydrothermal treatment seen in Eq. 1-4 [1].

$$10\ CaCO_3 + 6\ (NH_4)_2HPO_4 + 2\ H_2O \rightarrow$$

$$Ca_{10}(PO_4)_6(OH)_2 + 6\ (NH_4)_2CO_3 + 4\ H_2CO_3 \qquad \textbf{Eq. 1-4}$$

Another hydrothermal reaction involves calcium nitrate, diammonium phosphate, and urea where hydroxyapatite is crystallized. Several wet methods exist that can precipitate

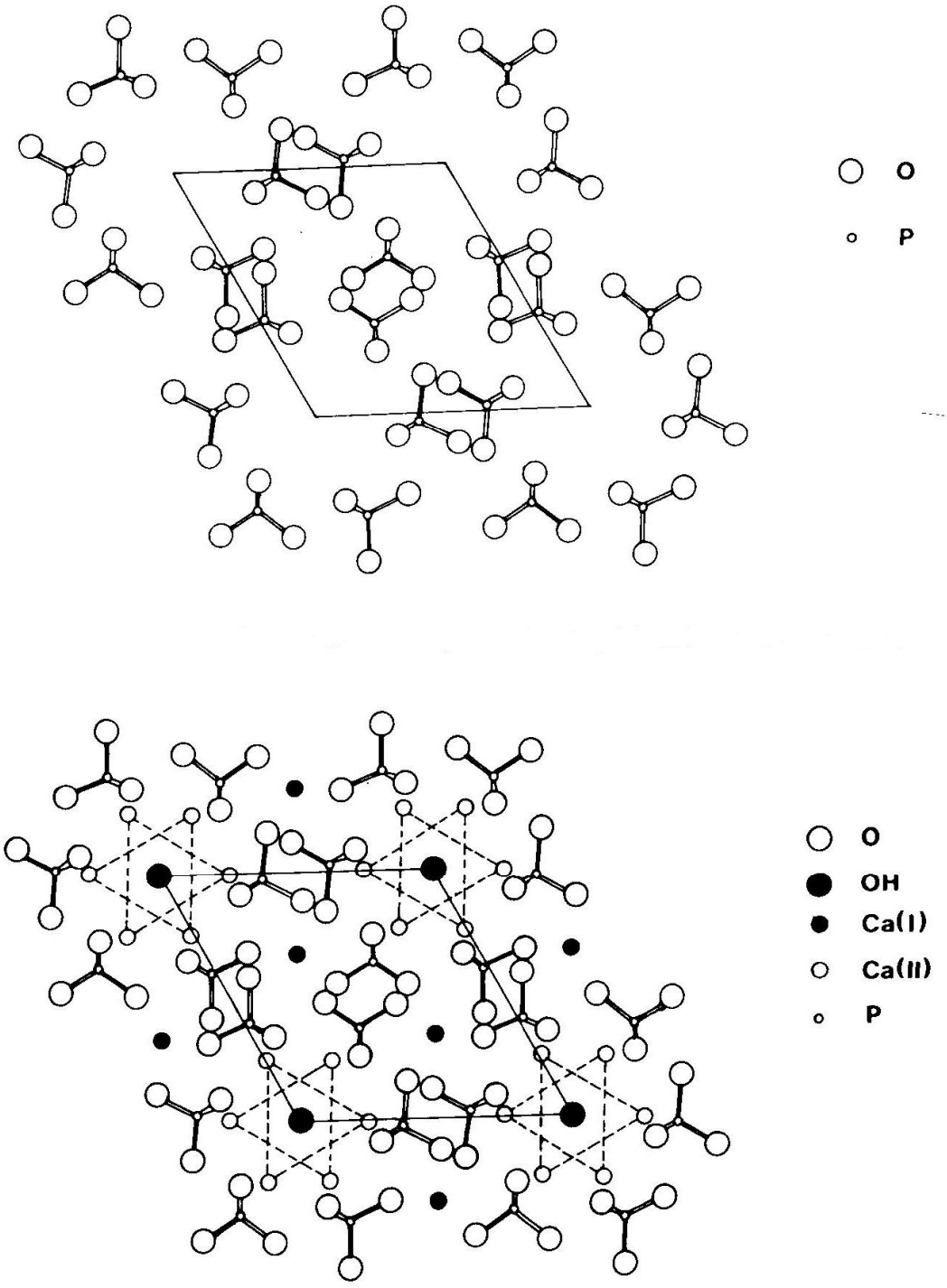

Figure 1-4: Structure representations of hydroxyapatite [51].

hydroxyapatite. A number of variations have been done in these wet method-reactions in an attempt to find the optimal conditions for synthesizing hydroxyapatite. With use of a surfactant, ultrasonic vibration, and heating at 50ºC, calcium nitrate and diammonium phosphate precipitated hydroxyapatite [52]. Another method uses calcium nitrate, phosphoric acid, and ammonia with an organic modifier to control crystal shape. Temperatures of 100-200ºC were needed to precipitate crystallized hydroxyapatite [53]. One study focused on different reactants with varying reflux period, aging period, and temperature of the reactions. The optimal conditions included a long reflux, prolonged aging periods (4 weeks and 4 months, respectably), and a temperature of 90ºC [54].

Sol-gel chemistry has been applied to the synthesis of hydroxyapatite. One route is a non-alkoxide method that implements phosphorous pentaoxide and calcium nitrate in ethanol. A temperature of 900ºC was required to have pure hydroxyapatite. A much lower calcination temperature (350ºC) was needed when triethyl phosphite and calcium nitrate were used as precursors along with water or ethanol.

CALCIUM PHOSPHATES

Calcium phosphate ceramics are biodegradable or bioresorbable: they dissolve inside the host tissue without causing any unfavorable tissue reaction [40]. They can aid in repairing deficiencies caused by tumors, trauma, surgery, and infections [38]. A ceramic glass has been made that contains hydroxyapatite and calcium pyrophosphate ($Ca_2P_2O_7$) that can be used as a implant material due to its bioresorbability.

Certain calcium phosphates, such as octacalcium phosphate and amorphous calcium phosphate, and hydroxyapatite were precipitated through a diffusion system. While the deposition took 20 hours to complete, pH had to be controlled within the

gelatin cup. Calcium chloride and disodium phosphate solutions were buffered with tris-HCl and sodium hydroxide [55]. Another implant material was prepared by sintering a glass mixture of calcium oxide and phosphorous pentaoxide. Both calcium pyrophosphate and calcium metaphosphate resulted, and this material was shown to be an effective resorbable bioglass [56].

CONCLUSION

These three different nanocrystalline materials: a garnet, a spinel, and a biomaterial, all can be synthesized by this newly-developed sol-gello process. This low-temperature route can control the precursor size allowing for faster reactions between the metal cations. The sol-gello method is facile and applicable to the synthesis of different materials. Record low crystallization temperatures are achieved.

CHAPTER II

YTTRIUM ALUMINUM GARNET

INTRODUCTION

Garnets are complex oxides with the formula $A_3B_2X_3O_{12}$. In yttrium aluminum garnet ($Y_3Al_5O_{12}$) (YAG), B and X are both aluminum. Therefore, the garnet has corner sharing AlO_6 octahedra and AlO_4 tetrahedra. The yttrium atoms reside in the eight coordinate locations of the distorted cubic framework [2].

YAG has applications in several material fields: mechanical and structural applications, as a laser host, and in electronics and optics. YAG is mechanically strong with relatively high resistance to thermal stress-induced fracture [57] and is used in ceramic composites to withstand high temperatures [12]. Bulk YAG can be used in the monolithic form or in a composite where YAG is in the matrix form. In order for YAG to be used for structural applications, the material needs to have a controlled grain size [58]. Both the flexural strength and fracture toughness are relatively high when grain size is controlled. High-temperature applications that include insulating or refractory coatings are possible for YAG because of its low electrical conductivity, high oxidation resistance, and low creep rate [18]. Due to its large thermal conductivity and stable lattice structure, YAG also has applications as an electronic device coating and as a laser host [18].

Among all the optical applications, YAG is probably most known as its use as a laser-host material. The Nd:YAG laser, for example, has medical applications that include being used as a laser catheter for lithotripsy and to treat plaque-filled coronary arteries [59]. When YAG is doped with terbium or europium, the resulting materials can be used in phosphor screens for visual applications. Both smaller particle size and higher brightness of the phosphors are a goal for cathode-ray tubes [9,10]. Other optical applications include doping the garnet to yield a transparent YAG [13] and the development of an optical pressure temperature sensor using Sm:YAG [8]. Since YAG is optically transparent and mechanically strong, it is currently being explored as an IR transparent missile dome material [7].

YAG can be synthesized by a variety of methods. Alumina and yttria powders can undergo a solid state reaction at high temperatures of 1600 to 1850ºC under vacuum to produce polycrystalline, transparent YAG [14]. Conventional methods have problems with controlling homogeneity, purity, particle shape and size, and size distribution. Chemical methods are an alternative to circumvent these problems. These synthesis methods include co-precipitation methods [21,60], a glycothermal synthesis route [20], alkoxide methods [23,24,61], and sol-gel and citrate gel techniques [17,58]. They all can be employed to lower the sintering temperature and pressure needed to make YAG. Thin YAG films were prepared for use as planar waveguides in lasers using an alkoxide method [62]. Micron-size agglomerates of YAG have been prepared using a solution combustion method using aluminum and yttrium nitrates and glycine [16].

Since nanoscaled phosphors have relatively high brightness and efficiency, nanocrystalline YAG doped with cerium has been made by co-precipitation methods

[63]. A similar method was used to make YAG nanopowder in order to be used in applications for high-performance transparent ceramics (e.g. Nd:YAG) [60]. Nanocrystalline YAG was prepared at a comparatively low temperature of 700ºC using an alkoxide method [24].

Often, chemical routes still have problems with homogeneity although they are marked improvement over the ceramic method. In the synthesis of YAG, other refractory phases can form such as hexagonal $YAlO_6$ and monoclinic $Y_4Al_2O_9$. These phases form due to an inhomogeneous distribution of metal ions in the ceramic precursors. To solve this challenge, having a more homogeneous precursor system is the key to forming YAG at relatively low temperatures at quicker rates. Using such a method allows control over particle size, surface area, and porosity.

The sol-gello method was developed to ensure that a more homogeneous precursor can be made. A gel can be used to equally distribute the cations. In this work of synthesizing YAG, the gelling agent is agar or gelatin. During hydrolysis, the agar or gelatin "freezes" the metal ions in place preventing them from segregating during the hydrolysis process. The gelling agent also helps to control the particle size. Having nanosize precursors allow the low preparative temperatures and quick rates. In this Chapter, hydrolysis of a precursor gel with evenly distributed yttrium and aluminum salts is discussed. Once the gel is heated, nanocrystalline YAG begins to form at relatively low temperatures.

EXPERIMENTAL

Chemicals:

The following chemicals were purchased and used without further purification. The chemicals used in this section were as follows: Yttrium chloride hexahydrate [$YCl_3 \cdot 6H_2O$, Strem]; aluminum chloride hexahydrate [$AlCl_3 \cdot 6H_2O$, Mallinckrodt]; agar [Sargent-Welch]; gelatin (Knox); aqueous ammonium hydroxide [NH_4OH, ACS Reagent, Pharmco]; agarase with buffer [ICN].

The following chemicals were purchased and purified before being used in this section. Cation Exchange 650C Dowex [Sigma-Aldrich] and Anion Exchange 550C Dowex [Aldrich] were rinsed with deionized water. Gelatin [Knox] was treated with the ion-exchange resins to rid the gelatin of impurities (NaCl, $Al_2(SO_4)_3$, and $CaSO_4$).

Preparation of Yttrium Aluminum Garnet (YAG) Precursor Using Agar:

A 2 wt % agar solution sample was prepared first. 3 mmol (0.9 g) of yttrium chloride hexahydrate and 5 mmol (1 g) of aluminum chloride hexahydrate were added to 20 g of deionized water. The solution was stirred. 1 g of agar was stirred into 30 g of boiling deionized water. Once the agar was dissolved, the metal chlorides solution was stirred into the agar solution for a total solvent mass of 50 g. The resulting mixture was cooled to 10ºC until it formed a transparent light yellow gel. Next, the gel was placed inside an ammonium hydroxide chamber. Initially, a temperature of 10ºC was used, but it was found that the gel was sufficiently stable at room temperature to allow later samples to be much more rapidly hydrolyzed. The ammonium hydroxide chamber was a closed container with aqueous ammonium hydroxide inside. As the hydrolysis occurred, the gel transformed from a transparent light yellow color to opaque white. The time necessary

for hydrolysis ranged from 1 – 6 days. The higher the agar content, the longer hydrolysis took. Once hydrolysis was completed, the opaque white solid was removed from the chamber and dried in a fume hood at room temperature for roughly a day followed by drying under vacuum for approximately a day.

The same procedure was used to prepare samples with a 15 wt % and 30 wt % agar solution. For the 15 wt % agar solution, 7.5 g of agar was dissolved in 30 g of boiling deionized water. The metal chlorides solution [3 mmol (0.9 g) of $YCl_3 \cdot 6H_2O$ and 5 mmol (1 g) of $AlCl_3 \cdot 6H_2O$ in 20 g of deionized water] was stirred into the agar solution. For the 30 wt % agar solution, 15 g of agar was dissolved in 40 g of boiling deionized water. The 40 g of water was needed to ensure that this large amount of agar would dissolve. The metal chlorides solution was prepared using 3 mmol (0.9 g) of $YCl_3 \cdot 6H_2O$ and 5 mmol (1 g) of $AlCl_3 \cdot 6H_2O$ in 10 g of deionized water. Then the metal chlorides solution was stirred into the agar solution. The total solvent mass for both the 15 and 30 wt % agar samples was 50 g each. After hydrolysis, with an increase of agar content, the gello color becomes darker.

A similar procedure was followed to prepare YAG precursor samples with an increased metal content. A metal chlorides solution was prepared that was three times concentrated. 9 mmol (3 g) of $YCl_3 \cdot 6H_2O$ and 15 mmol (4 g) of $AlCl_3 \cdot 6H_2O$ was stirred into 20 g of deionized water. Then 1 g of agar was dissolved in 30 g of boiling deionized water. The metal chlorides solution was stirred into the agar solution resulting in a 2 wt % agar solution (with a total mass of 50 g). 15 and 30 wt % agar YAG precursor samples were prepared as well. For the 15 wt % agar solution, 7.5 g of agar was dissolved in 30 g of boiling deionized water. The metal chlorides solution was prepared by dissolving 9

mmol (3 g) $YCl_3 \cdot 6H_2O$ of and 15 mmol (4 g) $AlCl_3 \cdot 6H_2O$ of in 20 g of deionized water. Then it was stirred into the agar solution resulting in 50 g of total solvent (15 wt % agar). The highest agar content YAG precursor sample was prepared by mixing the metal chlorides solution [9 mmol (3 g) $YCl_3 \cdot 6H_2O$ of and 15 mmol (4 g) $AlCl_3 \cdot 6H_2O$ of in 10 g of deionized water] into the agar solution (15 g of agar in 40 g of boiling deionized water). There was a total solvent mass of 50 g resulting in a 30 wt % agar sample.

Purification of the Agar YAG Precursor:

Purification techniques were employed to separate the agar from the gel prior to heating to form crystalline yttrium aluminum garnet. One method was a simple washing method. The precursor gel (after hydrolysis and drying) was placed in deionized water and heated to dissolve the agar. The temperature was kept below 100ºC to prevent the water from boiling. Then the solution was centrifuged and the agar-water solution was decanted. More hot water was added to the precipitate, shaken, and centrifuged again pouring off the agar-water supernatant. This step was repeated two more times. Then the precipitate was dried with acetone, and the acetone was centrifuged off. The precipitate was dried under vacuum.

Agarase was used in the second purification method to "eat away" the agar. A YAG precursor gel was prepared using 15 wt % agar. The YAG precursor gel was put in deionized water in order to soften the gel. The gel was washed with deionized water and the pH was monitored. Agarase has a broad range of activity at room temperature between 3.0 – 9.0 with the optimum pH being 7.0 [64]. Once the pH reached approximately 7, one milliliter of agarase was added to the gel. The gel and agarase was occasionally stirred for 48 hours.

Preparation of Yttrium Aluminum Garnet (YAG) Precursor Using Purified Gelatin:

The gelatin had to be purified before being used as the gelling agent in the synthesis of the YAG precursor. A 5 wt % solution of gelatin (Knox) in boiling deionized water (10 g of gelatin in 200 g of water) was prepared. 10 mL of Dowex Cation and 20 mL of Dowex Anion ion-exchange resins were added to the gelatin solution. (10 mL of each type of ion-exchange resin was found to be effective and used in subsequent batches.) The gelatin solution with the ion-exchange resins was stirred at low heat until the conductivity dropped significantly and leveled off. Then the gelatin solution was filtered to remove the Dowex resins from the gelatin. The gelatin solution was then dried under vacuum or in a dehydrator oven at approximately 50ºC.

The YAG precursor gel was made using the same procedure as discussed earlier. A 6.4 wt % solution of purified gelatin in boiling deionized water (3.2 g of purified gelatin in 30 g of water) was used with the metal chlorides solution. The metal chlorides solution was prepared using 5 mmol (1 g) of $AlCl_3 \cdot 6H_2O$ and 3 mmol (0.9 g) of $YCl_3 \cdot 6H_2O$ in 20 g of deionized water. The total solvent mass was 50 g. The mixture was cooled into a gel and then subjected to ammonia hydrolysis at room temperature. Similar to the hydrolysis with agar, the precursor gel transforms into an opaque white solid. After hydrolysis was completed, the white solid was dried in a fume hood at room temperature followed by drying under vacuum. The same procedure was used to prepare samples from a 19.2 wt % and a 32 wt % purified gelatin solution. The 19.2 wt % purified gelatin solution was prepared using 9.6 g of gelatin dissolved in 30 g of boiling deionized water. The metal chlorides solution [5 mmol (1 g) of $AlCl_3 \cdot 6H_2O$ and 3 mmol

(0.9 g) of $YCl_3 \cdot 6H_2O$ in 20 g of deionized water] was mixed into the purified gelatin solution for a solvent total of 50 g. The 32 wt % purified gelatin solution was made by dissolving 16 g of gelatin in 40 g of boiling deionized water. Like the 30 wt % agar solution, 40 g of water needed to ensure that the gelatin would dissolve. 3 mmol (0.9 g) of $YCl_3 \cdot 6H_2O$ and 5 mmol (1 g) of $AlCl_3 \cdot 6H_2O$ was dissolved in 10 g of deionized water. The metal chlorides solution was then mixed into the purified gelatin solution. The total solvent mass was 50 g.

Crystallization of Yttrium Aluminum Garnet (YAG)

The YAG precursor samples (from agar and gelatin) were heated to crystallize the samples into YAG. Heating occurred in an oven at temperatures ranging from 400 - 1000ºC in air.

Characterization:

The YAG precursors and YAG powders were characterized using thermogravimetric analysis, X-ray powder diffraction (XRD), infrared spectroscopy (IR), and scanning electron microscopy (SEM). Thermogravimetric analysis was done on a Seiko ExStar 6500 TGA/DTA instrument. A Bruker AXS D-8 Advance X-Ray powder diffractometer was used to record the XRD patterns of the powders using copper K_α radiation at ambient temperature. The phases were identified with the ICDD database. Crystallite sizes were calculated using the Pearson 7 model using Topas P version 1.01 software (Bruker Analytical X-ray systems, Madison, WI 48, USA 1998). The samples peak are profiled by the software along with the standard peaks, and then the WinCrysize program (version 3.05 program, Bruker Analytical X-ray systems, Madison, WI, USA,

1997) uses the line broadening method and Scherer's equation to estimate the crystallite size. The Scherer's equation is:

$$C = \lambda k / \beta \cos(2\theta) \qquad \textbf{Eq. 2-1}$$

where λ is the wavelength of the radiation, k is the crystallite shape constant, β equals $(\beta_t^2 - \beta_o^2)^{1/2}$ (where β_t and β_o are the angular peak width measured at half of the maximum intensity line for the measured and reference compounds, respectably), and θ is the maximum intensity peak angle.

A Nicolet Magna-IR 75 spectrometer was used to collect infrared spectra in the 4000-400 cm^{-1} region using a DRIFTS cell and diluted sample powders with potassium bromide. Scanning Electron Microscopy was performed using a JEOL JXM 6400 SEM.

RESULTS AND DISCUSSION

Crystallization of Yttrium Aluminum Garnet (YAG) From Agar Precursors

Thermogravimetric Analysis (TGA):

After a YAG precursor sample was prepared and hydrolyzed in the ammonium hydroxide chamber, an amorphous yttrium aluminum oxide/hydroxide product resulted along with a byproduct of ammonium chloride. Once the sample was dried, the solid was subjected to thermogravimetric analysis (TGA) so the temperature required for complete removal of water, hydroxide, agar, and ammonium chloride could be determined. Figure 2-1 shows the TGA profile for the 15 wt % agar YAG precursor sample. This figure is representative of other profiles of samples with varying amounts of agar. The first step was due to evaporation of water and was followed by sublimation of ammonium chloride in the second step. Next, the agar was burned out, a process that was completed at 510ºC

in the case of the 15 wt % agar sample. Once the extraneous species were removed, the amorphous yttrium aluminum oxide/hydroxide began to crystallize into YAG.

Infrared Spectroscopy:

Infrared spectroscopy demonstrated YAG formation at crystallization temperatures. In the agar YAG precursor gels seen in Figure 2-2, YAG began to form as evidence from the broad Al-O stretch at 700 cm^{-1} [17]. As the agar percentage increased for the precursor gels, the temperature at which YAG formation occurred decreased. The

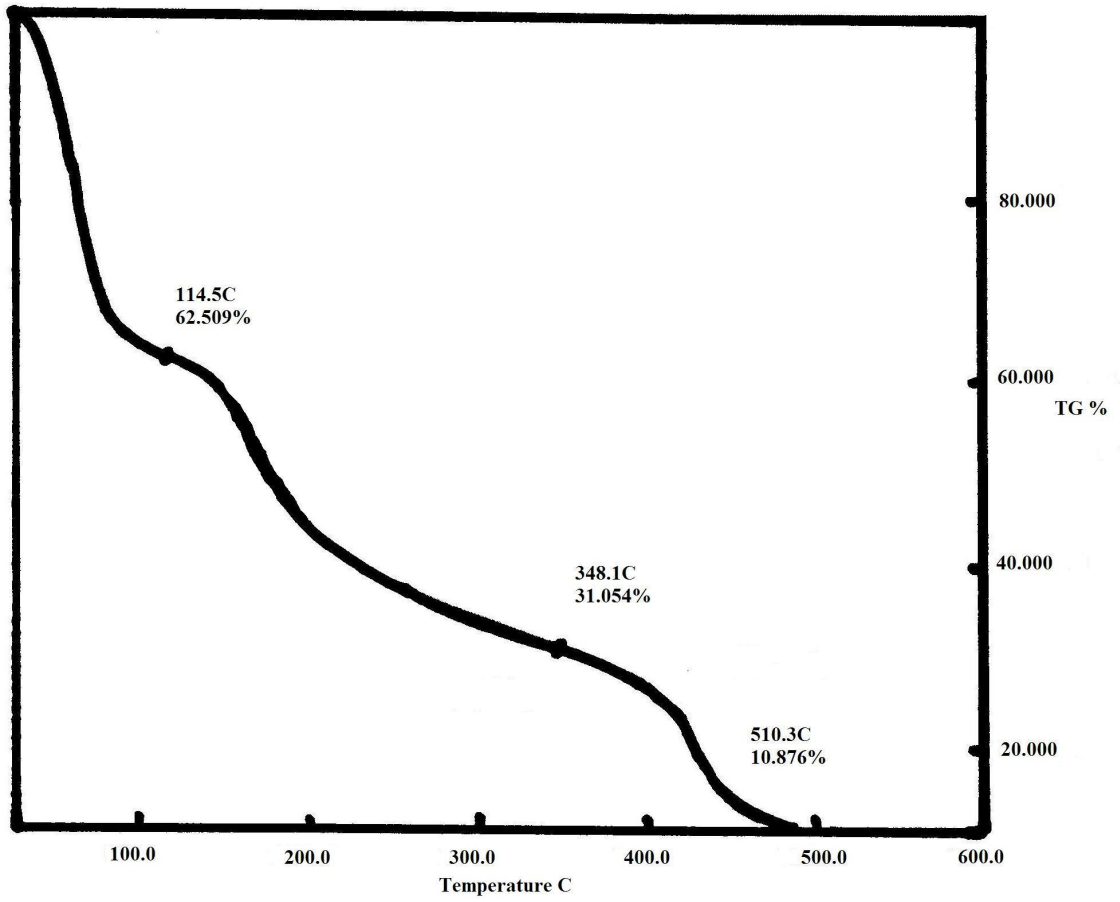

Figure 2-1: Thermal gravimetric analysis trace of 15 wt % agar YAG precursor gel.

O-H stretching band at 3500 cm^{-1} was present in all samples. This band is likely due to water or hydroxyls chemisorbed on the surface of the oxide powder.

Powder X-Ray Diffraction (XRD):

Powder X-Ray Diffraction (XRD) was used to identify the phase formation in samples. It was evident that as agar content was increased, the yttrium aluminum garnet (ICCD 33-0040) (YAG) phase begins to crystallize at lower temperatures. This trend can be seen in Figure 2-3 where the low agar content sample heated to 700ºC was amorphous while the high agar content sample heated to 700ºC had crystalline YAG present. A linear relationship exists between the initial crystallization temperature and agar content (Figure 2-4). The final crystallization temperature where only the YAG phase is present also shows a similar trend, but less linear. As the agar content increases, the final crystallization temperature decreases. No difference in crystallization temperature was seen when an increase of three times the metal content was used to prepare the samples.

Pure YAG formation occurred at the relatively low temperature of 600ºC when the agar content was 30 wt % (Figure 2-5). This is remarkable compared to the temperatures of conventional synthesis (1600-1850ºC) and even other chemical routes that use temperatures of 700-1100ºC [16,18,21,23,24,60-62]. Only a forced hydrolysis reaction with a temperature of 300ºC and a high pressure of 4 MPa has produced YAG at a lower temperature [20]. The width of the XRD reflections indicated that the material is nanocrystalline and was confirmed with an estimation of 11.4 nm.

Impurities such as $CaSO_4$, NaCl, and $Al_2(SO_4)_3$ from the agar were present. Some elements like calcium and chlorine have been shown to be bound to the agar so they are

difficult, if not impossible, to remove [65]. In Figure 2-5, the peaks not marked as YAG are anhydrite $CaSO_4$ (ICCD 37-1496).

Scanning Electron Microscopy (SEM):

SEM was used to observe the gels before calcinations and the powders once YAG began to crystallize. Figure 2-6 shows some of the images of 2 and 15 wt % agar content samples. The dried agar precursor YAG gels at room temperature have contorted surfaces (Figure 2-6A). The crystallized ammonium chloride is also seen on the surface of the gel. Once the sample was heated to 525ºC (Figure 2-6B), YAG began to crystallize. Irregular-shaped and different grain sizes are seen. An increase of agar content had similar effects as seen in Figure 2-6C where a 15 wt % agar content sample is heated to 510ºC. The grain sizes seem to have a smaller distribution of smaller sizes. As the 2 wt % agar sample was heated to a higher temperature of 800ºC, no visible change was observed in the morphology or gain size (Figure 2-6D).

Purification of Agar YAG Precursors:

The impurities from the agar were a concern since they could interfere with YAG crystallization. Purification methods for the Agar YAG precursors were initiated. At the start, the impurities were washed out of the agar. This was a cumbersome technique and not always effective.

Infrared Spectroscopy:

Infrared spectroscopy was used to study the effect impurities in the agar had on the system. Purification of the YAG precursor agar gels by washing out the impurities might have aided in the YAG formation as evidenced by IR (Figure 2-7). The 15 wt % agar YAG precursor heated to 510ºC shows more bands characteristic of YAG compared

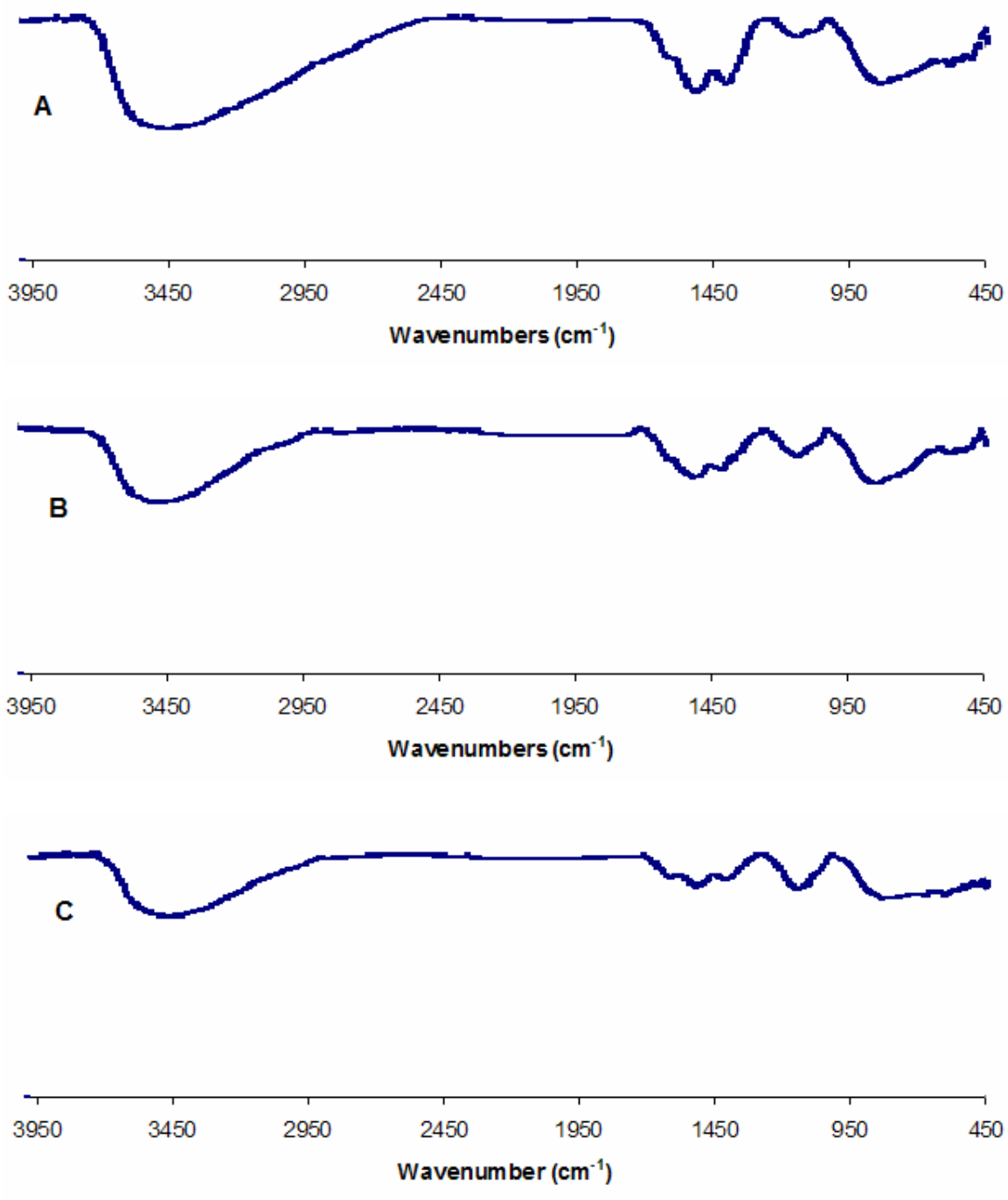

Figure 2-2: IR spectra of the YAG-agar precursors at A: 2 wt % agar fired at 525ºC; B: 15 wt % agar fired at 510ºC; and C: 30 wt % agar fired at 500ºC.

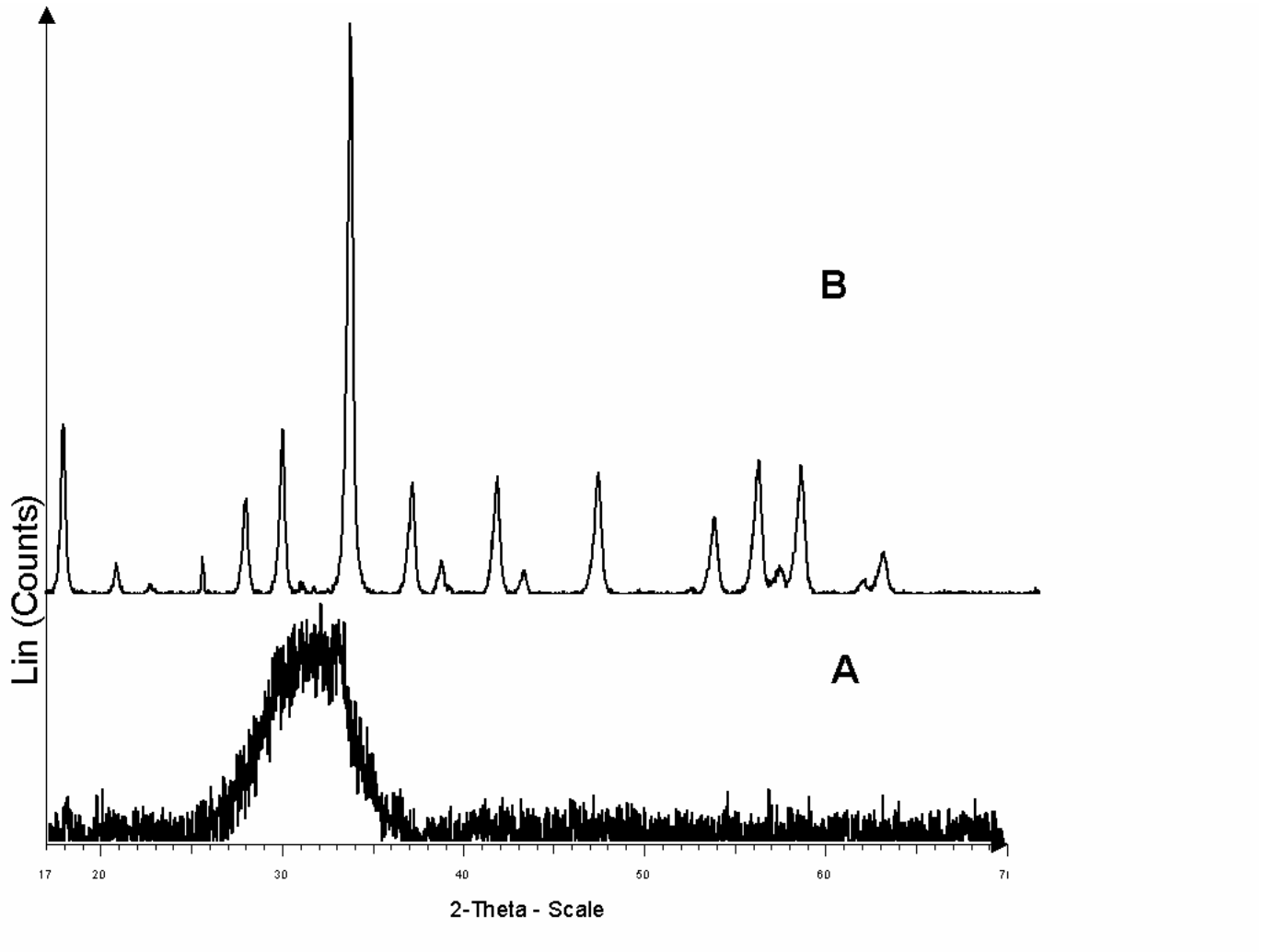

Figure 2-3: XRD Patterns for: A: 2 wt % agar YAG precursor sample fired at 700ºC and B: 30 wt % agar YAG precursor sample fired at 700ºC.

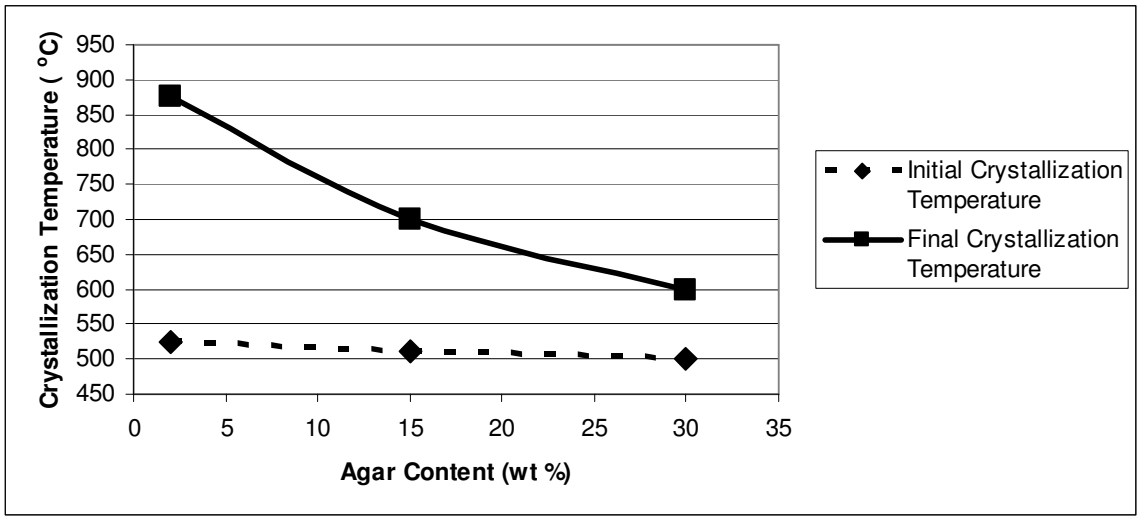

Figure 2-4: Linear trendlines for YAG agar precursor samples: Initial crystallization temperatures for: 2 wt % sample (525ºC), 15 wt % sample (510ºC), and 30 wt % sample (500ºC). Final crystallization temperatures for: 2 wt % sample (875ºC), 15 wt % sample (700ºC), and 30 wt % sample (600ºC).

to the unpurified 15 wt % agar YAG precursor sample heated to the same temperature (Figure 2-2B). Al-O vibrations are at 770 cm^{-1} and 690 cm^{-1} while a stretch at 569 cm^{-1} corresponds to Y-O vibrations [63].

Agarase Results:

After approximately 48 hours with occasional stirring the agarase and the sample, the gel was softer, but agar was still present. The agar must be bound tightly to the amorphous oxide solid so that is cannot be hydrolyzed by the agarase. Since neither the agarase approach nor the washing method was completely successful or necessary, the agar purification methods were abandoned.

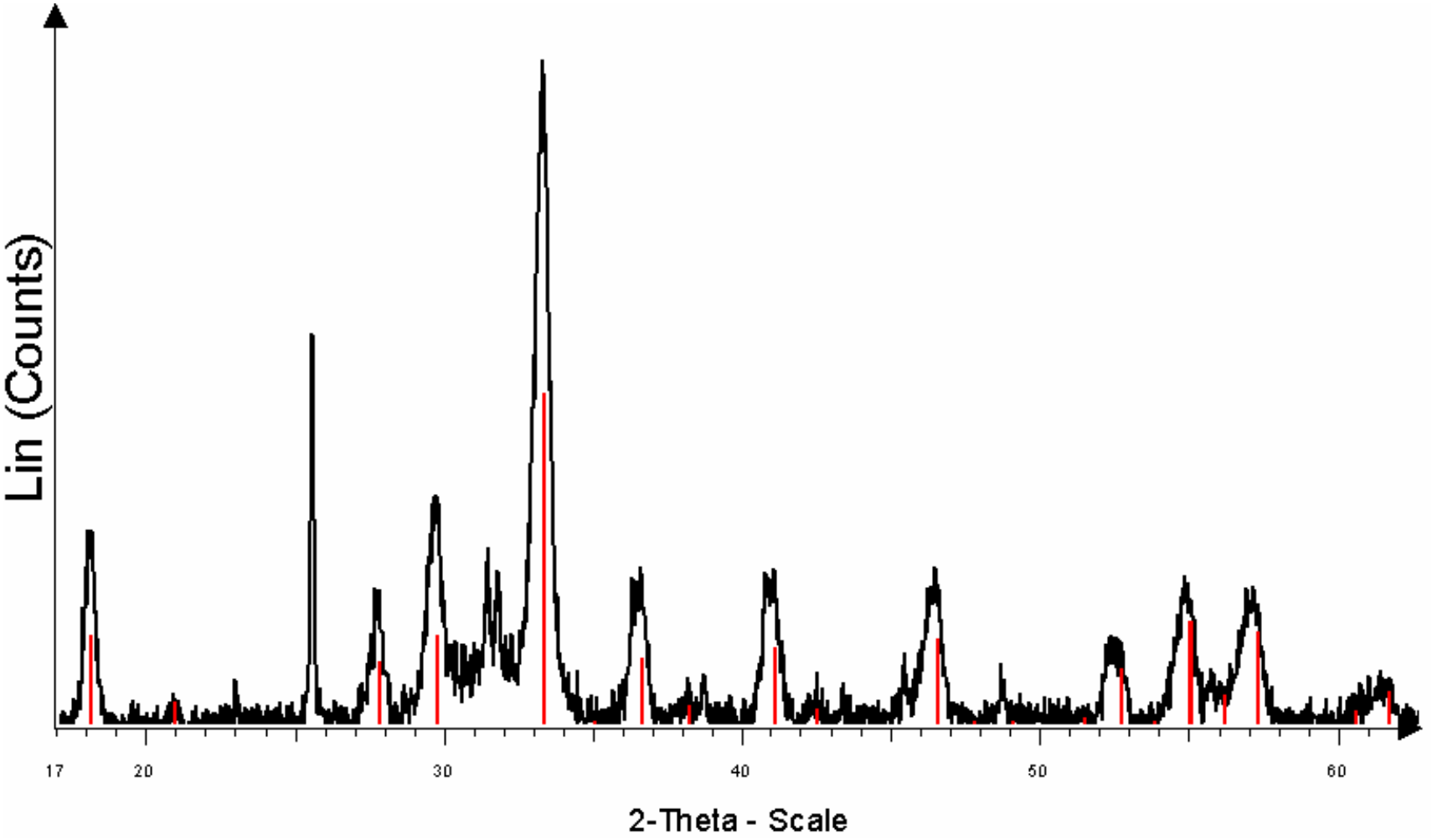

Figure 2-5: 30 wt % agar YAG precursor calcined at 600°C with $Y_3Al_5O_{12}$ identified. Peaks not labeled are from the impurity $CaSO_4$.

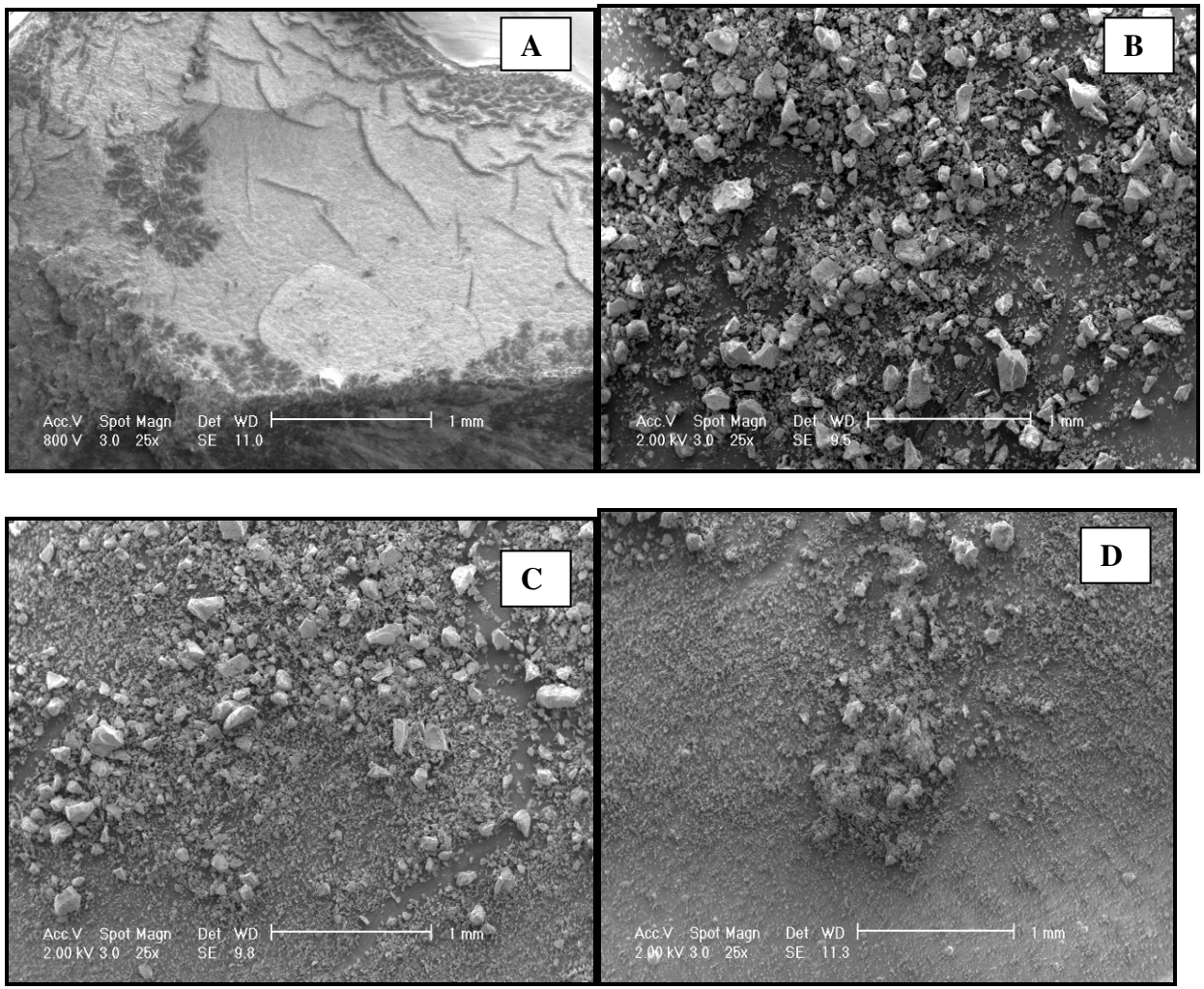

Figure 2-6: SEM images of A: 2 wt % agar YAG precursor gel, B: 2 wt % agar YAG powder calcined at 525ºC, C: 15 wt % agar YAG powder calcined at 510ºC, and D: 2 wt % agar YAG powder calcined at 800ºC.

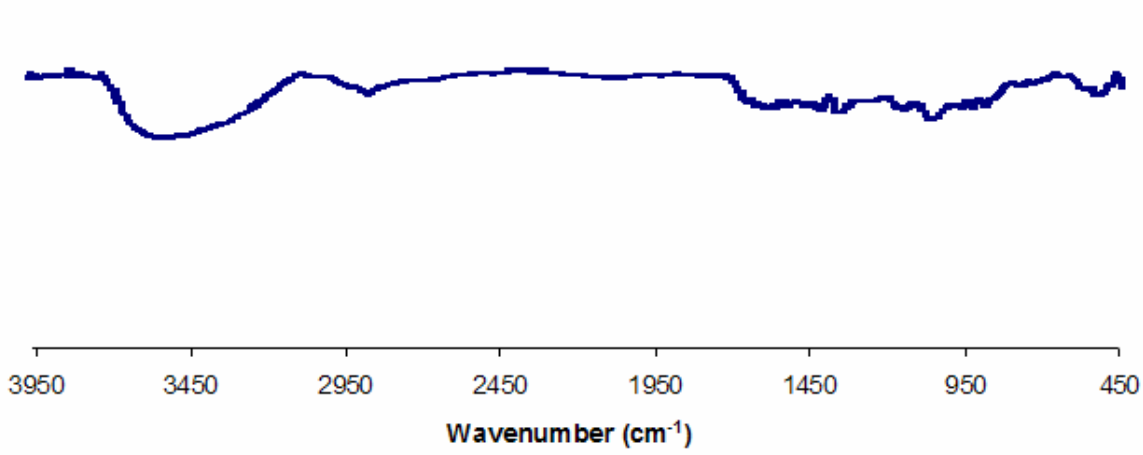

Figure 2-7: IR spectra of a purified YAG-agar precursor at 15 wt % agar fired at 510ºC.

Crystallization of Yttrium Aluminum Garnet (YAG) From Purified Gelatin

Precursors

Knox gelatin was purified and used for the synthesis of YAG precursors. The goal of this investigation was to see if having no impurities present affected the crystallization temperature of YAG.

Infrared Spectroscopy:

As the purified Knox gelatin precursor samples were heated, the gelatin was burned out as YAG crystallites began to form. Figure 2-8 shows the progression of a 6.4 wt % sample being heated from 400-900ºC. Bands due to water decreased as the sample was heated to higher temperatures (O-H stretching at 3500 cm^{-1} and O-H band at 1650 cm^{-1}) [60]. It seems the YAG formation is beginning once the sample is heated to 600ºC, and is complete at 900ºC where YAG stretches (789, 726, 567 cm^{-1}) are clearly apparent [66].

Powder X-Ray Diffraction (XRD):

Agar was tested as the gelling agent to determine whether it could result in formation of YAG at lower temperatures than gelatin. Even with purification, gelatin led to crystallization temperatures that were not as low as the precursors made with agar. Figure 2-9 shows a direct comparison of the results obtained with both gelling agents at a 30 wt % concentration. The oxide derived from gelatin was amorphous but that from agar was crystalline YAG. In fact, the gelatin YAG precursor had to be heated to 800ºC to yield pure crystalline YAG (Figure 2-10). Figure 2-11 demonstrates that samples made with agar as opposed to gelatin have a lower initial crystallization temperature.

The gelling agent allows for a homogeneous distribution of metal cations in each pore or "tiny beaker." Gelatin molecules are smaller than agar molecules. While an agar molecule is estimated to have a radius of 313 Å (molecular volume of 1.28×10^8 Å^3), a gelatin molecule has a radius of roughly 148 Å (molecular volume of 1.36×10^7 Å^3) [67]. Since agar has a larger molecular volume, the pores are smaller within the agar matrix. Smaller pores allows for quicker reactions between metal cations since there is less distance to cross. Another explanation centers around the molecular make-up of agar and gelatin. While agar is a polysaccharide (carbon, hydrogen, and oxygen atoms), gelatin is an amino acid (amine functional groups). It is quite possible that the gelatin weakly chelates to the metal ions slowing down reaction rates.

CONCLUSION

The sol-gello method used here to synthesize yttrium aluminum garnet (YAG) is simple and effective. Two different purification methods were used for the agar. The

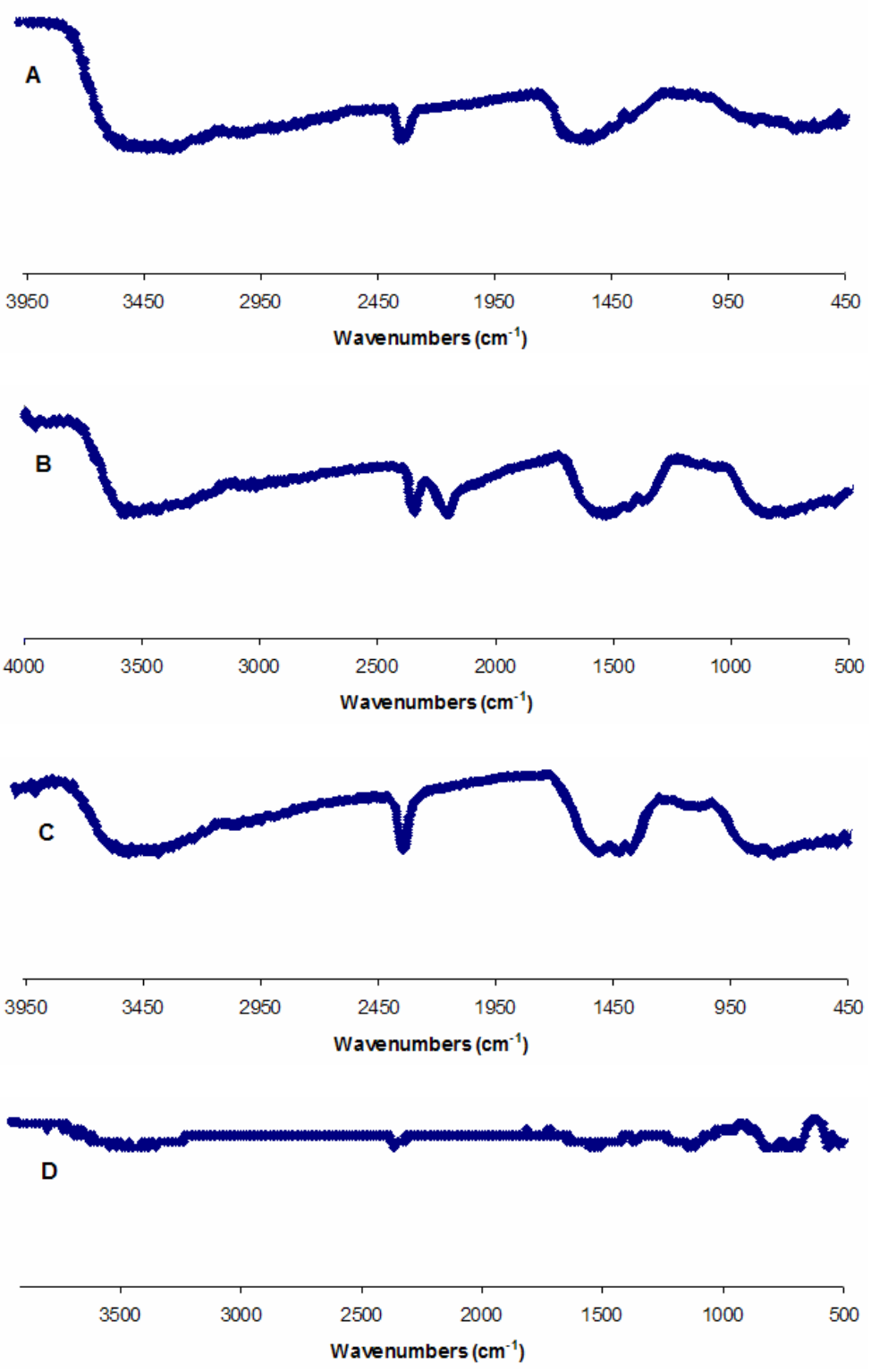

Figure 2-8: IR spectra of the YAG-purified gelatin precursors at A: 6.4 wt % gelatin fired at 400ºC; B: 6.4 wt % gelatin fired at 600ºC; C: 6.4 wt % gelatin fired at 700ºC; and D: 6.4 wt % gelatin fired at 900ºC.

washing method was not always effective and using agarase to dissolve the agar was also not successful. Since the impurities in the gelling agent do not effect YAG crystallization, unpurified agar was used and burned off as the samples are heated. Impurities such as calcium sulfate are innocuous when present with the YAG. Agar proved to be a more effective gelling agent than gelatin, and even purified gelatin. As agar content increases, the initial and final crystallization temperatures decrease. Nanocrystalline YAG was initially crystallized at 500ºC and only the YAG phase was present at the low temperature of 600ºC. To our knowledge, this is the lowest temperature that YAG has been synthesized without employing elevated pressures.

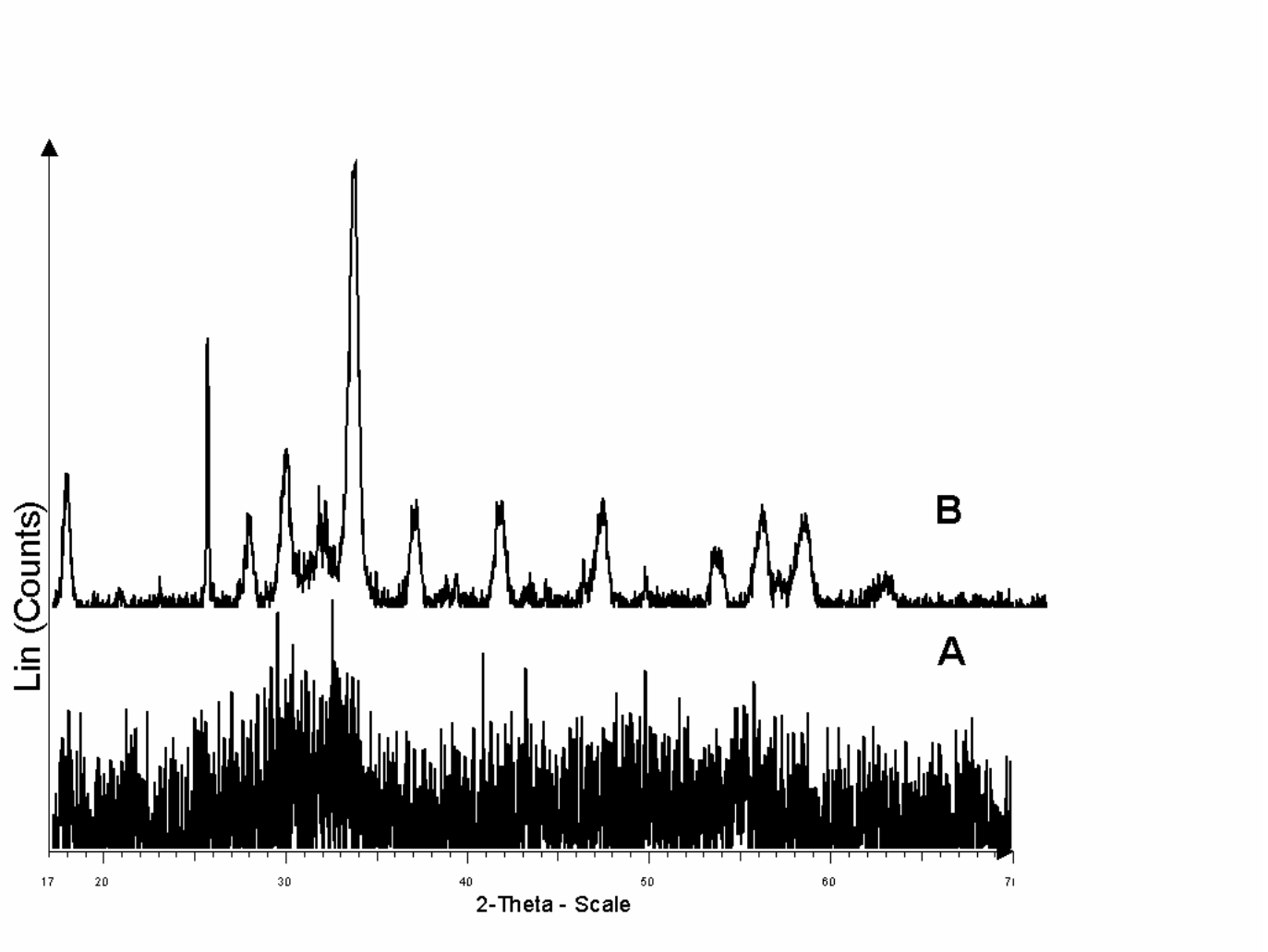

Figure 2-9: XRD Patterns for A: 32 wt % purified Knox gelatin YAG precursor sample fired at 600ºC and B: 30 wt % agar YAG precursor sample fired at 600ºC.

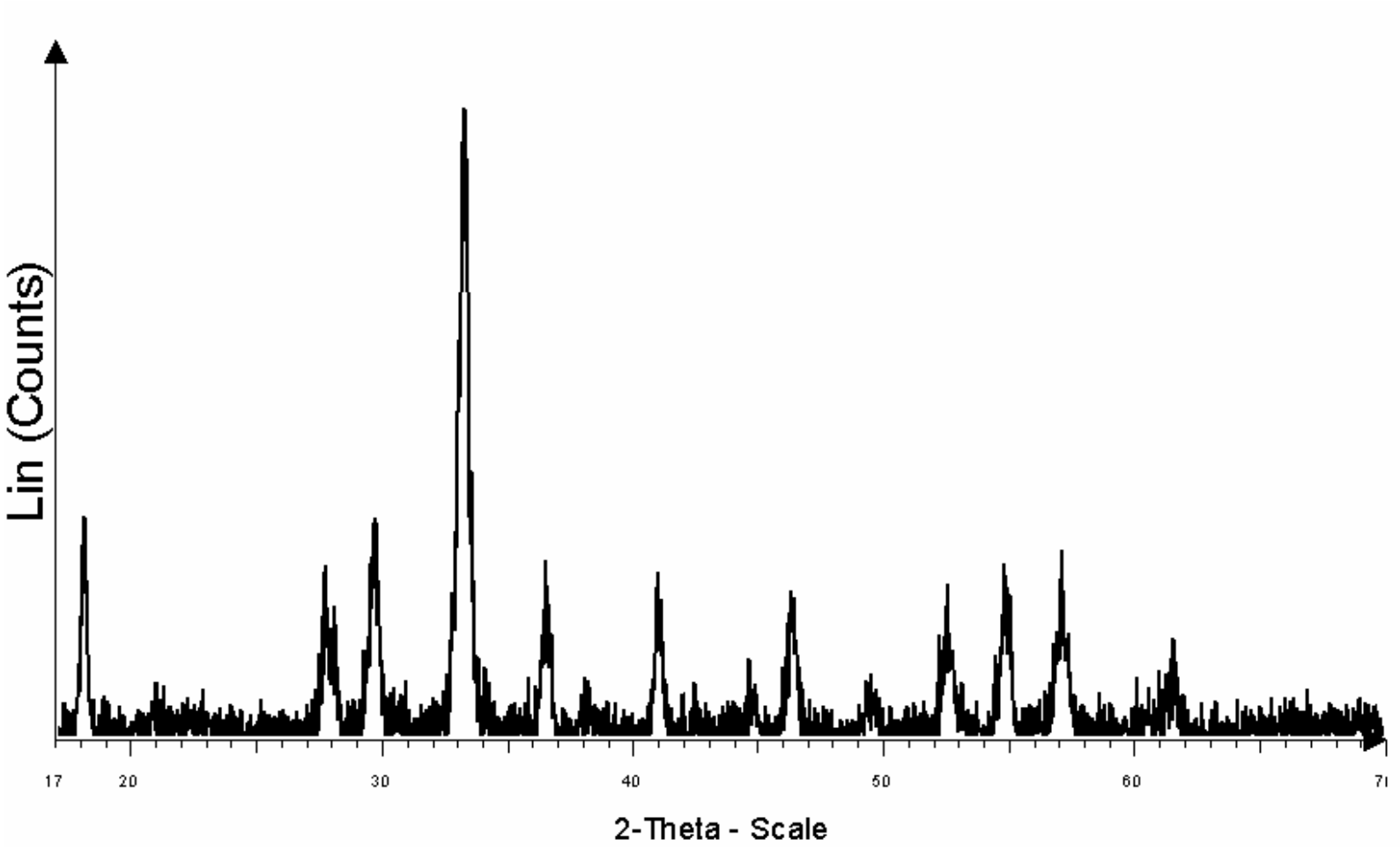

Figure 2-10: 30 wt % purified Knox Gelatin YAG precursor sample calcined at 800°C. Peaks correspond to $Y_3Al_5O_{12}$.

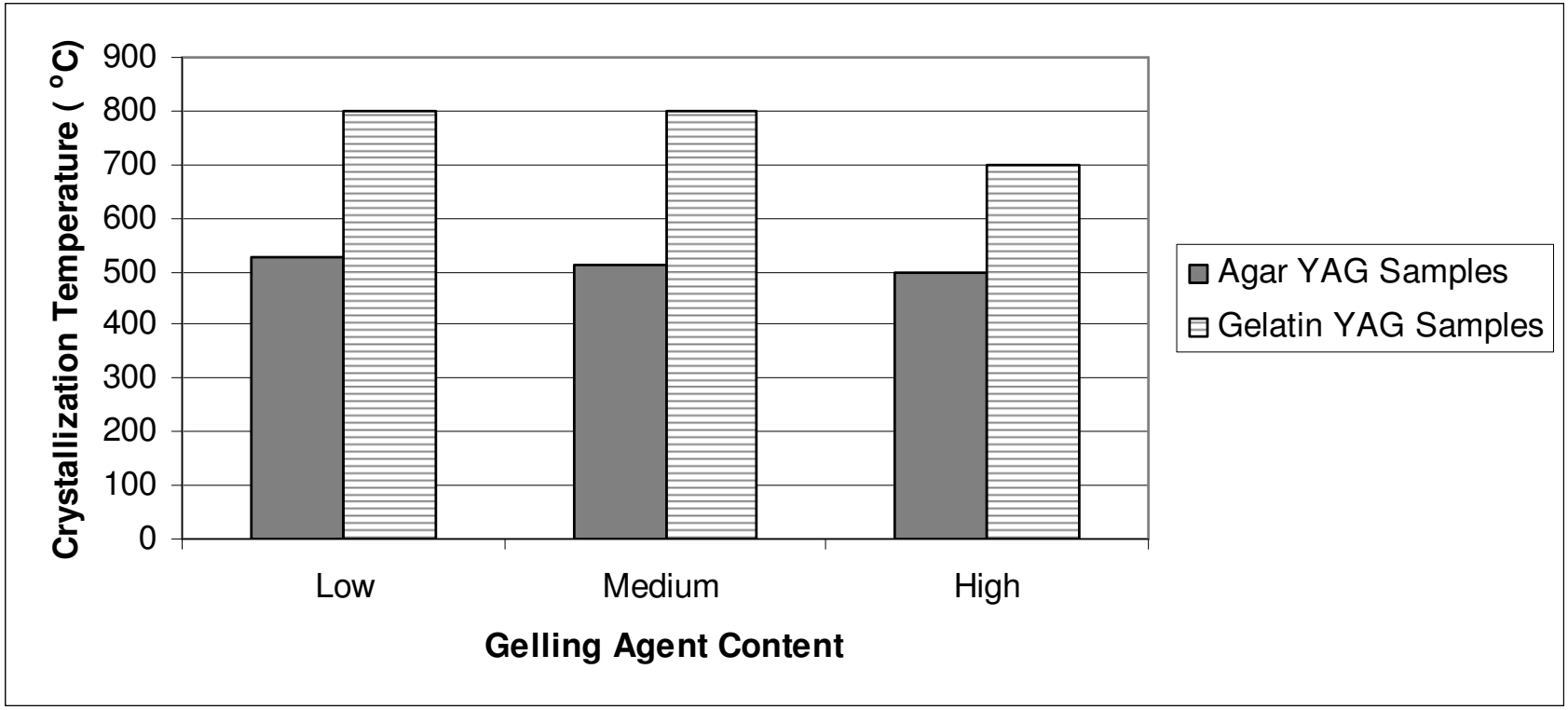

Figure 2-11: Initial crystallization temperatures for agar and gelatin YAG precursor samples. Agar: 2 wt % sample (525ºC), 15 wt % (510ºC), 30 wt % (500ºC). Gelatin: 6.4 wt % (800ºC), 19.2 wt % (800ºC), 32 wt % (700ºC).

CHAPTER III

SPINEL

INTRODUCTION

There are over 100 compounds with the spinel structure, and while some spinels are sulfides, selenides, and tellurides, most are oxides. The parent spinel has a close cubic packing arrangement of the anions and the structural formula AB_2O_4 [2]. One specific type of spinel ($MgAl_2O_4$) has been explored as an inorganic material made in a variety of different preparation methods due to its various applications. Spinel has a cubic structure that allows it to have isotropic expansion and high mechanical strength [32]. The most common application for spinel is as a refractory material. It can withstand 2135ºC temperatures so it is used in chrome-magnesite bricks [27] and as spinel bricks in electric and induction furnaces [26]. Another application is as an insulating material. Since spinel retains its strength and resists swelling in radiation, it can be used in fusion reactor cores [29]. Application as a catalyst support is another common use due to spinel's resistance to a reducing atmosphere [28]. For this purpose, it has been made with relatively high surface area of 96-160 m^2/g [68]. Spinel has also been investigated as an optical material since it has IR transparency in the 3-5 micron

range and is resistant to thermal shock. Compounds with those properties can have applications as materials for night vision, IR laser missile guidance, and IR security sensors [30]. Another possible application is as a humidity sensor. Spinel is also being explored as a material as such a sensor due to its open porosity [31].

Although spinel can be conventionally prepared via a solid state reaction [32], many other routes have been explored. Sol-gel methods are quite popular for the synthesis of spinel. For these methods, it seems that spinel is crystallized no lower than 600ºC. A citrate sol-gel process yielded an amorphous oxide phase that initially crystallized spinel at 600ºC with nanoparticles (~ 5 nm) [69]. Both an alkoxide approach and a traditional sol-gel method yielded spinel particles at that same temperature [70,71].

In our method, the sol-gello method is implemented to produce nanocrystalline spinel. The sol-gello method uses metal salt solutions and distribution of the metal ions throughout a gelatin matrix. The gelatin controls the purity and particle size of the spinel precursor. Once the precursor is heated, pure spinel can begin to crystallize at relatively low temperatures. The sol-gello method is a simple, quick way to make spinel.

EXPERIMENTAL

Chemicals:

The following chemicals were purchased and utilized without further purification: magnesium chloride hexahydrate [$MgCl_2 \cdot 6H_2O$, EMD]; aluminum chloride hexahydrate [$AlCl_3 \cdot 6H_2O$, Mallinckrodt]; gelatin [Knox]; gelatin [ICN]; agar [Sargent-Welch]; agarose (Low EEO Electrophoresis Grade) [Fisher Biotech]; HiPure Liquid Gelatin

("Fish Gelatin") (Norland); Photoengraving Glue Resist (Norland); aqueous ammonium hydroxide [NH_4OH, ACS Reagent, Pharmco].

The chemicals (Dowex and Knox gelatin) were purchased and purified. Cation Exchange 650C Dowex [Sigma-Aldrich] and Anion Exchange 550C Dowex [Aldrich] were rinsed with deionized water. Gelatin [Knox] was treated with the ion-exchange resins to rid the gelatin of impurities (NaCl, $Al_2(SO_4)_3$, and $CaSO_4$).

Preparation of $MgAl_2O_4$ (Spinel) Precursor Using Knox Gelatin:

A metal-chloride solution was made from 1 mmol (0.2 g) of magnesium chloride hexahydrate and 2 mmol (0.5 g) of aluminum chloride hexahydrate in 20 g of deionized water. 3.2 g of gelatin (Knox) was dissolved in 30 g of boiling deionized water. The metal salt solution was added to the hot gelatin solution with stirring. The total solvent mass was 50 g resulting in a 6.4 wt % gelatin solution. It was cooled to 10ºC until it formed a gel after approximately an hour. The gel was hydrolyzed with aqueous ammonium hydroxide at room temperature. Hydrolysis took place inside a closed ammonium hydroxide chamber. As hydrolysis occurred, the gel transforms from transparent light yellow into a transparent tan color. The time required for complete hydrolysis was typically about 72 hours. The higher the gelatin content, the longer hydrolysis took. After hydrolysis, the spinel precursor solid was removed from the chamber and dried in a fume hood at room temperature for approximately 24 hours, and then dried under vacuum overnight.

The same procedure was used to prepare samples with increasing gelatin contents: 12.8 wt %, 19.2 wt %, 25.6 wt %, and 32 wt %. The 12.8 wt % gelatin sample had 6.4 g of gelatin dissolved in 30 g of boiling deionized water. The 19.2 wt % gelatin sample

had 9.6 g of gelatin dissolved in 30 g of boiling deionized water while 12.8 g of gelatin was dissolved in 30 g of boiling deionized water for the 25.6 wt % gelatin sample. For the 12.8, 19.2, and 25.6 wt % gelatin samples, the metal chlorides solution [1 mmol (0.2 g) of magnesium chloride hexahydrate and 2 mmol (0.5 g) of aluminum chloride hexahydrate in 20 g of deionized water] was mixed into each gelatin solution. Each sample had a total solvent mass of 50 g. The 32 wt % gelatin sample was prepared by dissolving 16 g of gelatin in 40 g of boiling deionized water. The metal chlorides solution was prepared by dissolving 1 mmol (0.2 g) of magnesium chloride hexahydrate and 2 mmol (0.5 g) of aluminum chloride hexahydrate in 10 g of deionized water. Then the metal chlorides solution was mixed into the gelatin solution resulting in a total solvent mass of 50 g. After hydrolysis, with an increase of gelatin content, the color becomes less transparent.

Larger batch samples were prepared for the gelatin spinel precursors. The metal chlorides, gelatin, and water content were increased three times. For the 6.4 wt % gelatin sample, 9.6 g of gelatin was dissolved in 90 g of boiling deionized water. 3 mmol (0.6 g) of magnesium chloride hexahydrate and 6 mmol (1.5 g) of aluminum chloride hexahydrate was dissolved in 60 g of deionized water. The metal chlorides solution was mixed into the gelatin solution resulting in a total solvent mass of 150 g. Other samples were prepared in a similar fashion. The metal chlorides solution was prepared [3 mmol (0.6 g) of magnesium chloride hexahydrate and 6 mmol (1.5 g) of aluminum chloride hexahydrate dissolved in 60 g of deionized water] and stirred into the gelatin solution (29 g of gelatin dissolved in 90 g of boiling deionized water) resulting in a total solvent mass of 150 g (19 wt % gelatin sample). The high gelatin content of 25.6 wt % gelatin was

prepared by dissolving 38.4 g of gelatin in 90 g of boiling deionized water. 6 mmol (1.5 g) of aluminum chloride hexahydrate and 3 mmol (0.6 g) of magnesium chloride hexahydrate was dissolved in 60 g of deionized water. The metal chlorides solution was mixed into the gelatin solution (total solvent mass of 150 g). These larger-batch samples took approximately 24-72 hours longer to hydrolyze.

Preparation of $MgAl_2O_4$ (Spinel) Precursor Using Other Gelling Agents:

Other gelling agents were employed to make the spinel precursors as well. Norland's HiPure liquid gelatin ("fish gelatin") and photoengraving glue were explored as suitable gelling agents. Both substances are derived from fish skin which allows the gelatin to be liquid at room temperature. Because of the claim of higher purity, the liquid gelatin and glue were hopefully free of the salt impurities seen in Knox gelatin. The recommended 45 wt % liquid gelatin water solution (22.5 g of gelatin) was made along with an increased amount of liquid gelatin at 78 wt % (39 g of gelatin). As done with the precursor samples made with Knox gelatin, magnesium and aluminum chloride salts were added in a 1:2 molar ratio. 0.2 g magnesium chloride hexahydrate and 0.5 g of aluminum chloride hexahydrate was dissolved in 27.5 g of deionized water for the 45 wt % liquid gelatin sample and in 11 g of deionized water for the 78 wt % liquid gelatin sample. The metal chlorides solution was mixed into the liquid gelatin resulting in a total mass of 50 g. The mixtures were cooled to 10ºC where the sample became a solid. The gels were then placed inside ammonium hydroxide chambers and hydrolyzed at 10ºC. After approximately 6 days, the gels were removed from the chambers. Once gels reached room temperature, they became viscous liquids. Ammonia evaporated from the liquid mixtures in the fume hood with some stirring. The same procedure was used to make

spinel precursors with photoengraving glue resist (Norland). An 80 wt % glue solution with deionized water was utilized in this instance. Like the fish gelatin, the glue solution was liquid at room temperature and solid at 10ºC.

Laboratory-grade gelatin (ICN) was selected as another gelling agent to make the spinel precursors. 32 wt % solutions of gelatin and deionized water were made by heating so the gelatin would dissolve. The same chloride salts were used in the same molar ratio (1:2) to make the precursor gel. Once the gel was a solid at 10ºC, it was hydrolyzed with ammonium hydroxide at room temperature. Gels were dried in a fume hood and in a vacuum.

Agar and agarose were both investigated as alternative gelling agents as well. A 15 wt % solution of agar (Sargent-Welch) and deionized water was made with heating. Another water solution was made with Agarose Low EEO Electrophoresis Grade (Fisher Biotech) using an 8 wt %. Then the magnesium and aluminum chloride salts were added in a 1:2 molar ratio to each type of gel. The same hydrolysis and drying procedure was done as in the precursor preparation using ICN gelatin.

Purification of the Spinel Precursor:

Salt impurities in the gelatin (NaCl, $Al_2(SO_4)_3$, $CaSO_4$) interfered with spinel formation so purification techniques were employed. Initially, a facile washing method was used on the spinel precursors. After the precursor gel was calcined between 400-500ºC, the amorphous sample was mixed in deionized water on a rotary mill. Then the solution was centrifuged and the conductivity of the solution was recorded. The gelatin-salt-water solution was decanted. More water was added to the precipitate, mixed, centrifuged again, and followed by pouring off the supernatant. This step was repeated

until the conductivity reading dropped and leveled off to about 30 µS. Then the precipitate was dried with acetone, and the acetone was centrifuged off. This entire washing method usually lasted 24-48 hours. The precipitate was dried under vacuum.

Preparation of Spinel Precursor Using Purified Gelatin:

Since washing the spinel precursors was not effective in removing all the impurities, Knox gelatin was purified before being used as the gelling agent. A 5 wt % gelatin (Knox) solution was prepared. 10 mL of Dowex Cation and 20 mL of Dowex Anion ion-exchange resins were added to the gelatin solution. (10 mL of each type of ion-exchange resin was found to be effective and used in subsequent batches.) The gelatin solution was stirred at low heat, and the conductivity of the solution was monitored until there was a significant drop and leveling off. The Dowex resin was filtered out of the gelatin solution, and then the gelatin solution was dried under vacuum or in a dehydrator oven at approximately 50ºC.

Spinel precursor samples were prepared as before. A 6.4 wt % solution of gelatin was made by dissolving 3.2 g of purified gelatin in 30 g of boiling deionized water. A solution of 2 mmol (0.5 g) of aluminum chloride hexahydrate and 1 mmol (0.2 g) of magnesium chloride hexahydrate in 20 g of deionized water was made. The metal salt solution was stirred into the hot gelatin solution. There was a total mass of water of 50 g.

The resulting mixture was cooled to 10ºC until it became a transparent light yellow gel. Then the gel was placed inside an ammonium hydroxide chamber at room temperature. The ammonium hydroxide chamber was a closed container with aqueous ammonium hydroxide inside. Once hydrolysis was completed, the resulting transparent

solid was removed from the chamber and dried in a fume hood at room temperature, and then under vacuum. The same procedure was used to prepare samples from a 19 wt %, 22 wt % and 32 wt % purified gelatin solution.

Crystallization of Spinel:

The spinel precursor samples (using any gelling agent) were calcined to crystallize the sample into YAG. Heating was performed in an oven at temperatures ranging from 400 – 1000ºC.

Characterization:

The spinel precursors and spinel powders were characterized using X-ray powder diffraction (XRD), scanning electron microscopy (SEM), and the Brunauer-Emmett-Teller (BET) method. The XRD patterns of the powders were recorded with a Bruker AXS D-8 Advance X-ray powder diffractometer using copper K_α radiation at ambient temperature. The phases were identified with the ICDD database, and the crystallite sizes were calculated using the Pearson 7 model using Topas P version 1.01 software (Bruker Analytical X-Ray systems, Madison, WI 48, USA 1998). This software profiles the peaks and then the peaks of the standard. Then the Win-Crysize program (version 3.05 program, Bruker Analytical X-Ray systems, Madison, WI, USA, 1997) estimates crystallite size using the line broadening method and Scherer's equation. The Scherer's equation is:

$$C = \lambda k / \beta \cos(2\theta) \qquad \textbf{Eq. 3-1}$$

where λ is the wavelength of the radiation, k is the crystallite shape constant, β equals $(\beta_t^2 - \beta_o^2)^{1/2}$ (where β_t and β_o are the angular peak width measured at half of the maximum

intensity line for the measured and reference compounds, respectably), and θ is the maximum intensity peak angle.

Scanning electron microscopy was performed using a JEOL JXM 6400 SEM. The specific surface area for the samples were obtained using a Quantachrome Nova 1200 instrument and the conventional BET multilayer nitrogen adsorption method.

RESULTS AND DISCUSSION

Crystallization of Spinel from the Knox Gelatin Precursors:

The spinel precursors made from Knox gelatin began to crystallize at relatively low temperatures. Early in this study, the lowest initial crystallization temperature of spinel was 420ºC. To our knowledge, this is the lowest temperature where spinel begins to form. While many spinel syntheses call for initial crystallization temperatures of around 800ºC [34], there are a few groups that have achieved initial crystallization at 600ºC [69,71]. 420ºC is lower than both these temperatures. An example of initial spinel crystallization is shown in Figure 3-1.

From the beginning, it was apparent that as the gelatin content increased, spinel crystallization temperature decreased. Figure 3-2 demonstrates this relationship where 6.4 wt % and 32 wt % spinel precursor samples were both heated to 500ºC. Notice that the low gelatin content sample is still amorphous while the high gelatin content sample is beginning to form crystalline spinel. This relationship between gelatin content and crystallization temperature is discussed further when the purified gelatin is used. As expected, larger batch samples did not affect the crystallization temperature.

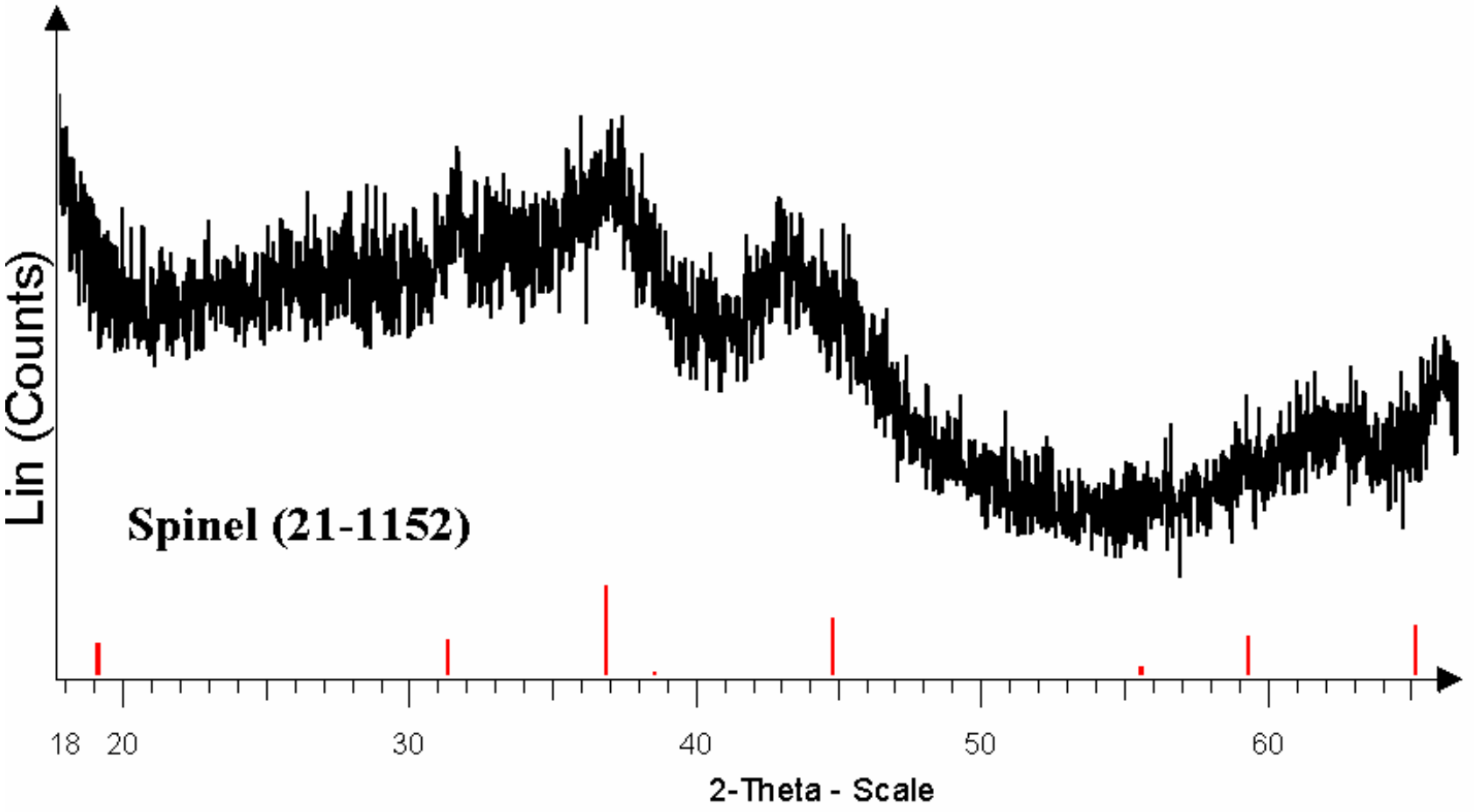

Figure 3-1: XRD pattern of 25.6 wt % Knox gelatin spinel precursor sample heated to 420°C. Spinel is beginning to crystallize.

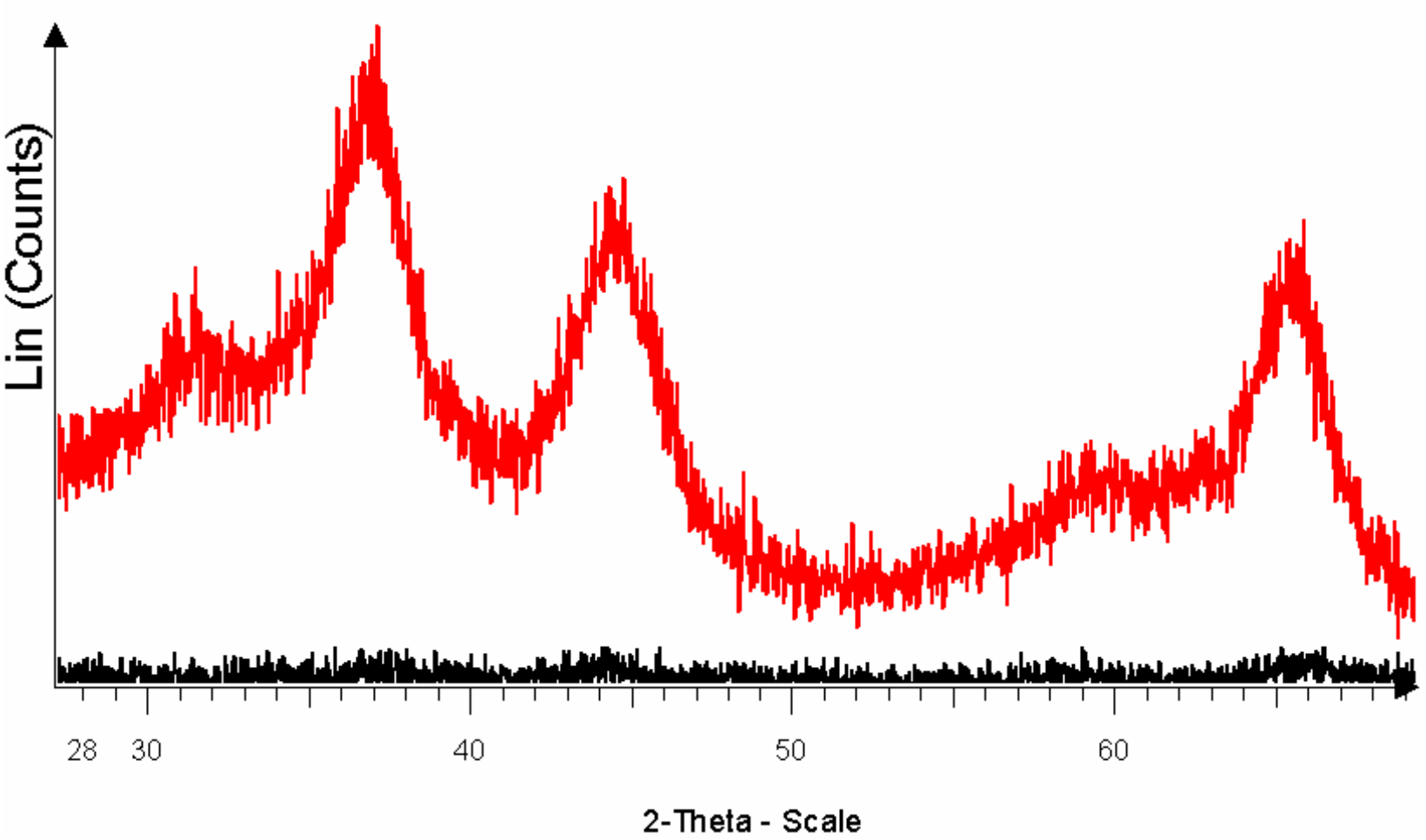

Figure 3-2: XRD pattern of two spinel Knox gelatin precursor samples heated to 500ºC. The bottom, amorphous pattern has the gelatin content of 6.4 wt %. The top pattern (32 gelatin wt %) shows spinel beginning to crystallize.

Many samples had impurities that were derived from the gelatin. These impurities included calcium sulfate and sodium chloride. While these impurities sublime out at higher temperatures, they cause the formation of undesired crystalline phases. Figure 3-3 shows the XRD patterns for a 32 wt % spinel sample. At 800ºC, the spinel phase is evident along with anhydrite calcium sulfate. At 1000ºC, the periclase (MgO) phase forms in addition to the spinel phase. The periclase phase likely forms when calcium sulfate decomposes to calcium oxide which subsequently reacts with the $MgAl_2O_4$ to give a slightly calcium-doped spinel and magnesium oxide.

Crystallization of Spinel from Precursors Made With Other Gelling Agents:

One way to rid the gelatin of the impurities was to wash the precursor samples. This method was extensively done for the YAG precursor samples and for a small group of the spinel precursor samples. The washings were not always effective, and it was cumbersome work. Since it was important to have a "purer" gelling agent, other gelling agents were explored.

Fish gelatin (Norland HiPure Liquid Gelatin) "is a specifically purified gelatin" and is "an alternative to regular gelatin" [72]. Because of these claims, it was explored as a gelling agent free of impurities. The spinel precursor samples made with fish gelatin had different results when heated. When heated to temperatures where spinel precursor samples made from Knox gelatin were beginning to crystallize (around 500ºC), the fish gelatin spinel precursor samples were still amorphous. At 700ºC, the samples made with the recommended 45 wt % fish gelatin content began crystallizing to spinel along with many other unidentified substances (Figure 3-4). The higher fish gelatin content (78 wt

%) and the photoengraving glue content never crystallized to spinel. Also, pure crystalline spinel was never obtained using fish gelatin.

Spinel precursor gels were made with three other gelling agents: laboratory-grade gelatin (ICN), electrophoresis-grade agarose (Fisher Biotech), and agar (Sargent-Welch). All the gelling agents had the same problem of having impurities such as sodium chloride and calcium sulfate. Spinel began to crystallize for the ICN gelatin and agar samples at a similar temperature (450-500ºC) as the samples made with Knox gelatin. Agarose samples began crystallizing spinel at 600ºC. All samples resulted in periclase forming at higher temperatures. Alternative gelling agents were abandoned for the synthesis of spinel.

Crystallization of Spinel From Purified Knox Gelatin Precursors:

Since a gelling agent that was pure enough could not be found, a method was developed to purify Knox gelatin. Once the gelatin was purified and dried, the gelatin was used to make spinel precursor gels. No impurities were detected at the lower calcinations temperatures. As the spinel crystallized at higher temperatures, no periclase phase ever formed (Figure 3-5). As long as the gelatin had been fully purified, spinel precursor gels made with different amounts of gelatin had only the spinel phase form. Figure 3-6 shows that with higher gelatin content, the spinel begins to crystallize at lower temperatures. These temperatures are similar to what was observed for samples using the unpurified Knox gelatin, except spinel crystallization began twenty degrees lower at 400ºC for the 19.2, 25.6, and 32 wt % gelatin samples. Figure 3-7 shows initial spinel crystallization XRD patterns for the 6.4, 12.8, and 32 wt % samples. There also seems to be a limit to how low the temperature can be to initialize spinel crystallization.

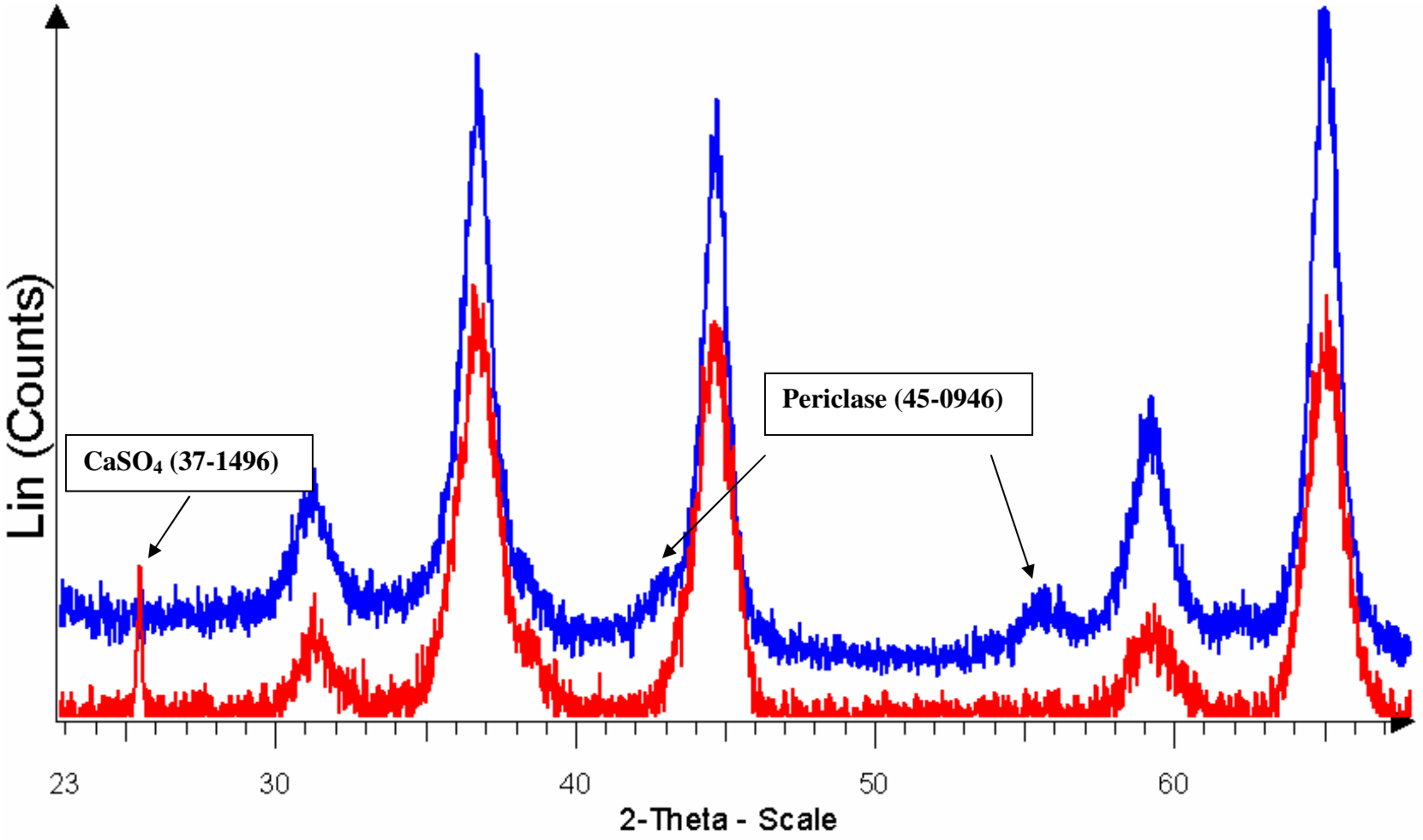

Figure 3-3: XRD patterns for a 32 wt % gelatin spinel sample. The gelatin impurity $CaSO_4$ is present with the spinel phase at the temperature of 800ºC (bottom pattern). At 1000ºC, while the impurity has sublimed out, both the periclase and spinel phases form (top pattern).

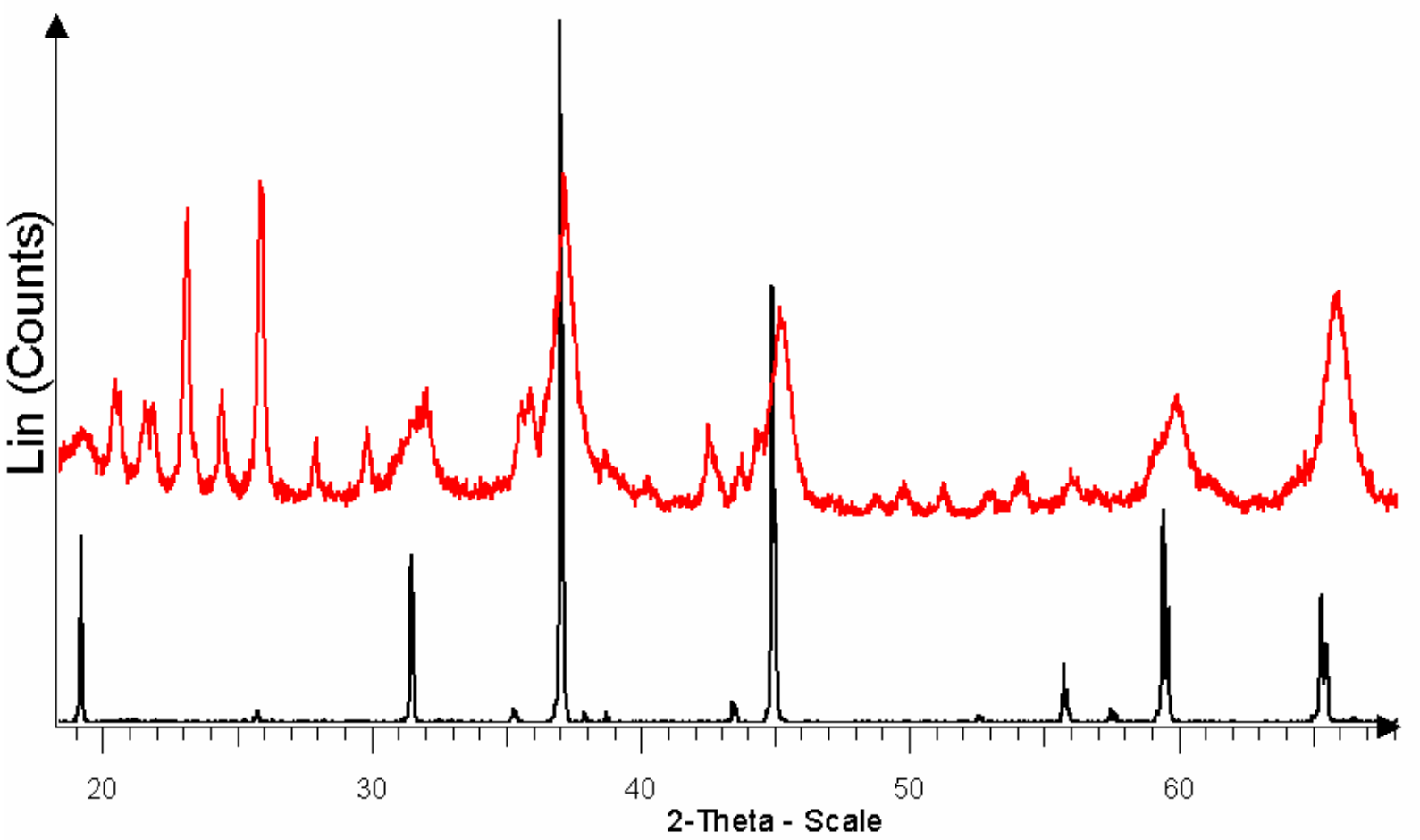

Figure 3-4: XRD patterns for spinel standard (bottom pattern) and spinel precursor samples made from 45 wt % fish gelatin (top pattern).

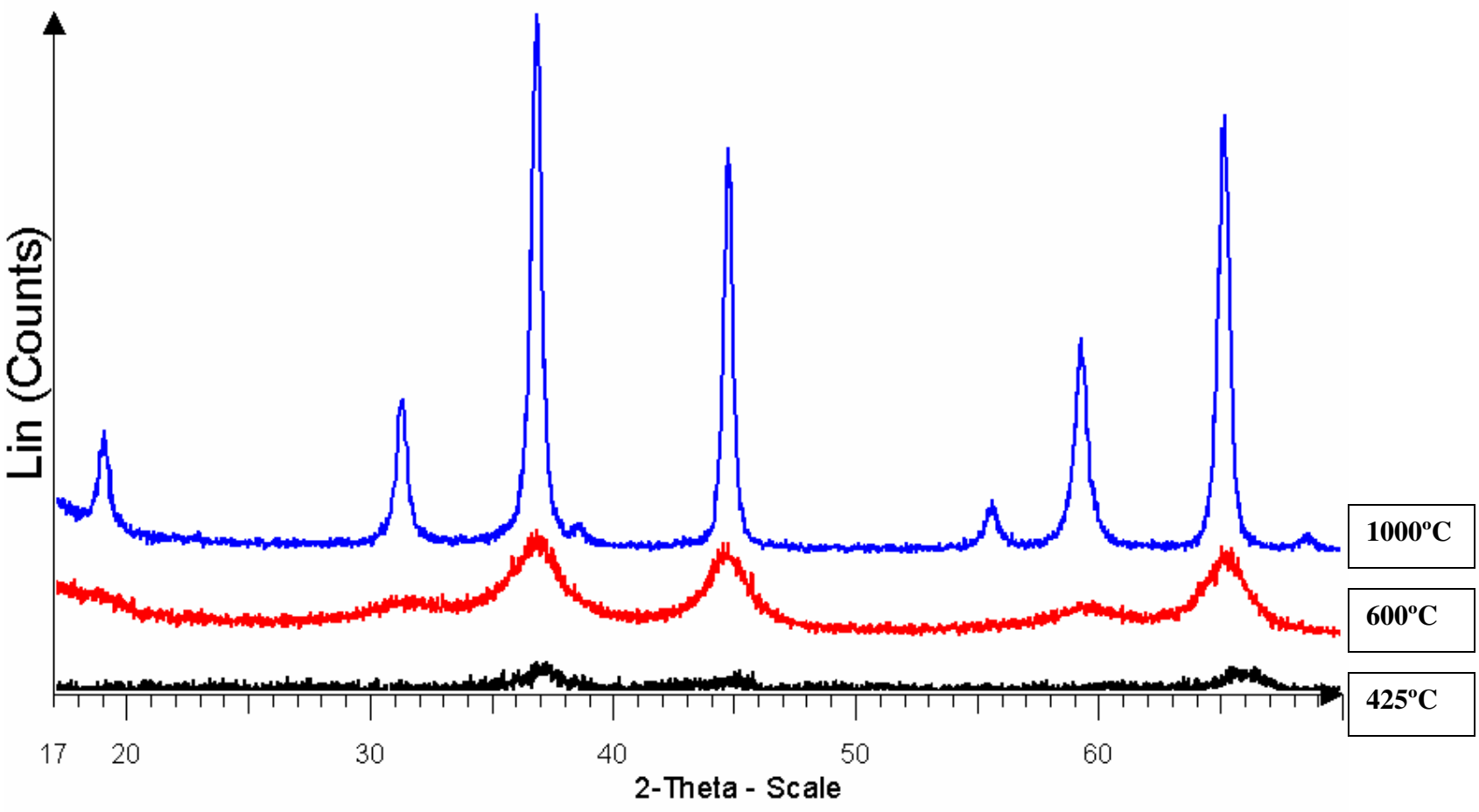

Figure 3-5: 12.8 wt % purified Knox gelatin spinel precursor samples heated to 425°C, 600°C, and 800°C. No impurities are detected. No periclase forms at 1000°C.

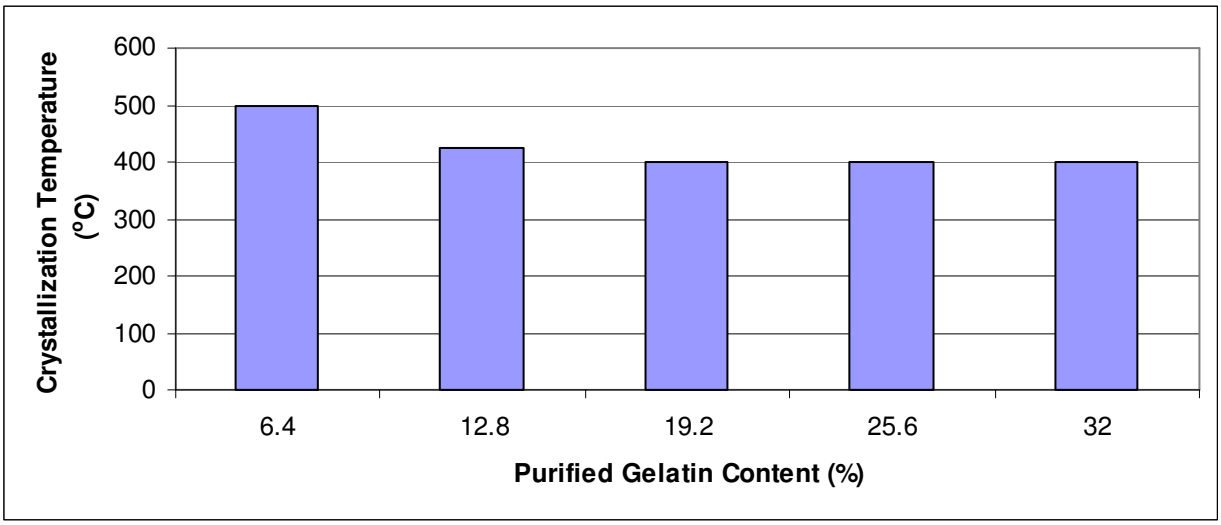

Figure 3-6: Initial crystallization temperature for spinel versus content of purified Knox gelatin.

Crystallite Size:

Crystallite sizes estimated from XRD patterns using the Scherrer's equation are summarized in Table 3-1. As the gelatin content of the precursor sample increases, the crystallite size of the spinel typically decreases. This expected trend is demonstrated with spinel samples that are heated to 500ºC, 600ºC, and 800ºC (Figure 3-8). The gelatin matrix of these precursor samples can be viewed as "mini beakers". These little beakers hold the metal salts where they are hydrolyzed. As the particles grow, the walls of the beakers control the size. As the gelatin content increases, there are more beakers, and the beakers are smaller. Hence, the particle size will be smaller when the samples are made with more gelatin. This trend is roughly followed with crystallite thicknesses with a small range of 1-4 nm.

Specific surface area for spinel samples were obtained using BET analysis then used to calculate the particle diameter. The equation,

$$d = 6 / [\rho S] \qquad \textbf{Eq. 3-2}$$

where d is the diameter, ρ is the density of spinel, and S is the specific surface area of the spinel powder was used. The theoretical density of spinel is 3.60 g/cm^3. Table 3-2 lists some of the surface area values along with the calculated particle diameters for low, medium, and high purified gelatin content spinel samples. Spinel powders at the lower temperatures have high surface areas, appropriate for some catalytic applications [68]*)*. The spinel powders formed at 700ºC have surface areas high enough to be used for catalysis. As expected, the surface areas decrease as the sample is heated to higher temperature because the particles are growing larger. As the gelatin content increased, the surface area roughly increased. Sometimes samples were ground between calcinations. This can aid in achieving smaller particle sizes [1]. Samples were most likely not ground adequately for the particle sizes that did not follow the trend.

SEM images show that the spinel powder is made up of particles that are not uniform in shape or size (Figure 3-9). Many of the particles are rounded and appear flat relative to their diameters. The synthesized spinel is similar in morphology to the spinel standard.

CONCLUSION

Spinel can be synthesized using the sol-gello process, but purification of Knox gelatin is necessary to make pure spinel. This is because impurities in the gelling agent interfere with pure spinel formation. The initial crystallization temperature (400-420ºC) is the lowest achieved for spinel so far. Spinel particles have nanoscaled thicknesses with some agglomeration present.

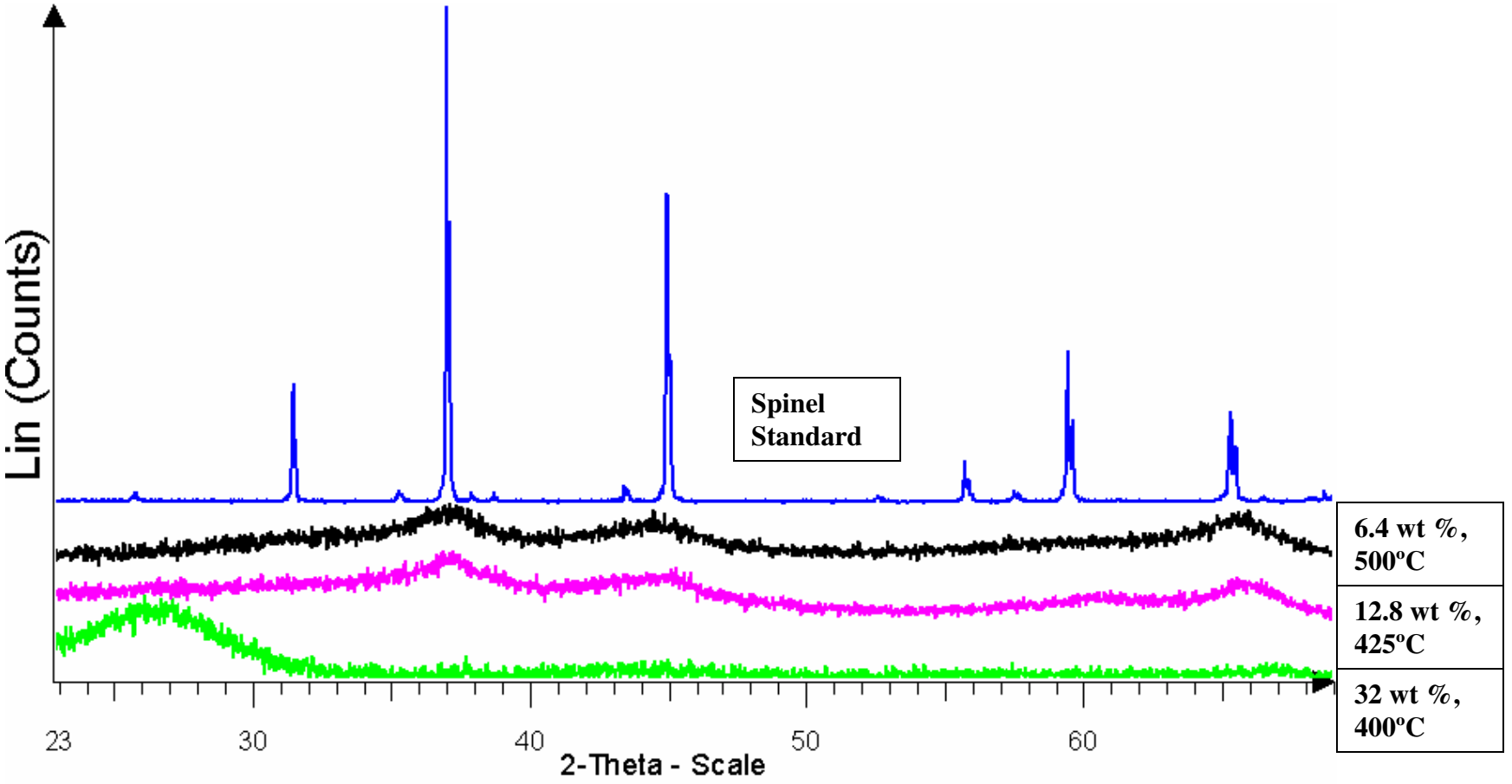

Figure 3-7: XRD patterns of initial crystallization of spinel. Samples include: spinel standard, 6.4 wt % purified Knox gelatin sample fired at 500ºC, 12.8 wt % purified Knox gelatin sample fired at 425ºC, 32 wt % purified Knox gelatin sample fired at 400ºC.

Gelatin Content (%)	Calcination Temperature (ºC)	Crystallite Thickness (nm)*	Gelatin Content (%)	Calcination Temperature (ºC)	Crystallite Thickness (nm)*
6.4	500	2.5	25.6	500	1.3
6.4	800	3.8	25.6	600	1.5
6.4	1000	4.5	25.6	800	1.2
12.8	425	0.8	25.6	1000	4.1
12.8	500	2.0	32	500	1.7
12.8	600	1.7	32	600	2.1
12.8	800	1.5	32	800	0.9
12.8	1000	4.3	32	900	4.0
19.2	500	2.0	32	1000	3.8
19.2	600	2.0	32	1100	4.2
19.2	800	3.5			
19.2	1000	5.2			

Table 3-1: Spinel samples of different Knox gelatin contents calcined at different temperatures.
***Crystallite Thickness is estimated from XRD patterns.**

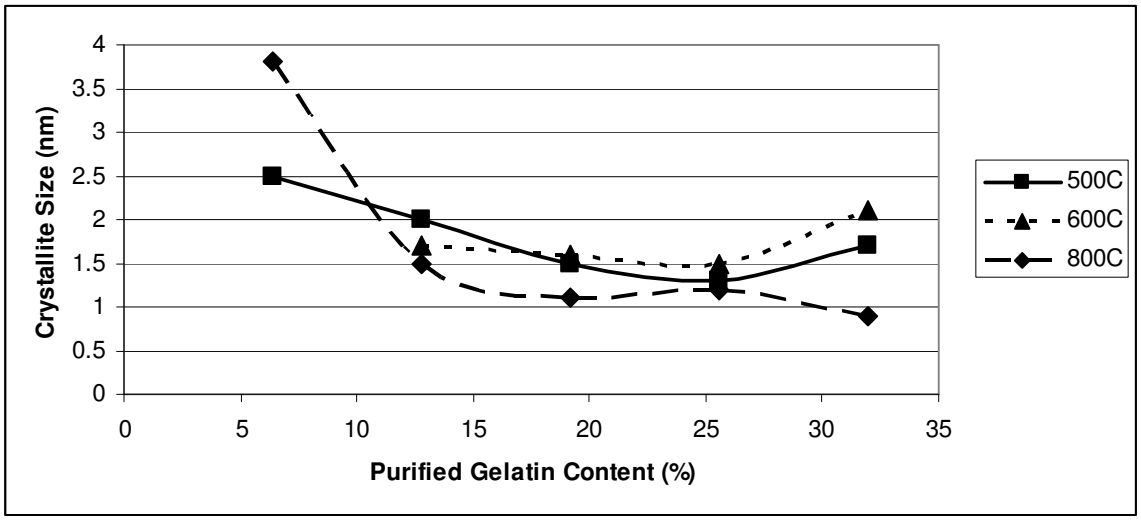

Figure 3-8: Crystallite samples of spinel calcined at 500ºC, 600ºC, and 800ºC with increasing gelatin content.

Gelatin Content (%)	Calcination Temperature (°C)	Specific Surface Area (m^2/g)	Diameter (nm)*
6.4	700	162.7	10.2
6.4	1000	49.89	33.4
19.2	700	97.11	17.2
19.2	1000	42.93	38.8
25.6	700	168.1	9.92
25.6	1100	17.32	96.2

Table 3-2: Specific surface area and particle diameter values for different gelatin content spinel samples calcined at different temperatures.
***Diameter was calculated from the specific surface area values. See text for details.**

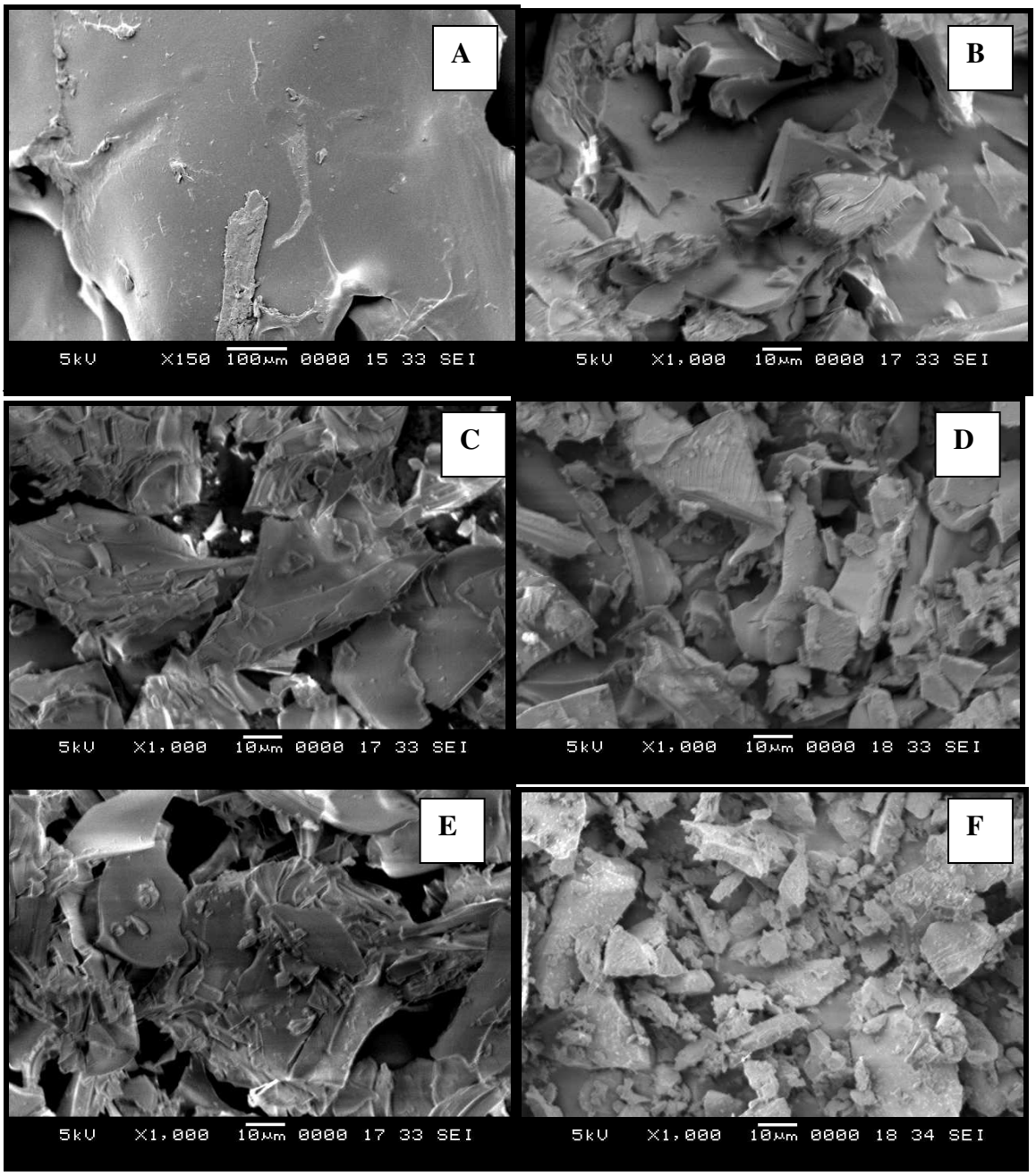

Figure 3-9: SEM images of purified gelatin spinel samples calcined at different temperatures. (A) 19.2 wt % spinel precursor gel at room temperature, (B) 25.6 wt % at 600ºC, (C) 25.6 wt % at 800ºC, (D) 19.2 wt % at 800ºC, (E) 25.6 wt % at 1000ºC, and (F) Spinel Standard.

CHAPTER IV

HYDROXYAPATITE

INTRODUCTION

Bone is a composite material made up of soft protein and collagen and the hard mineral hydroxyapatite [40]. The mineral component of bone, hydroxyapatite, provides the compressive strength. Bone has nanocrystals of hydroxyapatite with dimensions of 4 nm x 50 nm x 50 nm. Both dental enamel and dentin are comprised of hydroxyapatite as well [73]. Hydroxyapatite is a bioceramic material that has been extensively explored due to its successful applications for bone implants and cements. It serves as such an attractive implant material due to its bioactivity that allows the mineral to bond to both the surrounding bone and tissue [42]. Nano-sized hydroxyapatite is a subject of great interest because of the properties that hydroxyapatite nanocrystals hold including an increase in mechanical strength and better osteointegrative ability [52]. Osteointegrative ability is reflected in the osteoblast and osteoclast activity on nano-hydroxyapatite compared to conventional hydroxyapatite [74,75]. Another important aspect of hydroxyapatite is its open porosity which allows for it to have an osteophillic surface where bone and tissue can easily grow into the implanted hydroxyapatite [76].

Hydroxyapatite is a brittle and often weak material so it is usually implemented in non-load bearing applications or as a coating for implants [77]. Often, hydroxyapatite is combined with another material to either improve biocompatibility, strength, and/or flexibility.

Hydroxyapatite follows the general apatite formula of $Ca_5(PO_4)_3X$ with X as an hydroxide ion. The crystal structure has phosphate ions making up the tetrahedral skeleton [51]. Calcium and hydroxide ions are ordered around the phosphate frame. This hexagonal structure can be complicated with Ca/P molar ratios ranging from 1.5-1.67 [47]. The Ca/P molar ratio in natural hydroxyapatite varies due to its location in the body and the age of the bone [51]. The ratio tends to be smaller in younger, more metabolically active bones.

There are several methods that have proven effective in preparing hydroxyapatite, including wet, dry, hydrothermal, and alkoxide routes [78]. The wet method involves using either an acid-base solution reaction or a calcium and phosphate salts reaction [79]. A common acid-base combination is calcium hydroxide and phosphoric acid. The alkoxide method is a type of wet preparation. Dibasic ammonium phosphate and calcium ethoxide can be used as the reactants. Calcium ethoxide has also been used with phosphoric acid in forming hydroxyapatite [80].

The dry technique is simply a solid state reaction between a calcium phosphate compound and calcium carbonate or calcium hydroxide [81,82]. High temperatures (600-1250ºC) are needed to form hydroxyapatite. Hydroxyapatite whiskers have successfully been made using a hydrothermal route [83]. Calcium nitrate and dibasic ammonium phosphate were mixed with urea under hydrothermal conditions. Urea was

used as a homogeneous precipitation agent. A relatively low temperature of 90ºC was used in this method.

Sol-gel chemistry has been used to form nano-hydroxyapatite [84]. A sol solution of triethyl phosphate and calcium nitrate was mixed and hydrolyzed. Increasing the sol temperature and aging time resulted in purer hydroxyapatite samples. The hydroxyapatite crystallite size ranged from 40-100 nm. Another sol-gel method involving triethyl phosphite and calcium nitrate resulted in particles slightly larger (200-300 nm) [85]. Both methods involved heating up to 350-400ºC to acquire hydroxyapatite crystallization.

In this study, nano-hydroxyapatite is crystallized at room temperature using the sol-gello process. Phosphoric acid and calcium chloride are mixed in gelatin, and the resulting gello is placed in an ammonium hydroxide chamber. Phosphoric acid and ammonium hydroxide react followed by a reaction between the calcium and phosphate ions. The hydroxyapatite can be separated from the gello.

EXPERIMENTAL

Chemicals:

The chemicals listed below were purchased and employed without further purification: calcium chloride hexahydrate [$CaCl_2 \cdot 6H_2O$, Fisher]; phosphoric acid [H_3PO_4, Aldrich]; gelatin [Knox]; aqueous ammonium hydroxide [NH_4OH, ACS Reagent, Pharmco]; trypsin.

Preparation of Hydroxyapatite:

Ammonia is used to facilitate the reaction between phosphate and calcium ions resulting in nanocrystalline hydroxyapatite within the gelatin matrix at room temperature. Hydroxyapatite was synthesized by reacting phosphoric acid and ammonium hydroxide (Eq. 4-1) followed by a reaction between calcium ions and phosphate (Eq. 4-2).

$$H_3PO_4 + 3\ NH_4OH \rightarrow (NH_4)_3PO_4 + 3\ H_2O \qquad \textbf{(Eq. 4-1)}$$

$$10\ CaCl_2 \cdot 6\ H_2O + 6\ (NH_4)_3PO_4 + 2\ NH_4OH \rightarrow$$

$$Ca_{10}(PO_4)_6(OH)_2 + 20\ NH_4Cl + 60\ H_2O \qquad \textbf{(Eq. 4-2)}$$

Twenty mmol (4 g) of $CaCl_2 \cdot 6H_2O$ was dissolved in 10 g of deionized water. An excess amount [46 mmol (4.5 g)] of phosphoric acid was added to the calcium chloride solution and stirred. 7.2 g of gelatin was dissolved in 50 g of boiling deionized water (14.4 wt % solution). The calcium chloride-phosphoric acid solution was stirred into the gelatin solution. The mixture was cooled to 10ºC where the mixture sets into a "gello." A firm gello typically results after approximately two hours. Then the gello was placed inside an ammonium hydroxide chamber at 10ºC for about 72 hours. The reactions were complete once the gello changed from light yellow to white. The gel was air-dried in the fume hood where the ammonia can evaporate.

Variables in the preparation process included gelatin amount, reaction temperature, and reactants amounts. Varying amounts of gelatin were used to make other hydroxyapatite samples. Gelatin solutions included 6.4 wt % and 19.2 wt %. The reactions do not require the gello in the ammonium hydroxide chamber to be at 10ºC so other samples were made at room temperature. The typical 10:6 mole ratio of $CaCl_2 \cdot 6H_2O$ and H_3PO_4 was also used to prepare hydroxyapatite.

Sample Purification Methods

The gelatin needed to be separated from the product in order for the latter to be fully characterized. Trypsin was explored as a method to remove the gelatin. Once the reactions were completed, the gello was removed from the ammonium hydroxide chamber and put in the fume hood. The gello was rinsed with water and then the pH of the water was taken. The water was poured off of the gello. Since, trypsin has an optimal pH range of 7 – 9 [86], the gello was washed with water until the pH was approximately 8. Then 0.4 g of trypsin was added to the gello.

Another method to separate the gelatin from the hydroxyapatite was a simple washing method. Gelatin was removed from the samples by dissolving the gellos in hot water. After centrifuging, the gelatin solution was poured off leaving the product as a white powder. After at least three washings, the hydroxyapatite was rinsed with acetone removing the water from the product. The product was dried under vacuum.

Crystallization:

The hydroxyapatite samples were heated to 670ºC to dehydrate them and crystallize other calcium phosphate phases. The heating took place under air for approximately 10 hours.

Characterization:

The hydroxyapatite and calcium phosphate powders were characterized using thermogravimetric analysis, X-ray powder diffraction (XRD), infrared spectroscopy (IR), scanning electron microscopy (SEM). Thermogravimetric analysis was performed on a Seiko ExStar 6500 TGA/DTA instrument. A Bruker AXS D-8 Advance X-ray powder diffractometer was used to record the XRD patterns of the powders using copper K_α

radiation at ambient temperature. The phases were identified with the ICDD database. The Pearson 7 model using Topas P version 1.01 software (Bruker Analytical X-ray systems, Madison, WI 48, USA 1998) was used to calculate the crystallite sizes. This software profiles the samples peak along with the standard peaks, and then the WinCrysize program (version 3.05 program, Bruker Analytical X-ray systems, Madison, WI, USA, 1997) uses the line broadening method and Scherer's equation to estimate the crystallite size. The Scherer's equation is:

$$C = \lambda k / \beta \cos(2\theta) \qquad \textbf{(Eq. 4-3)}$$

where λ is the wavelength of the radiation, k is the crystallite shape constant, β equals $(\beta_t^2 - \beta_o^2)^{1/2}$ (where β_t and β_o are the angular peak width measured at half of the maximum intensity line for the measured and reference compounds, respectably), and θ is the maximum intensity peak angle.

A Nicolet Magna-IR 75 spectrometer was used to collect infrared spectra in the 4000-400 cm^{-1} region by diluting the sample powders with potassium bromide. Scanning Electron Microscopy was done using a JEOL JXM 6400 SEM.

RESULTS AND DISCUSSION

Preparation of Hydroxyapatite at Room Temperature

Once the gello was prepared and dried, thermogravimetric analysis (TGA) was carried out on a small portion. Figure 4-1 shows the TGA profile for the 14.4 wt % gelatin hydroxyapatite sample. Once the water is evaporated, the ammonium chloride sublimes out, and the gelatin is then burned away. The hydroxyapatite dehydrates and eventually separates into other calcium phosphate phases by 670ºC.

Characterization

White powder was separated from the gelatin by washing away the water and drying the product. It was identified as hydroxyapatite using infrared spectroscopy (IR) and powder X-ray diffraction (XRD). The product powder was identified as hydroxyapatite (ICCD 09-0346) according to XRD (Figure 4-1). The widths of the peaks

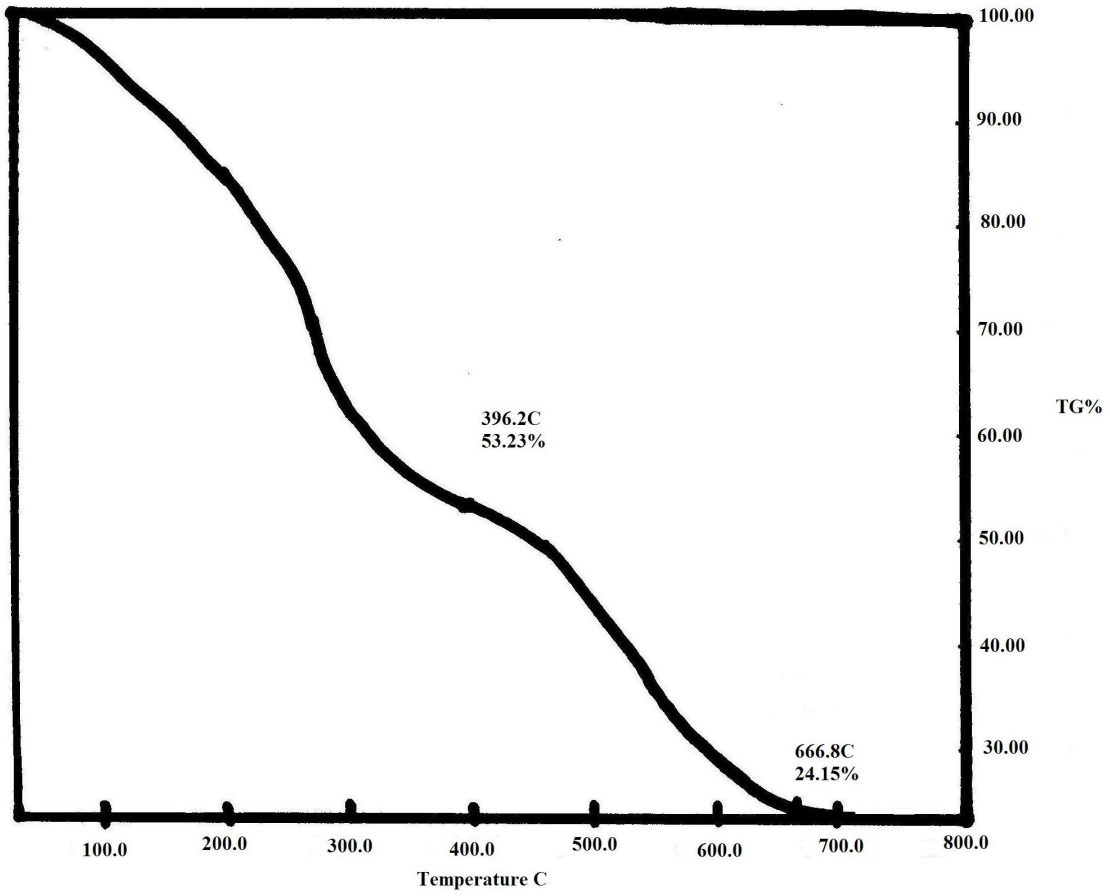

Figure 4-1: Thermal gravimetric analysis trace of 14.4 wt % gelatin hydroxyapatite sample.

suggest that the material is nanocrystalline. This was confirmed using Scherrer's equation that gave an estimated crystalline thickness of approximately 2.5 nm for the 14.4 wt % gelatin-hydroxyapatite sample. Other samples made with 6.4 and 19.2 wt %

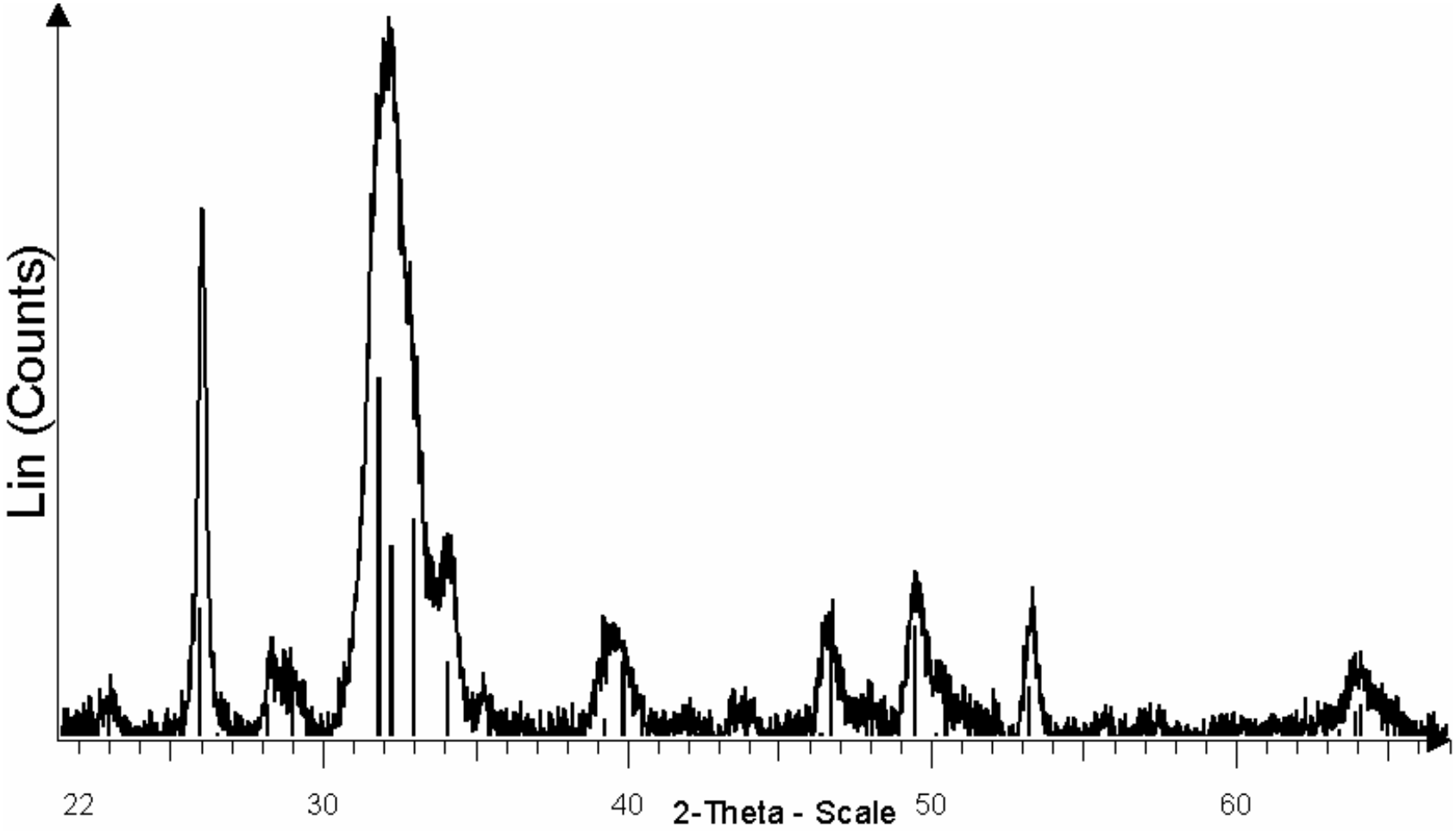

Figure 4-2: XRD pattern for the product isolated from the gello acquired at room temperature. Identified as hydroxyapatite.

gelatin solutions also had pure hydroxyapatite powder at room temperature. While the 19.2 wt % gelatin-hydroxyapatite sample was nanocrystalline, the 6.4 wt % gelatin-hydroxyapatite sample was not. For the low gelatin content samples, the walls of the gelatin matrix are further apart allowing the hydroxyapatite crystals a large area to grow.

Figure 4-3 shows the infrared spectrum of the sample at room temperature. The broad peak at 3400 cm^{-1} is most likely absorbed water in the hydroxyapatite [54]. Other bands can be attributed to hydroxyapatite [54,83]. Due to the broad water peak, the hydroxyapatite hydroxyl group stretching at 3570 cm^{-1} cannot be seen. The asymmetric stretching of PO_4^{3-} leads to bands at 1100, 1070, and 1030 cm^{-1}. Symmetric stretching of the P-O bond is seen at 860 cm^{-1}. Bands at 560 and 600 cm^{-1} can be attributed to bending of the O-P-O bond. Some gelatin might still be present in the sample since bands characteristic of gelatin are still present (amide N-H bond at 1650, 1540, and 1200 cm^{-1}).

SEM images were taken of the gello dried at room temperature without separation of gelatin. As seen in Figure 4-4, the samples are agglomerates of hydroxyapatite-gelatin nanocomposite. This combination is similar to bone. The gelatin part of the composite is soft like protein and collagen while the hydroxyapatite is the source of mechanical strength.

Purification Methods

Attempts to remove the gelatin from the samples with trypsin were not successful. The trypsin-gello mixture was stirred occasionally for several days. After ten days, it appeared that most of the gelatin was dissolved. The white solid material was washed with water. After centrifuging, the water was decanted. This was repeated three times.

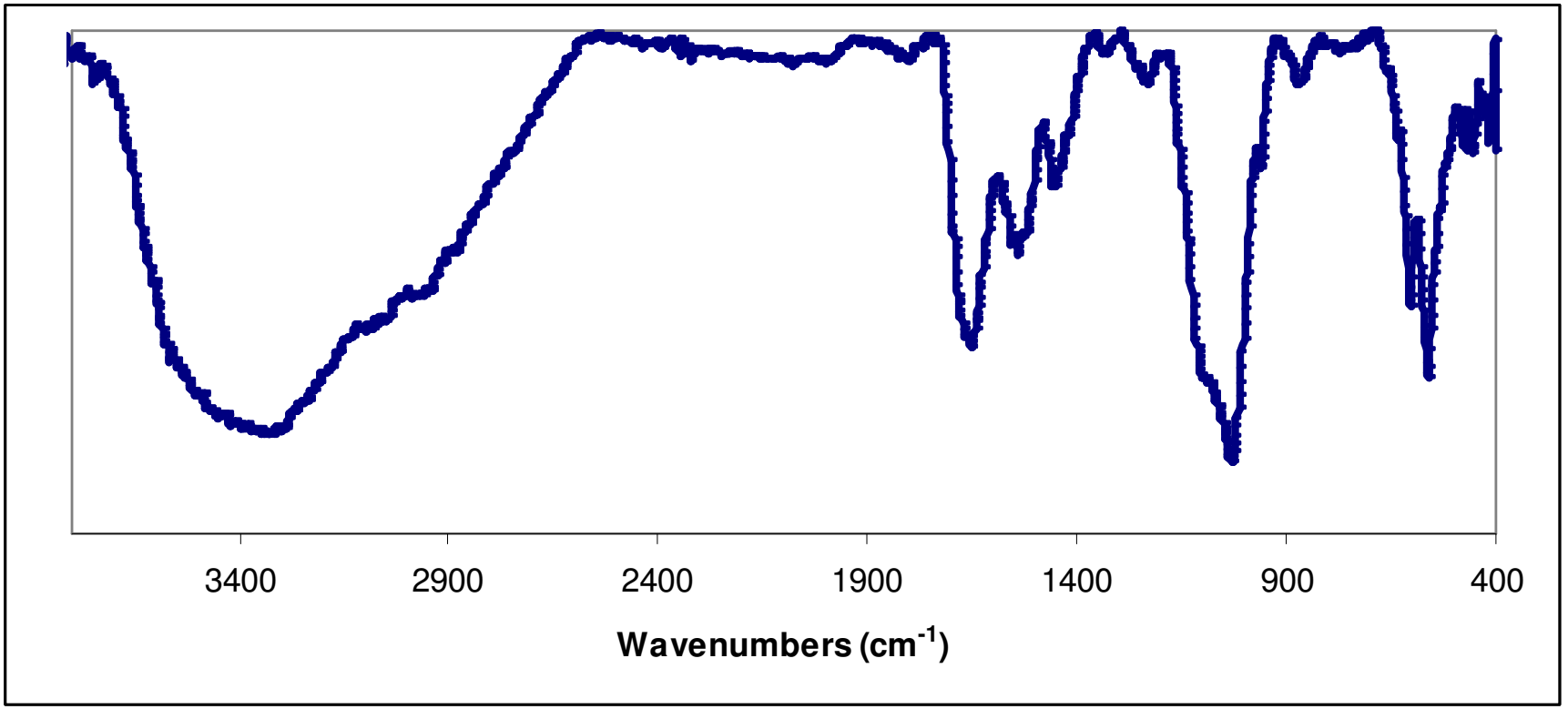

Figure 4-3: Infrared spectrum of hydroxyapatite isolated from 14.4 wt % gelatin sample by the washing method.

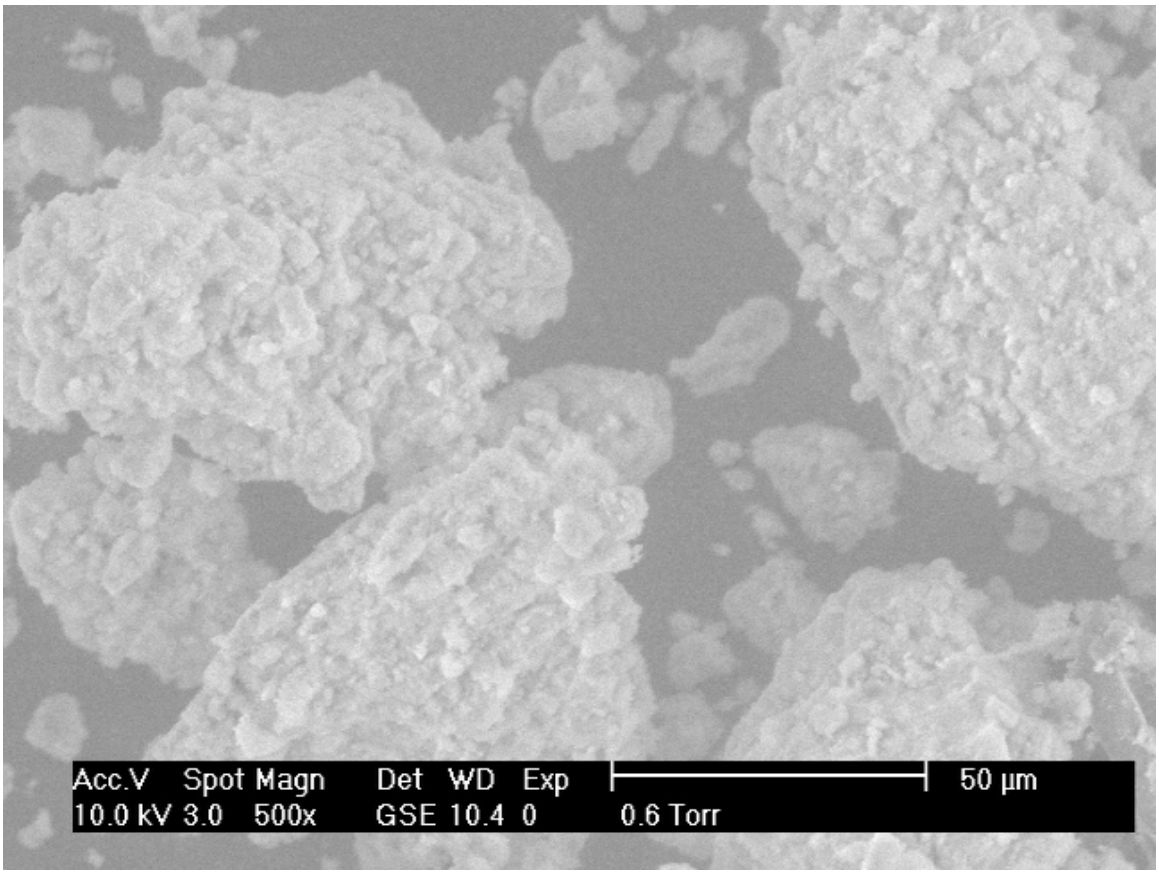

Figure 4-4: SEM image of 14.4 wt % gelatin-hydroxyapatite gello sample.

Then the sample was dried under vacuum. XRD showed that hydroxyapatite had formed (Figure 4-5). Peak widths are similar in width to the pattern peaks from the hydroxyapatite that was isolated from the gello by simply washing. Hence, hydroxyapatite from the gello that was purified with trypsin had a crystallite thickness of about 2.5 nm.

Infrared spectroscopy agreed that hydroxyapatite had been synthesized in the trypsin-purified sample. Bands characteristic of hydroxyapatite were present with the PO_4^{3-} asymmetric stretching at 1100 and 1030 cm^{-1}, the P-O symmetric stretching at 860 cm^{-1}, and the O-P-O bending at 600 and 560 cm^{-1}. Apparently, both water (3400 cm^{-1})

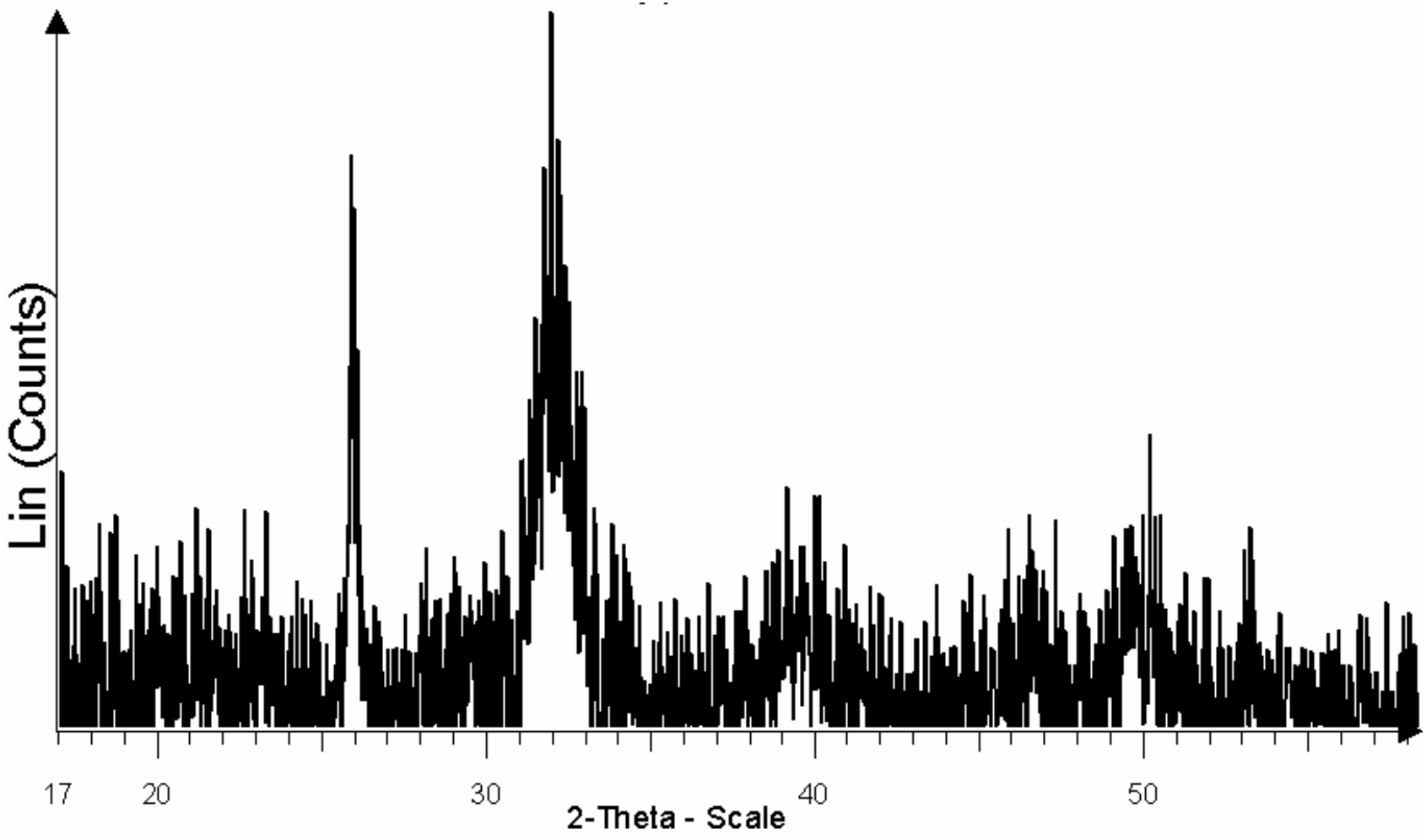

Figure 4-5: XRD pattern for the 14.4 wt % gelatin-hydroxyapatite sample with trypsin used to isolate the hydroxyapatite.

and gelatin (1660, 1540, and 1200 cm^{-1}) were still present in the hydroxyapatite sample (Figure 4-6).

Other preliminary work had been done with gelatin and trypsin when trying to form yttrium iron garnet (YIG). The same procedure as used for the hydroxyapatite samples had been used to try to remove the gelatin from the YIG-precursor samples. Trypsin could not successfully remove the gelatin from these samples. Much like what was observed for the yttrium aluminum garnet (YAG)-precursor agar samples when agarase was added, the YIG-precursor gels became softer, but the gelatin was still noticeably present. The gelling agent must be securely adjoined to the amorphous solid and difficult to remove with a protease. It is interesting that the gelling agent seems to not be as bound up with a crystalline material, in this case, hydroxyapatite.

Although the trypsin was able to remove most of the gelatin for the hydroxyapatite samples, water washings still had to be done to isolate the hydroxyapatite. Therefore, future samples were purified of the gelatin by the simple washing method.

Preparation of Calcium Phosphates

Once the hydroxyapatite powder was heated to 670ºC, calcium phosphate phases formed as expected. As shown in Figure 4-7, XRD reveals that these phases are calcium pyrophosphate ($Ca_2P_2O_7$) and calcium metaphosphate (CaP_2O_6). Both of these phases have been explored as a bioactive ceramic and shown promise as use in bioglass and bone implants [56,87].

The infrared spectrum for the powder heated at 670ºC is shown in Figure 4-8. Not surprisingly, there are no bands associated with water or gelatin since these have

been burned off by this temperature. Various P_2O_7 bonds from calcium pyrophosphate are seen at 570, 600, 960, 1030, 1100, and 1140 cm^{-1} [88]. Bands characteristic of calcium metaphosphate include PO_2 stretching (220 and 1040 cm^{-1}) and P-O stretching (980 and 795 cm^{-1}) [89].

CONCLUSION

Nanocrystalline hydroxyapatite was prepared at room temperature using the sol-gello process. Two purification methods were used: washing with water and using the protease trypsin to dissolve the gelatin. Both methods were successful at isolating the hydroxyapatite with some traces of gelatin left. Heating the hydroxyapatite crystallizes out calcium phosphate phases that are important as a bioceramic material as well.

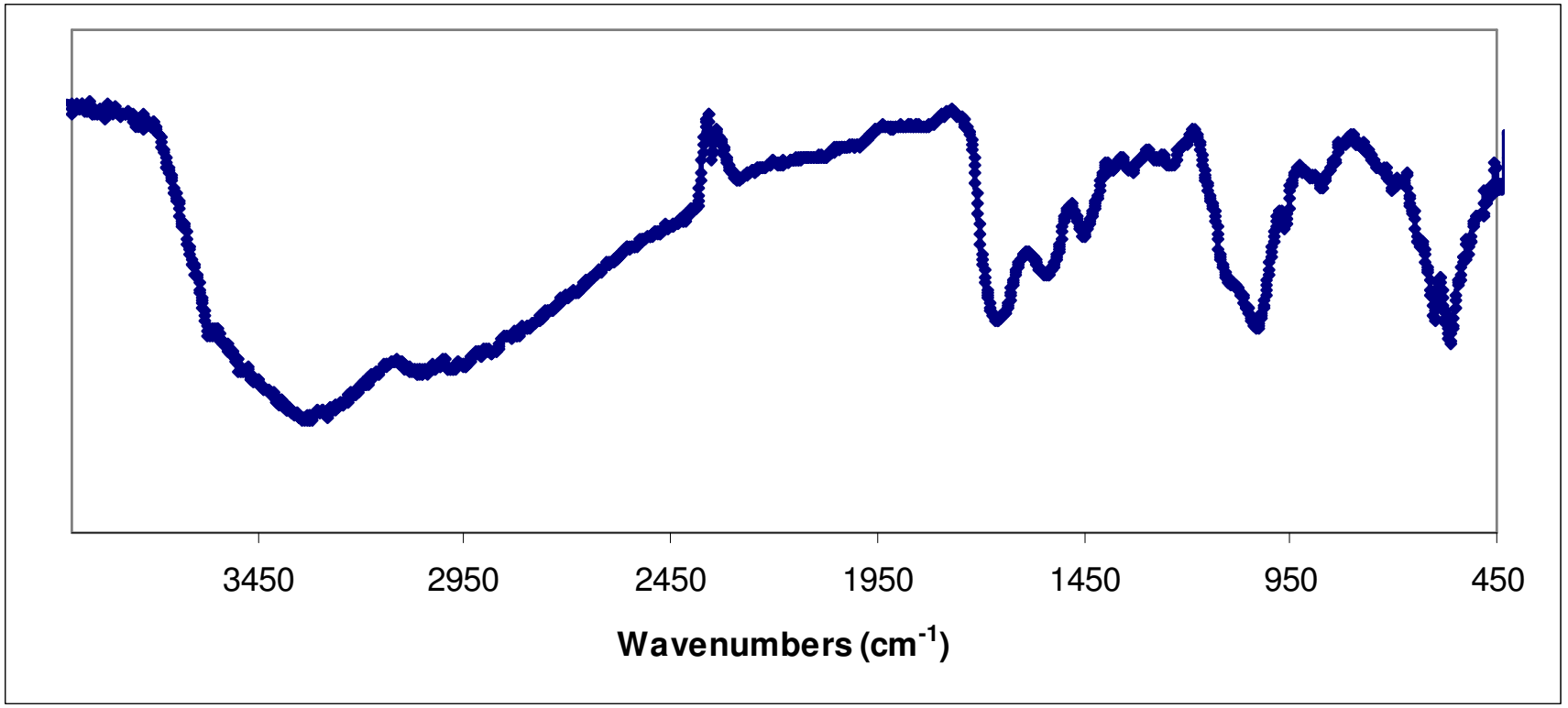

Figure 4-6: IR spectrum for the 14.4 wt % gelatin-hydroxyapatite sample purified with trypsin.

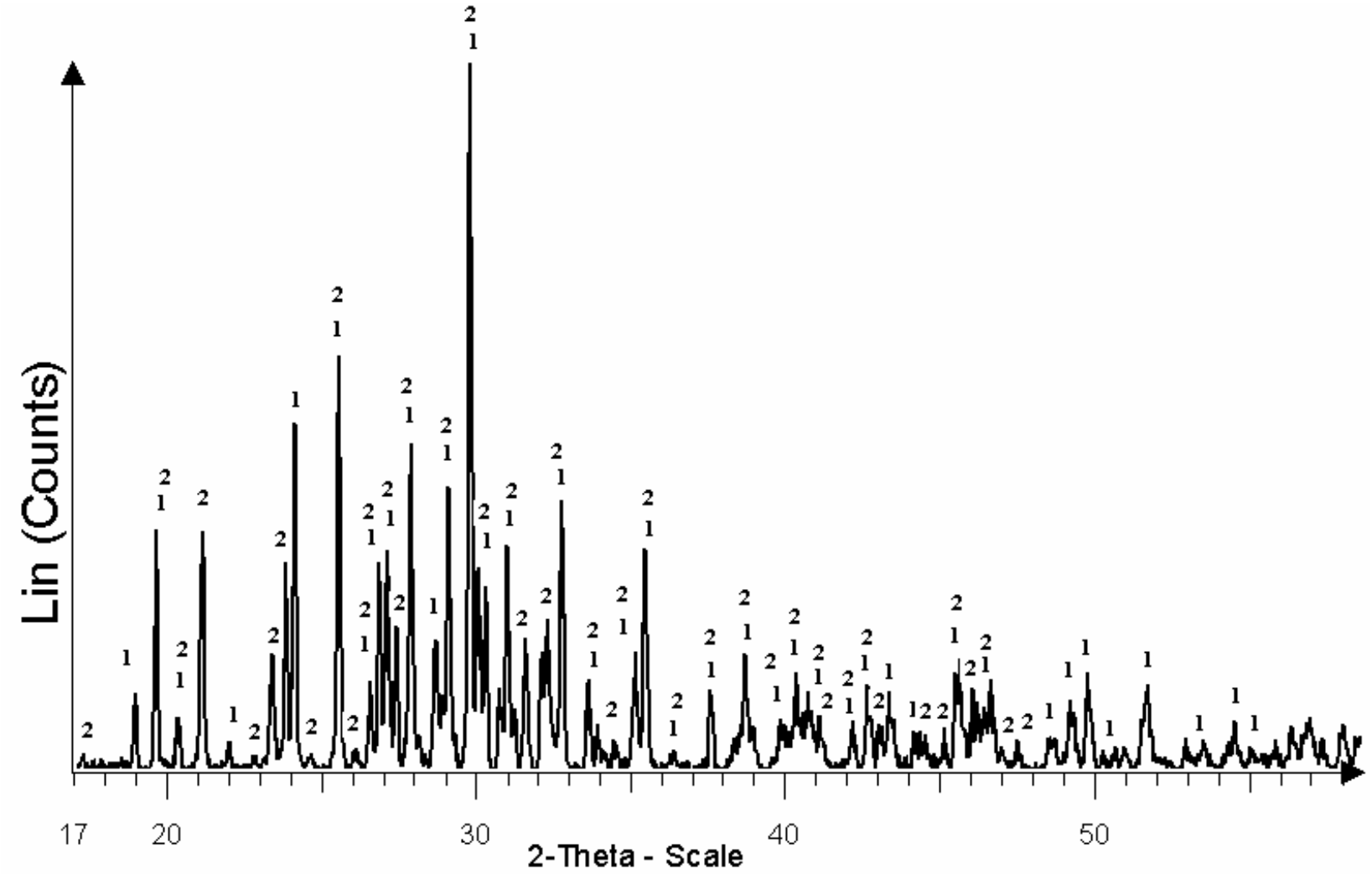

Figure 4-7: XRD pattern for the hydroxyapatite powder heated to 670ºC identified two calcium phosphate phases: $Ca_2P_2O_7$ (ICCN: 09-0346) (1) and CaP_2O_6 (ICCN: 11-0039) (2).

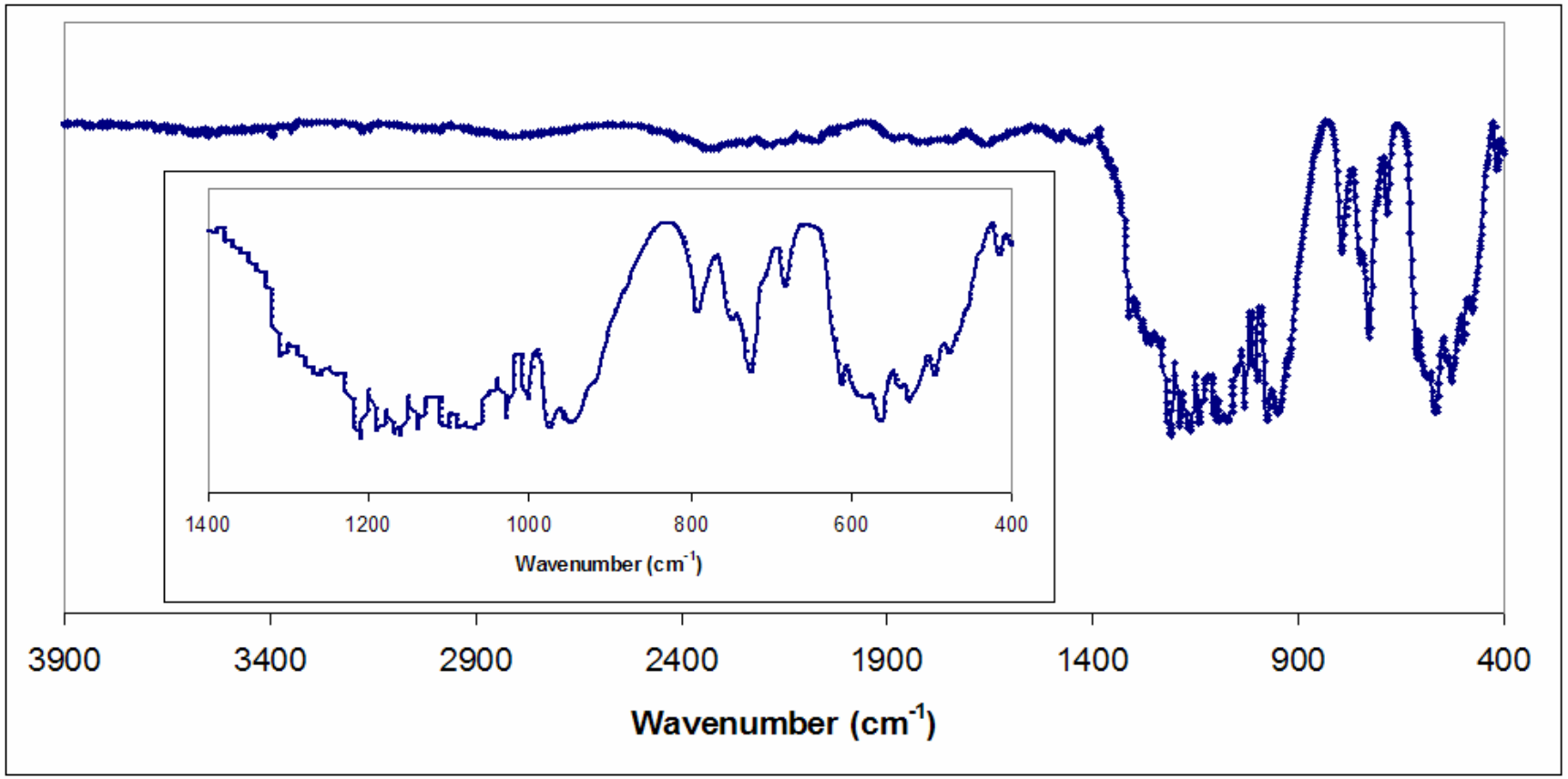

Figure 4-8: IR spectrum of the calcium phosphates.

CHAPTER V

CONCLUSIONS AND FUTURE DIRECTIONS

CONCLUSIONS

The sol-gello method was successful in the synthesis of three nanocrystalline materials: yttrium aluminum garnet (YAG), spinel, and hydroxyapatite. This approach is a simple, straight-forward technique for the preparation of materials. All of these materials were prepared at record low temperatures due to controlling the precursor size. Locking the metal cations into small pores within the gel matrix allows the formation of a hydrolysis product that converts to the desired crystalline ceramic at low temperature. Variations of the sol-gello method that included the gelling agent type, content, purity, and removal were explored.

While YAG can be prepared using any of the gelling agents (agar, gelatin, and purified gelatin), agar proved to be the most effective, allowing YAG to start crystallization at 500ºC and complete it at 600ºC. Lower crystallization temperatures were achieved with an increase of agar content. The YAG crystallite size was estimated to be 11.4 nm when 30% by weight of agar was used.

Spinel was prepared using the purified gelatin since impurities in the gelatin hinder pure spinel formation. An initial crystallization temperature of 420ºC is a record low in the synthesis of spinel. Crystallite sizes slightly decreased as the gelatin content increased. Crystallite sizes were estimated to be in the range of 1-5 nm.

Hydroxyapatite crystals were prepared at room temperature estimating approximately 2.5 nm. While a hydroxyapatite-gelatin composite is applicable, separation techniques were explored for isolating the hydroxyapatite from the gelatin. Both methods, washing with water and dissolving the gelatin with the protease trypsin, were somewhat successful with some traces of gelatin left. Useful bioceramic calcium phosphate phases were crystallized when hydroxyapatite was heated to 670ºC.

FUTURE DIRECTIONS

There are some recommendations for the future direction of this research. One of the gelling agents, fish gelatin, is a liquid and was used in an attempt to synthesize spinel. Though that attempt was unsuccessful, a gelling agent that is liquid at room temperature could hold interesting promise. A temperature of at least 400ºC has to be reached to burn the conventional gelatin off. An alternative might be removing liquid fish gelatin via centrifugation at room temperature that might allow for even lower crystallization temperatures to be reached.

Another gelling agent used for an unsuccessful attempt in preparing pure spinel was the photoengraving glue. Since Norland describes that baking the glue will convert it into an acid-resistant polymer [90], the glue could be used to make a cement-acid-resistant-polymer composite. One study made an alumina cement-acid-resistant-polymer composite for use in concrete structures exposed to an acidic environment [91].

The sol-gello method is a facile technique and applicable to the synthesis of many different materials. Current work in our lab has focused upon using the sol-gello method to prepare iron nanoparticles and molybdenum hydrogen bronzes. Iron nanoparticles can

be prepared by the reduction of iron chloride [92] and along with iron oxide nanoparticles can be used for arsenic remediation [93,94]. Iron oxide-polymer nanocomposites have been prepared for applications as a room temperature transparent magnet [95]. Our preliminary work has shown that iron gellos can be prepared using the sol-gello method. Molybdenum hydrogen bronzes can be used as explosives detection and neutralization [96] and for heavy metal removal from water [97]. Metal oxides, such as superconducting oxides [98], and metal phosphates [99] could probably be prepared using this same sol-gello process. It would be interesting to see if doped YAG as phosphors could be prepared as well [8-10,24,63].

One of the popular areas of research currently involves hydroxyapatite. Hydroxyapatite-polymer hybrids and hydroxyapatite-gelatin nanocomposites have been explored as drug-delivery systems for antibiotic drugs [100,101]. Other useful drugs that treat osteoporosis and rheumatoid arthritis could be loaded into hydroxyapatite-gelatin nanocomposites [102]. Implementing the sol-gello process would be an easier method in preparing the nanocomposites for drug-delivery systems. Some research has explored the use of microbial silver in hydroxyapatite for biomedical applications [103,104]. Attempting to dope hydroxyapatite via the sol-gello process could yield an important implant material with a facile preparation method.

REFERENCES CITED

[1] Schubert, U.; Husing, N., *Synthesis of Inorganic Materials*. Wiley-VCH: Weinheim, 2000.

[2] West, A. R., *Basic Solid State Chemistry*. John Wiley & Sons: Chichester, 1988; p 415.

[3] Wang, F. F. Y., Physical and Chemical Properties of Garnets. In *Treatise on Materials Science and Technology*, Herman, H., Ed. Academic Press: New York, 1973; Vol. 2, pp 279-384.

[4] Dillon, J. F., Jr., Ferrimagnetic resonance in yttrium iron garnet. *Phys. Rev.* **1957,** 105, 759-60.

[5] Pauthenet, R., Spontaneous magnetization of some garnet ferrites and the aluminum-substituted garnet ferrites. *Journal of Applied Physics* **1958,** 29, 253-5.

[6] Iino, T.; Tsukada, T.; Fujino, K., A magnetic bubble device for revolution counters. *IEEE Transactions on Magnetics* **1999,** 35, (5, Pt. 2), 3664-3666.

[7] Huie, J. C.; Dudding, C. B.; McCloy, J., Polycrystalline yttrium aluminum garnet (YAG) for IR transparent missile domes and windows. *Proceedings of SPIE-The International Society for Optical Engineering* **2007,** 6545, (Window and Dome Technologies and Materials X), 65450E/1-65450E/12.

[8] Hess, N. J.; Exarhos, G. J., Pressure-temperature sensors: solution deposition of rare-earth-doped garnet films. *Journal of Non-Crystalline Solids* **1994,** 178, 91-7.

[9] Ohno, K.; Abe, T., The synthesis and particle growth mechanism of bright green phosphor YAG:Tb. *Journal of the Electrochemical Society* **1994,** 141, (5), 1252-4.

[10] Rao, R. P., Preparation and characterization of fine-grain yttrium-based phosphors by sol-gel process. *Journal of the Electrochemical Society* **1996,** 143, (1), 189-97.

[11] Hazel, B. T.; Murphy, J. A.; Skoog, A. J. Strain-tolerant corrosion protecting coating and spray method of application on gas turbine engine parts. 2006-126417 1798311, 20061218., 2007.

[12] Nakagawa, N.; Ohtsubo, H.; Mitani, A.; Shimizu, K.; Waku, Y., High temperature strength and thermal stability for melt growth composite. *Journal of the European Ceramic Society* **2005,** 25, (8), 1251-1257.

[13] De With, G.; Van Dijk, H. J. A., Translucent yttrium aluminium oxide (Y3Al5O12) ceramics. *Materials Research Bulletin* **1984,** 19, (12), 1669-74.

[14] Ikesue, A.; Furusato, I.; Kamata, K., Fabrication of polycrystalline, transparent YAG ceramics by a solid-state reaction method. *Journal of the American Ceramic Society* **1995,** 78, (1), 225-8.

[15] Messier, D. R.; Gazza, G. E., Synthesis of MgAl2O4 and Y3A15O12 by thermal decomposition of hydrated nitrate mixtures. *American Ceramic Society Bulletin* **1972,** 51, (9), 692-4, 697.

[16] Kakade, M. B.; Ramanathan, S.; Roy, S. K., Synthesis of YAG powder by aluminum nitrate-yttrium nitrate-glycine reaction. *Journal of Materials Science Letters* **2002,** 21, (12), 927-929.

[17] Vaqueiro, P.; Lopez-quintela, M. A., Synthesis of yttrium aluminum garnet by the citrate gel process. *Journal of Materials Chemistry* **1998,** 8, (1), 161-163.

[18] Vaidhyanathan, B.; Binner, J. G. P., Microwave assisted synthesis of nanocrystalline YAG. *Journal of Materials Science* **2006,** 41, (18), 5954-5957.

[19] Puttbach, R. C.; Monchamp, R. R.; Nielsen, J. W., Hydrothermal growth of Y3Al5O12. *Journal of Physics and Chemistry of Solids, Supplement* **1967,** 1, 569-71.

[20] Inoue, M.; Otsu, H.; Kominami, H.; Inui, T., Synthesis of yttrium aluminum garnet by the glycothermal method. *Journal of the American Ceramic Society* **1991,** 74, (6), 1452-4.

[21] He, J.; Bell, A., Co-Precipitation Synthesis of Nano-Sized Yttrium Aluminum Garnet (YAG) Powders. *Ceramic Transactions* **2006,** 172, 71-78.

[22] Apblett, A. W.; Reinhardt, L. E.; Walker, E. H., Jr., Liquid metal carboxylates as precursors for aluminum-containing ceramics. *Comments on Inorganic Chemistry* **1998,** 20, (2-3), 83-99.

[23] Sim, S. M.; Keller, K. A.; Mah, T. I., Phase formation in yttrium aluminum garnet powders synthesized by chemical methods. *Journal of Materials Science* **2000,** 35, (3), 713-717.

[24] Veith, M.; Mathur, S.; Kareiva, A.; Jilavi, M.; Zimmer, M.; Huch, V., Low temperature synthesis of nanocrystalline Y3Al5O12 (YAG) and Ce-doped Y3Al5O12 via different sol-gel methods. *Journal of Materials Chemistry* **1999,** 9, (12), 3069-3079.

[25] De la Rosa, E.; Diaz-Torres, L. A.; Salas, P.; Arredondo, A.; Montoya, J. A.; Angeles, C.; Rodriguez, R. A., Low temperature synthesis and structural characterization of nanocrystalline YAG prepared by a modified sol-gel method. *Optical Materials (Amsterdam, Netherlands)* **2005,** 27, (12), 1793-1799.

[26] Searle, A. B., *Refractory Materials: Their Manufacture and Uses*. Charles

Griffin: London, 1924.

[27] Chesters, J. H., *Refractories: Production and Properties*. Iron and Steel Institute: London, 1973.

[28] Szmigiel, D.; Rarog-Pilecka, W.; Miskiewicz, E.; Kaszkur, Z.; Kowalczyk, Z., Ammonia decomposition over the ruthenium catalysts deposited on magnesium-aluminum spinel. *Applied Catalysis, A: General* **2004,** 264, (1), 59-63.

[29] Sharafat, S.; Ghoniem, N. M.; Cooke, P. I. H.; Martin, R. C.; Najmabadi, F.; Schultz, K. R.; Wong, C. P. C.; et al., Materials analysis of the TITAN-I reversed-field-pinch fusion power core. *Fusion Engineering and Design* **1993,** 23, (2-3), 99-113.

[30] Carts, Y. A., Hard Materials Shine in Infrared Applications. *Laser Focus World* **1992,** 28, (12), 89-94.

[31] Gusmano, G.; Montesperelli, G.; Nunziante, P.; Traversa, E., Study of the conduction mechanism of magnesium aluminum oxide (MgAl2O4) at different environmental humidities. *Electrochimica Acta* **1993,** 38, (17), 2617-21.

[32] McColm, I. J., *Ceramic Science for Materials Technologists*. Chapman and Hall: New York, 1983.

[33] Foll, H. Ionic Crystals. http://www.techfak.uni-kiel.de/matwis/amat/def_en/kap_2/basics/b2_1_6.html

[34] Vestal, C. R.; Zhang, Z. J., Normal micelle synthesis and characterization of MgAl2O4 spinel nanoparticles. *Journal of Solid State Chemistry* **2003,** 175, (1), 59-62.

[35] Osseo-Asare, K., Microemulsion-Mediated Synthesis of Nanosize Oxide Materials. In *In Handbook of Microemulsion Science and Technology*, Kumar, P.; Mittal, K. L., Eds. Markel Dekker: New York, 1999; pp 549-603.

[36] Waldner, K. F.; Laine, R. M.; Dhumrongvaraporn, S.; Tayaniphan, S.; Narayanan, R., Synthesis of a Double Alkoxide Precursor to Spinel (MgAl2O4) Directly from Al(OH)3, MgO, and Triethanolamine and Its Pyrolytic Transformation to Spinel. *Chemistry of Materials* **1996,** 8, (12), 2850-2857.

[37] Parmentier, J.; Richard-Plouet, M.; Vilminot, S., Influence of the sol-gel synthesis on the formation of spinel MgAl2O4. *Materials Research Bulletin* **1998,** 33, (11), 1717-1724.

[38] Gresser, J. D.; Lewandrowski, K.-U.; Trantola, D. J.; Wise, D. L.; Hsu, Y.-Y., Soluble Calcium Salts in Bioresorbable Bone Grafts. In *Biomaterials Engineering and Devices: Human Applications*, Wise, D. L.; Trantola, D. J.; Lewandrowski, K.-U.; Gresser, J. D.; Cattaneo, M. V.; Yaszemski, M. J., Eds. Humana Press: Totowa, NJ, 2000; Vol. 2: Orthopedic, Dental, and Bone Graft Applications, pp 171-188.

[39] Shetty, R. H., Surface Hardening of Orthopedic Implants. In *Biomaterials Engineering and Devices: Human Applications*, Wise, D. L.; Trantola, D. J.; Lewandrowski, K.-U.; Gresser, J. D.; Cattaneo, M. V.; Yaszemski, M. J., Eds. Humana Press: Totowa, NJ, 2000; Vol. 2: Orthopedic, Dental, and Bone Graft Applications, pp 191-202.

[40] Patka, P., Haarman, H.J.Th.M., van der Elst, M., Bakker, F.C., Artificial Bone: Hydroxyapatite Reconstruction of Tibial Plateau Fractures. In *Biomaterials Engineering and Devices*, Wise, D. L.; Trantola, D. J.; Lewandrowski, K.-U.; Gresser, J. D.; Cattaneo, M. V.; Yaszemski, M. J., Eds. Humana Press: Totowa, NJ, 2000; Vol. 2: Orthopedic, Dental, and Bone Graft Applications, pp 95-109.

[41] Korkusuz, P.; Korkusuz, F., Hard Tissue - Biomaterial Interactions. In

Biomaterials in Orthopedics, Yaszemski, M. J.; Trantola, D. J.; Lewandrowski, K.-U.; Hasirci, V.; Altobelli, D. E.; Wise, D. L., Eds. Marcel Dekker, Inc.: NY, 2004; pp 1-40.

[42] Heimke, G.; Willmann, G., Follow-up-Study-Based Wear Debris Reduction with Ceramic-Metal-Modular Hip Replacements. In *Biomaterials Engineering and Devices: Human Applications*, Wise, D. L.; Trantola, D. J.; Lewandrowski, K.-U.; Gresser, J. D.; Cattaneo, M. V.; Yaszemski, M. J., Eds. Humana press: Totowa, NJ, 2000; Vol. 2: Orthopedic, Dental, and Bone Graft Applications, pp 223-251.

[43] Kim, H. M., Ceramic bioactivity and related biomimetic strategy. *Current Opinion in Solid State & Materials Science* **2003,** 7, (4-5), 289-299.

[44] Kokubo, T.; Kim, H.-M.; Kawashita, M., Novel bioactive materials with different mechanical properties. *Biomater.* **2003,** 24, (13), 2161-2175.

[45] Payten, W. M.; Ben-Nissan, B., Development of a Modular Ceramic Knee Prosthesis. In *Biomaterials Engineering and Devices: Human Applications*, Wise, D. L.; Trantola, D. J.; Lewandrowski, K.-U.; Gresser, J. D.; Cattaneo, M. V.; Yaszemski, M. J., Eds. Humana Press: Totowa, NJ, 2000; Vol. 2: Orthopedic, Dental, and Bone Graft Applications, pp 309-336.

[46] Trantola, D. J.; Lewandrowski, K.-U.; Gresser, J. D.; Wise, D. L., Injectable and Bioresorbable Poly(Propylene Glycol-Co-Fumaric Acid) Bone Cement. In *Biomaterials Engineering and Devices: Human Applications*, Wise, D. L.; Trantola, D. J.; Lewandrowski, K.-U.; Gresser, J. D.; Cattaneo, M. V.; Yaszemski, M. J., Eds. Humana Press Totowa, NJ, 2000; Vol. 2: Orthopedic, Dental, and Bone Graft Applications, pp 291-308.

[47] Elliott, J. C., *Structure and chemistry of the apatites and other calcium*

orthophosphates. Elsevier: Amsterdam [The Netherlands] New York ;, 1994; p xiii, 387 p.

[48] Van Raemdonck, W.; Ducheyne, P.; De Meester, P., Calcium Phosphate Ceramics. In *Metal and Ceramic Biomaterials*, Ducheyne, P.; Hastings, G. W., Eds. CRC Press, Inc.: Boca Raton, 1984; Vol. 2: Strength and Surface, pp 143-166.

[49] Cao, J. M.; Feng, J.; Deng, S. G.; Chang, X.; Wang, J.; Liu, J. S.; Lu, P.; Lu, H. X.; Zheng, M. B.; Zhang, F.; Tao, J., Microwave-assisted solid-state synthesis of hydroxyapatite nanorods at room temperature. *Journal of Materials Science* **2005,** 40, (23), 6311-6313.

[50] Orlovskii, V. P.; Komlev, V. S.; Barinov, S. M., Hydroxyapatite and Hydroxyapatite-Based Ceramics. *Inorganic Materials (Translation of Neorganicheskie Materialy)* **2002,** 38, (10), 973-984.

[51] Raemdonck, W. V.; Ducheyne, P.; De Meester, P., Calcium Phosphate Ceramics. In *Metal and Ceramic Biomaterials: Volume II Strength and Surface*, Ducheyne, P.; Hastings, G. W., Eds. CRC Press, Inc.: Boca Raton, 1984; Vol. 2, pp 143-166.

[52] Meng, Y. H.; Tang, C. Y.; Tsui, C. P.; Chen, D. Z., Fabrication and characterization of needle-like nano-HA and HA/MWNT composites. *Journal of Materials Science: Materials in Medicine* **2008,** 19, (1), 75-81.

[53] Wang, A.; Liu, D.; Yin, H.; Wu, H.; Wada, Y.; Ren, M.; Jiang, T.; Cheng, X.; Xu, Y., Size-controlled synthesis of hydroxyapatite nanorods by chemical precipitation in the presence of organic modifiers. *Materials Science & Engineering, C: Biomimetic and Supramolecular Systems* **2007,** 27, (4), 865-869.

[54] Koutsopoulos, S., Synthesis and characterization of hydroxyapatite crystals: a

review study on the analytical methods. *Journal of Biomedical Materials Research* **2002,** 62, (4), 600-612.

[55] Teng, S.; Shi, J.; Chen, L., Formation of calcium phosphates in gelatin with a novel diffusion system. *Colloids and Surfaces, B: Biointerfaces* **2006,** 49, (1), 87-92.

[56] Chin, T. S.; Wu, D. C.; Liu, H. S.; Hung, M. P.; Wang, C. P., The resorbable bioglass ceramics based on calcium biphosphate. *Materials Research Society Symposium Proceedings* **1992,** 252, (Tissue-Inducing Biomaterials), 103-8.

[57] Payne, S. A.; Albrecht, G. F., Solid-State Lasers. In *Encyclopedia of Lasers and Optical Technology*, Meyers, R. A., Ed. Academic Press, Inc.: San Diego, 1991; pp 603-624.

[58] Manalert, R.; Rahaman, M. N., Sol-gel processing and sintering of yttrium aluminum garnet (YAG) powders. *Journal of Materials Science* **1996,** 31, (13), 3453-3458.

[59] Tariyal, B. K.; Cherin, A. H., Optical Fiber Communications. In *Encyclopedia of Lasers and Optical Technology*, Meyers, R. A., Ed. Academic Press, Inc.: San Diego, 1991; pp 411-455.

[60] Su, J.; Zhang, Q. L.; Gu, C. J.; Sun, D. L.; Wang, Z. B.; Qiu, H. L.; Wang, A. H.; Yin, S. T., Preparation and characterization of Y3Al5O12 (YAG) nano-powder by co-precipitation method. *Materials Research Bulletin* **2005,** 40, (8), 1279-1285.

[61] Iida, Y.; Towata, A.; Tsugoshi, T.; Furukawa, M., In situ Raman monitoring of low-temperature synthesis of YAG from different starting materials. *Vibrational Spectroscopy* **1999,** 19, (2), 399-405.

[62] Wu, N.-L.; Wang, S.-Y.; Rusakova, I. A., Inhibition of crystallite growth in the

sol-gel synthesis of nanocrystalline metal oxides. *Science (Washington, D. C.)* **1999,** 285, (5432), 1375-1377.

[63] Nien, Y.-T.; Chen, Y.-L.; Chen, I.-G.; Hwang, C.-S.; Su, Y.-K.; Chang, S.-J.; Juang, F.-S., Synthesis of nano-scaled yttrium aluminum garnet phosphor by co-precipitation method with HMDS treatment. *Materials Chemistry and Physics* **2005,** 93, (1), 79-83.

[64] Morrice, L. M.; McLean, M. W.; Williamson, F. B.; Long, W. F., b-Agarases I and II from Pseudomonas atlantica. Purifications and some properties. *European Journal of Biochemistry* **1983,** 135, (3), 553-8.

[65] Scholten, H. J.; Pierik, R. L. M., Agar as a gelling agent. Chemical and physical analysis. *Plant Cell Reports* **1998,** 17, (3), 230-235.

[66] Hofmeister, A. M.; Campbell, K. R., Infrared spectroscopy of yttrium aluminum, yttrium gallium, and yttrium iron garnets. *Journal of Applied Physics* **1992,** 72, (2), 638-46.

[67] Dudman, W. F., Precipitation of tobacco mosaic virus by macromolecules; a method for estimating molecular volumes. *Nature (London, United Kingdom)* **1966,** 211, (5053), 1049-50,1067.

[68] Guo, J.; Lou, H.; Zhao, H.; Wang, X.; Zheng, X., Novel synthesis of high surface area MgAl2O4 spinel as catalyst support. *Materials Letters* **2004,** 58, (12-13), 1920-1923.

[69] Zhang, H.; Jia, X.; Liu, Z.; Li, Z., The low temperature preparation of nanocrystalline MgAl2O4 spinel by citrate sol-gel process. *Materials Letters* **2004,** 58, (10), 1625-1628.

[70] Colomban, P., Structure of oxide gels and glasses by infrared and Raman scattering. Part 1. Alumina. *Journal of Materials Science* **1989,** 24, (8), 3002-10.

[71] Stathopoulos, V. N.; Pomonis, P. J., Low-temperature synthesis of spinels MAl2O4 (M=Mg, Co, Ni, Cu, Zn) prepared by a sol-gel method. *Progress in Colloid & Polymer Science* **2001,** 118, (Trends in Colloid and Interface Science XV), 17-21.

[72] Norland HiPure Liquid Gelatin. https://www.norlandprod.com/fishgel/hipure.html

[73] *Handbook of Biomaterial Properties*. 1st ed.; Chapman Hall: New York, 1998.

[74] Webster, T. J.; Ergun, C.; Doremus, R. H.; Siegel, R. W.; Bizios, R., Enhanced functions of osteoblasts on nanophase ceramics. *Biomaterials* **2000,** 21, (17), 1803-1810.

[75] Webster, T. J.; Ergun, C.; Doremus, R. H.; Siegel, R. W.; Bizios, R., Enhanced osteoclast-like cell functions on nanophase ceramics. *Biomaterials* **2001,** 22, (11), 1327-1333.

[76] Yoshikawa, H.; Myoui, A., Bone tissue engineering with porous hydroxyapatite ceramics. *Journal of Artificial Organs* **2005,** 8, 131-136.

[77] Lacefield, W. R., Hydroxylapatite Coatings. In *An Introduction to Bioceramics*, Hench, L. L.; Wilson, J., Eds. World Scientific: Singapore, 1993; Vol. 1, pp 223-238.

[78] Aoki, H., *Science and Medical Applications of Hydroxyapatite*. Takayama Press System Center Co., Inc.: Tokyo, 1991.

[79] Wei, M.; Ruys, A. J.; Milthorpe, B. K.; Sorrell, C. C., Precipitation of hydroxyapatite nanoparticles: Effects of precipitation method on electrophoretic deposition. *Journal of Materials Science: Materials in Medicine* **2005,** 16, (4), 319-324.

[80] Zakharov, N. A.; Polunina, I. A.; Polunin, K. E.; Rakitina, N. M.; Kochetkova, E. I.; Sokolova, N. P.; Kalinnikov, V. T., Calcium Hydroxyapatite for Medical Applications.

Inorganic Materials (Translation of Neorganicheskie Materialy) **2004,** 40, (6), 641-648.

[81] Fazan, F.; Shahida, K. B. N., Fabrication of synthetic apatites by solid-state reactions. *Med J Malaysia FIELD Full Journal Title:The Medical journal of Malaysia* **2004,** 59 Suppl B, 69-70.

[82] Rhee, S.-H., Synthesis of hydroxyapatite via mechanochemical treatment. *Biomaterials FIELD Full Journal Title:Biomaterials sanghoon@krict.re.kr***2002,** 23, (4), 1147-52.

[83] Neira, I. S.; Guitian, F.; Taniguchi, T.; Watanabe, T.; Yoshimura, M., Hydrothermal synthesis of hydroxyapatite whiskers with sharp faceted hexagonal morphology. *Journal of Materials Science* **2008,** 43, (7), 2171-2178.

[84] Eshtiagh-Hosseini, H.; Housaindokht, M. R.; Chahkandi, M., Effects of parameters of sol-gel process on the phase evolution of sol-gel-derived hydroxyapatite. *Materials Chemistry and Physics* **2007,** 106, (2-3), 310-316.

[85] Liu, D.-M.; Troczynski, T.; Tseng Wenjea, J., Aging effect on the phase evolution of water-based sol-gel hydroxyapatite. *Biomaterials FIELD Full Journal Title:Biomaterials deanmo@interchange.ubc.ca***2002,** 23, (4), 1227-36.

[86] Sipos, T.; Merkel, J. R., Effect of calcium ions on the activity, heat stability, and structure of trypsin. *Biochemistry* **1970,** 9, (14), 2766-75.

[87] Safina, M. N.; Safronova, T. V.; Lukin, E. S., Calcium phosphate based ceramic with a resorbable phase and low sintering temperature. *Glass and Ceramics* **2007,** 64, (7-8), 238-243.

[88] Yonggang, Y.; Wolke, J. G. C.; Yubao, L.; Jansen, J. A., The influence of discharge power and heat treatment on calcium phosphate coatings prepared by RF

magnetron sputtering deposition. *J Mater Sci Mater Med FIELD Full Journal Title:Journal of materials science. Materials in medicine* **2007,** 18, (6), 1061-9.

[89] Meyer, K.; Hobert, H.; Barz, A.; Stachel, D., Infrared spectra and structure of various crystalline ultraphosphates and their glasses. *Vibrational Spectroscopy* **1994,** 6, (3), 323-32.

[90] Norland Photoengraving Glue. https://www.norlandprod.com/fishgel/photoglue.html

[91] Sakakibara, H.; Wakasugi, M.; Sugiura, A.; Fukada, K.; Uchibata, S.; Kitora, T. Acid-resistant polymer type cement for repairing of concrete structures exposed to acidic environment. 2003-351553 2005112689, 20031010., 2005.

[92] Huang, K.-C.; Ehrman, S. H., Synthesis of Iron Nanoparticles via Chemical Reduction with Palladium Ion Seeds. *Langmuir* **2007,** 23, (3), 1419-1426.

[93] Kanel, S. R.; Nepal, D.; Manning, B.; Choi, H., Transport of surface-modified iron nanoparticle in porous media and application to arsenic(III) remediation. *Journal of Nanoparticle Research* **2007,** 9, 725-735.

[94] Apblett, A. W.; Kuriyavar, S. I.; Kiran, B. P., Preparation of micron-sized spherical porous iron oxide particles. *Journal of Materials Chemistry* **2003,** 13, (5), 983-985.

[95] Ziolo, R. F.; Giannelis, E. P.; Weinstein, B. A.; O'Horo, M. P.; Ganguly, B. N.; Mehrotra, V.; Russell, M. W.; Huffman, D. R., Matrix-mediated synthesis of nanocrystalline g-ferric oxide: a new optically transparent magnetic material. *Science (Washington, DC, United States)* **1992,** 257, (5067), 219-23.

[96] Apblett, A. W.; Kiran, B. P.; Malka, S.; Materer, N. F.; Piquette, A., Nanotechnology for neutralization of terrorist explosives. *Ceramic Transactions* **2006,** 172, (Ceramic Nanomaterials and Nanotechnologies IV), 29-35.

[97] Kiran, B. P.; Apblett, A. W., Process for selective removal and concentration of actinides and heavy metals from water. *Ceramic Transactions* **2004,** 155, (Environmental Issues and Waste Management Technologies in the Ceramic and Nuclear Industries IX), 371-380.

[98] Kakihana, M., "Sol-gel" preparation of high temperature superconducting oxides. *Journal of Sol-Gel Science and Technology* **1996,** 6, (1), 7-55.

[99] Dinamani, M.; Kamath, P. V., Electrochemical synthesis of metal phosphates by cathodic reduction. *Materials Research Bulletin* **2001,** 36, 2043-2050.

[100] Kim, H.-W.; Knowles, J. C.; Kim, H.-E., Development of hydroxyapatite bone scaffold for controlled drug release via poly(e-caprolactone) and hydroxyapatite hybrid coatings. *Journal of Biomedical Materials Research, Part B: Applied Biomaterials* **2004,** 70B, (2), 240-249.

[101] Kim, H.-W.; Knowles Jonathan, C.; Kim, H.-E., Porous scaffolds of gelatin-hydroxyapatite nanocomposites obtained by biomimetic approach: characterization and antibiotic drug release. *J Biomed Mater Res B Appl Biomater FIELD Full Journal Title:Journal of biomedical materials research. Part B, Applied biomaterials hwkim@snu.ac.kr***2005,** 74, (2), 686-98.

[102] Rodan, G. A.; Martin, T. J., Therapeutic approaches to bone diseases. *Science (Washington, D. C.)* **2000,** 289, (5484), 1508-1514.

[103] Clupper, D. C.; Hench, L. L., Bioactive response of Ag-doped tape cast Bioglass

45S5 following heat treatment. *Journal of Materials Science: Materials in Medicine* **2001,** 12, (10/11/12), 917-921.

[104] Kim, T. N.; Feng, Q. L.; Kim, J. O.; Wu, J.; Wang, H.; Chen, G. C.; Cui, F. Z., Antimicrobial effects of metal ions (Ag+, Cu2+, Zn2+) in hydroxyapatite. *Journal of Materials Science: Materials in Medicine* **1998,** 9, (3), 129-134.

VITA

Amanda J. Nichols

Candidate for the Degree of

Doctor of Philosophy

Thesis: A SOL-GELLO APPROACH TO THE SYNTHESIS OF NANOCRYSTALLINE MATERIALS

Major Field: Chemistry

Biographical:

Personal Data: Born in Tucson, Arizona on January 10, 1981, daughter of Brian and Kimberly McCormack. Married to Joshua Nichols in December 2000. Mother of Joshua Casen Nichols.

Education: Received Bachelor of Science Degree in Chemistry from Oklahoma Christian University, Oklahoma City, Oklahoma in April 2003. Completed the requirements for the Doctor of Philosophy in Chemistry at Oklahoma State University, Stillwater, Oklahoma in July, 2008.

Experience: Employed as a summer intern lab technician for the Citgo Gas and Oil Production plant in Oklahoma City, Oklahoma in 2002. Employed as a teaching assistant and research assistant by Oklahoma State University, Department of Chemistry between 2003-2008. As a chemistry instructor in Fall of 2007.

Professional Memberships: American Chemical Society (ACS), Phi Lambda Upsilon (PLU) National Honorary Chemical Society

Name: Amanda J. Nichols Date of Degree: July, 2008

Institution: Oklahoma State University Location: Stillwater, Oklahoma

Title of Study: A SOL-GELLO APPROACH TO THE SYNTHESIS OF NANOCRYSTALLINE MATERIALS

Pages in Study: 96 Candidate for the Degree of Doctor of Philosophy

Major Field: Chemistry

Scope and Method of Study: A sol-gello approach has been developed for the synthesis of nanocrystalline materials. This facile approach allows for the preparation of precursor nanoparticles that have higher reactivity at lower temperatures. Three materials have been prepared using this method: Yttrium aluminum garnet (YAG), hydroxyapatite, and spinel ($MgAl_2O_4$). The first material (YAG) can be synthesized by adding yttrium and aluminum salts to a gelling agent solution. While YAG can be prepared using any of the gelling agents (agar, gelatin, and purified gelatin), agar proved to be the most effective. For the synthesis of spinel, an ion-exchange purification method was implemented to rid the gelatin of impurities. Magnesium and aluminum salts were added to the gelatin, trapping the metal ions in a homogeneous distribution. Hydroxyapatite, a bioactive material, was formed when a calcium salt and phosphoric acid were added to the gelatin. Ammonia was used to facilitate the reaction between phosphate and calcium ions. Two purification methods were used: washing with water and using the protease trypsin to dissolve the gelatin. Both methods were successful at isolating the hydroxyapatite with some traces of gelatin left.

Findings and Conclusions: YAG was crystallized at 650ºC compared to the conventional preparation temperature of 1600ºC. Lower crystallization temperatures were achieved with an increase of agar content. The YAG crystallite size was estimated to be 11.4 nm when 30% by weight of agar was used. For the synthesis of spinel, ammonia hydrolysis resulted in amorphous solids. Spinel began to crystallize as low as 420ºC compared to the solid state reaction temperature of 1600ºC. Because of the gelatin purification, only the spinel phase was present at higher temperatures. Crystallite sizes slightly decreased as the gelatin content increased. Crystallite sizes were estimated to be in the range of 1-5 nm. Nanocrystalline hydroxyapatite was formed within the gelatin matrix at room temperature estimating approximately 2.5 nm. Other important bioceramic calcium phosphate phases were crystallized once the solid was heated.

ADVISER'S APPROVAL: Dr. Allen Apblett